Editorial Team

JAEHR
Journal of Advances in Environmental Health Research
Kurdistan Environmental Health Research Center
Kurdistan University of Medical Sciences

Information for Authors

AIM AND SCOPE

*Journal of Advances in Environmental Health Research (JAEHR)*is a quarterly peer-reviewed scientific journal published by Kurdistan University of Medical Sciences. The manuscripts on the topic of environmental science and engineering will be published in this journal. This contains all aspects of solid waste management, air pollution, water and wastewater, environmental monitoring and modeling, innovative technologies and studies related to the environmental science.

Instruction to Authors

MANUSCRIPTS

Manuscripts containing original material are accepted for consideration if neither the article nor any part of its essential substance, tables, or figures has been or will be published or submitted elsewhere before appearing in the *Journal of Advances in Environmental Health Research*. This restriction does not apply to abstracts or press reports published in connection with scientific meetings. Copies of any closely related manuscripts must be submitted along with the manuscript that is to be considered by the *Journal of Advances in Environmental Health Research*. Authors of all types of articles should follow the general instructions given below.

HUMAN AND ANIMAL RIGHTS

The research involves human beings or animals must adhere to the principles of the Declaration of Helsinki (http://www.wma.net/e/ethicsunit/helsinki.htm).

Types of Articles

- *Original article* which reports the results of an original scientific research should be less than 4000 words.
- *Review article* which represents the researches and works on a particular topic.
- *Brief communication* is a short research article and should be limited to 1500 words. This article contains all sections of an original article.
- *Case report* is a detailed report of an individual patient that may represent a previously non-described condition and contains new information about different aspects of a disease. It should be less than 2000 words.
- *Letter to the Editor* must be less than 400 words in all cases.
- *Book Review* must be less than 1000 words on any book topics related to the scope of *Journal of Advances in Environmental Health Research*.

SUBMISSION

- Only online submission is acceptable. Please submit online at: http://www.jaehr.muk.ac.ir
- This manuscripts should be divided into the following sections: (1) Title page, (2) Abstract and Keywords, (3) Introduction, (4) Materials and Methods, (5) Results and Discussion, (6) Acknowledgements, (7) Author contribution, (8) References, (9) Figure legends, (10) Tables and (11) Figures (figures should be submitted in separate files if the file size exceeds 2 Mb).
- Please supply a word count in title page.
- Use normal page margins (2.5 cm), and double-space throughout the manuscript.
- Use Times New Roman (12) font throughout the manuscript.
- Prepare your manuscript text using a Word processing package (save in .doc or .rtf format). Submissions of text in the form of PDF files are not permitted.

COVER LETTER

A covering letter signed by all authors should identify the corresponding author (include the address, telephone number, fax number, and e-mail address). Please make clear that the final manuscript has been seen and approved by all authors, and that the authors accept full responsibility for the design and conduct of the study, had access to the data, and controlled the decision to publish.

Authors are also asked to provide the names and contact information for three potential reviewers in their cover letter. However, the journal is not obliged to use the suggested reviewers. Final selection of reviewers will be determined by the editors.

AUTHORSHIP

As stated in the Uniform Requirements for Manuscripts Submitted to Biomedical Journals (http://www.icmje.org/icmje-recommendations.pdf), credit for authorship requires substantial contributions to: 1. Substantial contributions to the conception or design of the work; or the acquisition, analysis, or interpretation of data for the work; AND 2. Drafting the work or revising it critically for important intellectual content; AND 3. Final approval of the version to be published; AND 4. Agreement to be accountable for all aspects of the work in ensuring that questions related to the accuracy or integrity of any part of the work are appropriately investigated and resolved. Each author must sign authorship form attesting that he or she fulfills the authorship criteria. There should be a statement in manuscript explaining contribution of each author to the work. Acknowledgments will be limited to one page of *Journal of Advances in Environmental Health Research*, and those acknowledged will be listed only once.

Any change in authorship after submission must be approved in writing by all authors.

ASSURANCES

In appropriate places in the manuscript please provide the following items:

- If applicable, a statement that the research protocol was approved by the relevant institutional review boards or ethics committees and that all human participants gave written informed consent
- The source of funding for the study
- The identity of those who analyzed the data
- Financial disclosure, or a statement that none is necessary

TITLE PAGE

With the manuscript, provide a page giving the title of the paper; titles should be concise and descriptive (not declarative). Title page should include an abbreviated running title of 40 characters, the names of the authors, including the complete first names, the name of the department and institution in which the work was done, the institutional affiliation of each author. The name, post address, telephone number, fax number, and e-mail address of the corresponding author should be separately addressed. Any grant support that requires acknowledgment should be mentioned on this page. Word count of abstract and main text as well as number of tables and figures and references should be mentioned on title page. If the work was derived from a project or dissertation, its code should also be stated.

Affiliation model: Department, Institute, City, Country.
Example: Department of Environmental Health Engineering, School of Health, Kurdistan University of Medical Sciences, Sanandaj, Iran.

ABSTRACT

Provide on a separate page an abstract of not more than 250 words. This abstract should consist of ONE paragraph (Non-structured Abstract). It should briefly describe the problem being addressed in the study, how the study was performed, the salient results, and what the authors conclude from the results respectively. Three to seven keywords may be included. Keywords are preferred to be in accordance with MeSH (http://www.ncbi.nlm.nih.gov/mesh) terms.

CONFLICT OF INTEREST

Authors of research articles should disclose at the time of submission any financial arrangement they may have with a company whose product is pertinent to the submitted manuscript or with a company making a competing product. Such information will be held in confidence while the paper is under review and will not influence the editorial decision, but if the article is accepted for publication, a disclosure will appear with the article.
Because the essence of reviews and editorials is selection and interpretation of the literature, the *Journal of Advances in Environmental Health Research* expects that authors of such articles will not have any significant financial interest in a company (or its competitor) that makes a product discussed in the article.

REVIEW AND ACTION

Submitted papers will be examined for the evidence of plagiarism using some automated plagiarism detection service. Manuscripts are examined by members of the editorial staff, and two thirds are sent to external reviewers. Communications about manuscripts will be sent after the review and editorial decision-making process is complete within **3-6 weeks** after receiving the manuscript. After acceptance, editorial system makes a final language and scientific edition. No substantial change is permitted by authors after acceptance. It is the responsibility of corresponding author to answer probable questions and approve final version.

COPYRIGHT

Journal of Advances in Environmental Health Research is the owner of all copyright to any original work published by the

JAEHR. Authors agree to execute copyright transfer forms as requested with respect to their *Journal of Advances in Environmental Health Research* has the right to use, reproduce, transmit, derive works from, publish, and distribute the contribution, in the *Journal* or otherwise, in any form or medium. Authors will not use or authorize the use of the contribution without the Journal Office' written consent

JOURNAL STYLE

Tables

Double-space tables and provide a title for each.

Figures

Figures should be no larger than 125 (height) x 180 (width) mm (5 x 7 inches) and should be submitted in a separate file from that of the manuscript. The name of images or figures files should be the same as the order that was used in manuscript (fig1, fig2, etc.). Only JPEG, tif, gif and eps image formats are acceptable with CMYK model for colored image at a resolution of at least 300 dpi. Graphs must have the minimum quality: clear text, proportionate, not 3 dimensional and without disharmonic language. Electron photomicrographs should have internal scale markers.

If photographs of patients are used, either the subjects should not be identifiable or the photographs should be accompanied by written permission to use them. Permission forms are available from the Editorial Office.

Scientific illustrations will be created or recreated in-house. If an outside illustrator creates the figure, the *Journal of Advances in Environmental Health Research* reserves the right to modify or redraw it to meet our specifications for publication. The author must explicitly acquire all rights to the illustration from the artist in order for us to publish the illustration. Legends for figures should be an editable text as caption and should not appear on the figures.

References

The Vancouver style of referencing should be used. References must be double-spaced and numbered as **superscripts** consecutively as they are cited. References first cited in a table or figure legend should be numbered so that they will be in sequence with references cited in the text at the point where the table or figure is first mentioned. List all authors when there are six or fewer; when there are seven or more, list the first six, then "et al." The following are sample references:

1. Maleki A, Shahmoradi B, Daraei H, Kalantar E. Assessment of ultrasound irradiation on inactivation of gram negative and positive bacteria isolated from hospital in aqueous solution. J Adv Environ Health Res 2013; 1(1): 9-14.

2. Buckwalter JA, Marsh JL, Brown T, Amendola A, Martin JA. Articular cartilage injury. In: Robert L, Robert L, Joseph V, editors. Principles of Tissue Engineering. 3rd ed. Burlington, MA: Academic Press; 2007. p. 897-907.

3. Kuczmarski RJ, Ogden CL, Grammer-Strawn LM, Flegal KM, Guo SS, Wei R, et al. CDC growth charts: United States. Advance data from vital and health statistics. No. 314. Hyattsville, Md: National Center for Health Statistics, 2000. (DHHS publication no. (PHS) 2000-1250 0-0431)

4. World Health organization. Strategic directions for strengthening nursing and midwifery services [online]. Available from: URL:http://www.wpro.who.int/themesfocuses/theme3/focus2/nursingmidwifery.pdf2002

Units of Measurement

Authors should express all measurements in conventional units, with Système International (SI) units given in parentheses throughout the text. Figures and tables should use conventional units, with conversion factors given in legends or footnotes. In accordance with the Uniform Requirements, however, manuscripts containing only SI units will not be returned for that reason.

Abbreviations

Except for units of measurement, abbreviations are discouraged. Consult Scientific Style and Format: The CBE Manual for Authors, Editors, and Publishers (Sixth edition. New York: Cambridge University Press, 1994) for lists of standard abbreviations. Except for units of measurement, the first time an abbreviation appears, it should be preceded by the words for which it stands.

Chemical Structure

Structures should be produced with a chemical drawing program, preferably ChemDraw 4.5 or higher, and submitted in TIFF format to allow use of electronic files in production. Structures should also be submitted in native file formats, e.g., RDX.

For any more detail about the writing style for your manuscripts refer to:

http://www.jaehr.muk.ac.ir

Authorship Form

Title of the manuscript:

.....

.....

We, the undersigned, certify that we take responsibility for the conduct of this study and for the analysis and interpretation of the data. We wrote this manuscript and are responsible for the decisions about it. Each of us meets the definition of an author as stated by the International Committee of Medical Journal Editors (see http://www.icmje.org/icmje-recommendations.pdf). We have seen and approved the final manuscript. Neither the article nor any essential part of it, including tables and figures, will be published or submitted elsewhere before appearing in the *Journal of Advances in Environmental Health Research* [All authors must sign this form or an equivalent letter.]

Name of Author	**Contribution**	**Signature**

Please scan this form and upload it as a supplementary file in "Step 4" of submitting articles.

Table of Contents

Original Article(s)

JAEHR Journal of Advances in Environmental Health Research

The effect of ergonomic intervention in reducing musculoskeletal disorders by Snook table method in a steel industry

Omid Giahi[1], Mansur Sarabi[2], Jamshid Khoubi[1], Ebrahim Darvishi[1]

1 Department of Occupational Health, School of Health AND Kurdistan Environmental Health Research Center, Kurdistan University of Medical Sciences, Sanandaj, Iran
2 Qorveh Public Health Center, Kurdistan University of Medical Sciences, Qorveh, Iran

Original Article

Abstract

The most frequent and expensive cause category of compensable loss is manual material handling (MMH). Casting workers who handle oxygen (O_2) cylinders manually are at risk for work-related musculoskeletal disorders (WMSDs). The aim of this study was to assess manual handling of O_2 cylinders by casting workers and to implement ergonomic intervention to reduce the risk of musculoskeletal disorders (MSDs). This interventional study was conducted on 30 male workers of casting unit in a steel industry. Nordic Musculoskeletal Questionnaire was used to determine the prevalence of MSDs in workers. Snook tables and its software were used to assess manual handling risk of O_2 cylinders. Manual handling of O_2 cylinders was totally excluded using the box with 16 cylinders that can be moved by crane. The most common MSDs in 1 year prior to the study were low back pain (43%), shoulders (33%), and hand/wrist and knee disorders (16%), respectively. The Snook tables' results indicated that 86% of lifting/lowering, 100% of carrying, and 50% of pulling tasks were appropriate for <10% of casting workers. About 94% of O_2 cylinders pushing were appropriate for 17% casting workers. With the implementation of ergonomic intervention, the risk of WMSDs and explosion of cylinders was decreased, and safety of workers was improved.

KEYWORDS: Manual Material Handling, Snook Tables, Ergonomics Intervention, Nordic Musculoskeletal Questionnaire, Oxygen Cylinders, Musculoskeletal Disorders

Date of submission: 30 Dec 2013, ***Date of acceptance:*** 07 Mar 2014

Citation: Giahi O, Sarabi M, Khoubi J, Darvishi E. **The effect of ergonomic intervention in reducing musculoskeletal disorders by Snook table method in a steel industry.** J Adv Environ Health Res 2014; 2(2): 65-71.

Introduction

Manual materials handling (MMH) tasks (pushing, puling, lifting, lowering, and carrying) are very common in workplaces and are carried out in most industrial plants.[1,2] MMH tasks are in many industry sectors, including manufacturing and service occupations.[3] However, the technology is developed in many industries, MMH has remained essentially the concern.[4,5] About 10% of jobs require extensive MMH.[6] The risk level of MMH depends on the load characteristics [weight, size, shape, coupling, and imbalance (i.e., changing center of gravity)], the task or method of handling (include repetitively, moving the load over large distances, accuracy and precision required because of fragile loads, hazardous movements or postures, etc.), environmental factors and workplace physical conditions (such as obstacles and floor surfaces (e.g., slippery, uneven or damaged, distance of route, temperature, lighting, and noise) and operator characteristics

Corresponding Author:
Ebrahim Darvishi
Email: darvishi.hse@gmail.com

(physical factors and psychological factors, like stress).[7,8] MMHs are the leading source of fatigue, musculoskeletal disorders (MSDs), low back pain and workers compensation claims in the workplace. MSDs often involve strains and sprains to the low back, shoulders, and upper limbs.[6] Annually, over half a million cases of MSDs reported in the United States due to MMH.[9,10] More than one-fourth of all compensable work injuries are associated with MMH tasks. National Institute for Occupational Safety and Health (NIOSH) has reported that 60% of the injury claims for low back pain is associated with MMH and 20% with pushing and pulling.[11] MMH is a frequent (36% of all claims) and costly (35% of total cost) category of compensable loss in the USA.[12]

Limitations and acceptable loads in MMH have been analyzed using a wide spectrum of techniques including physiological, psychophysical, subjective, biomechanical, observational, postural analysis and a combination of the above. "Snook tables" were developed at Liberty Mutual Insurance Company and described by Snook.[13] Snook tables are based on psychophysical measurements rather than biomechanical. They have more general use rather than the revised NIOSH lifting equation because they are applied in many of tasks.[13,14] Snook tables have been used in various studies and industries, including agriculture, mines, and construction sites.[10,15,16] Furthermore, these tables have been used in order to survey physiological and psychophysical responses in handling maximum acceptable weights (MAWs) in male Chinese workers performing combined MMH tasks, the effects of box size, vertical distance, and height on lowering tasks for male and female industrial workers.[17-19] Scientific studies indicate that effective ergonomic interventions can decrease the physical demands of MMH tasks, as a result lowering the prevalence and severity of the musculoskeletal discomfort.[2] Their potential to reduce discomfort associated with costs alone makes the ergonomic interventions useful tool for improving a product quality, company's productivity and overall business competitiveness. The best ergonomic intervention measure is to remove the need for workers to carry out MMH tasks.[17,18]

Mechanical handling devices or aids can often remove the task itself or facilitate the demands on the worker. Hence, it is not possible for MMH tasks to be designed base on to the workers' capabilities. Workers are facing with ergonomics hazards such as overload in manual handling of O_2 cylinders tasks in blast furnace unit, which expose them to risk of work-related musculoskeletal disorders (WMSDs). Thus, the aim of this study was to evaluate prevalence of WMSDs and to investigate MMH tasks by Snook tables among casting workers and ergonomics intervention in manual handling of O_2 cylinders in a steel industry.

Materials and Methods

The current experiment is an intervention study that was conducted on 30 male workers of the casting unit in a steel industry. All the subjects dressed in the same working overalls. They were provided with similar shoes to ensure consistent coefficients of friction on the ground. All the subjects examined by an occupational medicine specialist to identify people had experienced significant low back pain or other MSDs.

In steel industry, purified O_2 is used to take the hot metal out of the blast furnace and conduct it into the cauldron and casting molds to produce steel ingots. O_2 reduces the viscosity of the hot metal flow. Thus, O_2 consumption in steel industry is very high. In the studied steel industry, 40 rechargeable O_2 cylinders with weight and dimensions of 153 pounds (70 kg) and 146 × 23 cm, respectively, were used per day. Workers performed 14 variations of Lifting, carrying, lowering, pushing and pulling of cylinders, manually (MMH). O_2 cylinders were placed horizontally on each other in a truck and

were carried to the company. Workers lifted cylinders and carried it vertically to 2 m in the truck, then lowered to 1 m onto ground. In most cases, this necessitated some degree of body twisting during lifting and lowering (Figure 1). The lifting and lowering tasks were performed at frequencies of 2 and 1/min. Workers carried the O_2 cylinders from the floor to body height distances of 2.1 m. Combination of The lifting, carrying and lowering task was performed at frequency rate of 1/min. Pulling tasks were performed at a distance of 2.6 m and at frequency of 0.2 and 1/min. A 1.1 m pushing task was performed 1/min. Workers pushed and pulled at a height midway between knuckle and elbow height (88.1 cm).

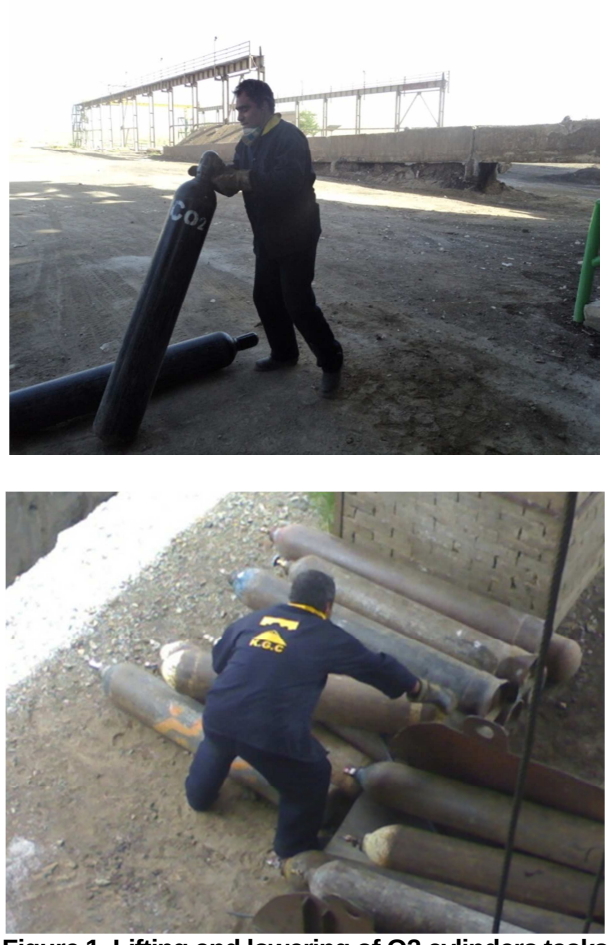

Figure 1. Lifting and lowering of O2 cylinders tasks

By unloading the truck, the O_2 cylinders were laid horizontally on the ground and on each other (Figure 2). Cylinders must be connected to the valve and oxygen consumption device that are used separately. Cylinders loading have been done manually for recharging in the factory after discharging. Workers complained of MMH tasks because they had to handle many cylinders daily.

Figure 2. Oxygen cylinders position before the intervention

Nordic Musculoskeletal Questionnaire (NMQ) was used to determine the prevalence of MSDs in workers. NMQ included questions about risks and discomfort during the last 12 months and 1 week before the study.[20]

Furthermore, the psychophysical methodology described by Ciriello and Snook[14] and Ciriello and Snook[18] was used in this experiment. This methodology includes measurement of oxygen consumption, heart rate, and anthropometric characteristics. This methodology is well-known as Snook tables. These tables are based on controlled experiments using psychophysical evaluation, and can be used to find the percent of an industrial population capable of sustaining the efforts tabulated in lifting, lowering, pushing, pulling, and carrying. These tables included 20 tables for MAW for lifting, lowering, pulling, pushing and carrying tasks. These tables are

presented separately for males and females. The result is specified as a percentage of the population of males and females who are able to carry out manual handling tasks. MMH tasks must be designed for more than 75% of the female or male work population to be able to do it. Designing these manual tasks for more than 90% of the female work population will offer a more appropriate level of protection from manual handling injuries. The force exerted to lifting/lowering, pushing/pulling, and carrying cylinders tasks were measured using a model of FG-5100 potentiometer. These tasks were evaluated using the software Snook.

Ergonomics intervention (designed box and handling mechanization of the cylinders)

Among the different options to improve a particular MMH task, it is important to choose the one, which will work best for that task. In the current study, a cubic rectangular box was designed to eliminate the manual handling of cylinders. Box dimensions were 150 × 150 × 170 cm. Box frame was made of steel. Sixteen O_2 cylinders were fixed inside the box vertically. The cylinders were connected to each other using copper pipes. Finally, inlet and outlet in the cylinders were designed for O_2 consumption and charging, respectively. Regulator and manometer were installed at the inlet and outlet of the cylinders. Two hooks were installed in the top of the box for connection of the crane. There were overhead cranes in all the units with the application of O_2 cylinders (Figure 3).

Results and Discussion

Mean (± SD) of 30 studied male workers' age, height, body weight, and work experience were 35.8 (± 5.5) years, 175.8 (± 4.2) cm, 65.0 (± 5.6) kg, and 14.5 (± 5.5) years, respectively.

The results of NMQ showed that 84% of workers had experienced pain at least once in one of the organs during the 12 months before the study. The most common MSDs were low back pain (43%), shoulders (33%) and hand/wrist and knee disorders (16%), respectively, in 1 year prior to the study (Table 1). Furthermore, four of them had suffered significant musculoskeletal injuries.

The measurements included finding the percentage of male workers population for O_2 cylinder lifting/lowering.

O_2 cylinder weights were 153 pounds (70 kg). Hand distances away from the body of 7 in. an initial hand height at the start of 10 and 15 in. O_2 cylinders were lifted once every 1, 5, and 480 min.

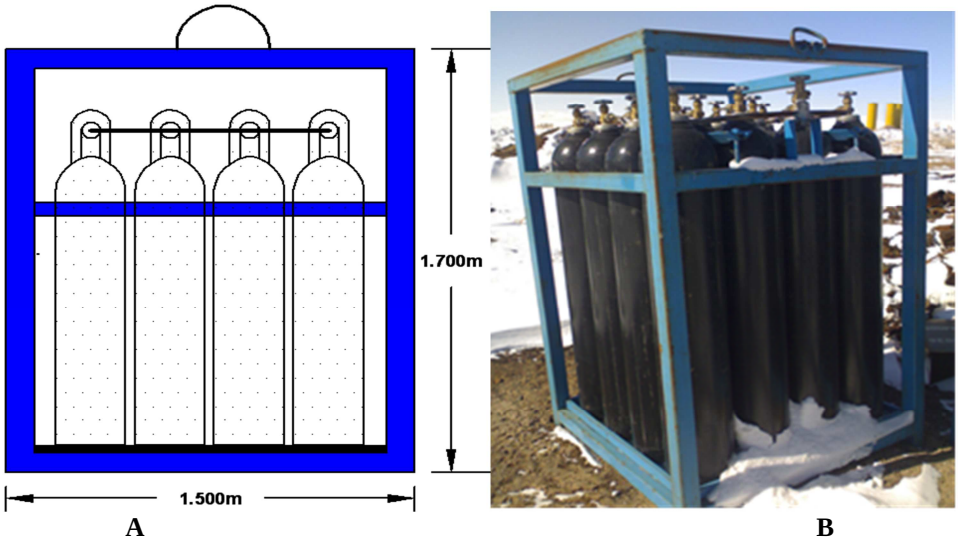

Figure 3. (A) Cylinder box plan, (B) Made cylinder box

Table 1. Musculoskeletal symptoms in various body regions during the 12 months and 1 week before the study

Organs	Musculoskeletal disorders	
	Frequency during the last 1 week (%)	Frequency during the last 12 months (%)
Neck	3 (10.0)	4 (13.0)
Shoulders	5 (16.0)	10 (33.0)
Elbow	1 (3.3)	2 (6.6)
Hand/wrist	1 (3.3)	5 (16.0)
Low Back	10 (33.0)	13 (43.0)
Thigh/hip	0 (0.0)	1 (3.3)
Knee	3 (10.0)	5 (16.0)
Foot	1 (3.3)	3 (10.0)

The percentages of population capable of sustaining the efforts of lifting/lowering were estimated using the software Snook for 30 workers (Table 2).

The results of the carrying O_2 cylinder tasks are presented in table 3.

The percentage male workers able to perform these tasks (lifting, lowering, and carrying of O_2 cylinders) were very low. MAWs and forces were appropriate for < 10% of them.

Maximum hands and lifting/lowering distances were 15 and 20 in., respectively. Most lifting and lowering tasks were performed in the frequency of 1 and 5 min and least of them were performed once every 8 h.

Table 4 contains the population percentage estimated for pushing/pulling O_2 cylinder tasks and maximum acceptable forces of push/pull of the subjects.

Table 2. Population percentage estimated for lifting/lowering O2 cylinder tasks and maximum acceptable lifting/lowering weights for workers (kg)

States	Lifting/lowering						
	Frequency states	Force exertion (kg/p)	Hand distance (cm/in.)	Distance (cm/in.)	Frequency once every	Percentage population	Maximum acceptable weights
1	0.330	38/84	38/15	51/20	1 min	Less than 10	13
2	0.130	38/84	25/10	51/20	1 min	Less than 10	13
3	0.400	38/84	38/15	51/20	5 min	Less than 10	13
4	0.033	38/84	25/10	25/10	5 min	22	14
5	0.066	38/84	25/10	25/10	1 min	17	14
6	0.033	38/84	25/10	25/10	8 h	48	17

Table 3. Population percentage estimated for carrying O2 cylinder tasks and maximum acceptable carrying weights for workers (kg)

Carrying states	Frequency states	Force exertion to carrying (kg/p)	Hand height (cm/in.)	Carrying distance (m/feet)	Frequency one carrying every	Percentage population	Maximum acceptable weights
1	0.86	70/153	84/33	4.3/14	30 s	Less than 10	13
2	0.14	70/153	84/15	8.5/28	1 min	Less than 10	13

Table 4. Population percentage estimated for pushing/pulling O2 cylinder tasks and maximum acceptable forces of push/pull for workers (kg)

Task	States	Frequency states	Initial force (kg/p)	Sustained forces (kg/p)	Hand height (cm/in.)	Frequency one every	Percentage population	Maximum Acceptable (kg)	
								Initial forces	Sustained forces
Pulling	1	0.260	43/95	52/115	94/37	5 min	29	44	36
	2	0.166	43/95	52/115	94/37	1 min	20	43	31
	3	0.500	43/95	52/115	94/37	30 s	Less than 10	44	31
	4	0.080	43/95	52/115	94/37	8 h	60	45	36
Pushing	1	0.944	46/100	53/116	145/57	30 s	17	44	30
	2	0.066	46/100	53/116	145/57	1 min	15	53	36

The results indicated that 84% of workers have experienced musculoskeletal discomfort in the low back, shoulders, hands, and wrists in the year prior to the study. These discomforts were due to extra weight cylinders, forceful exertions and awkward postures during tasks, repetitive and forceful movements, poor workstation design and the MMH tasks. High prevalence of wrist, low back, shoulders, and neck disorders in casting workers in the steel plant have been reported by Armstrong et al.[21]

The results of the assessment of manual handling of O_2 cylinders tasks in the casting workers showed that these tasks were appropriate for < 10%. More than 90% of casting workers confronted with the risk of suffering from MSDs, especially in the low back. About 86% of cylinders lifting/lowering tasks were appropriate for < 10% of workers and MAW for cylinders lifting/lowering was 13 kg, which was more than the recommended limit. The low percentage of workers population in lifting, lowering, and carrying cylinders tasks were due to weight factor. The study of manual material handling assessment by Snook tables in casting workshops in Iran has been studied by Faghih et al. The Snook tables' results indicated that in most of the cases exerted loads exceeded suggested weights.[22] Therefore, the results showed the significant decreases in MAWs with cylinders weight. About 50% of cylinders pulling tasks were appropriate for < 10% of workers population and maximum acceptable initial and sustained forces to pull cylinders were 44 and 31 kg, respectively. About 94% of cylinders pushing tasks were appropriate for 17% of workers population and maximum acceptable initial and sustained forces to push them were 43 and 30 kg, respectively. Results of a study on Indian male and female workers showed that the maximum acceptable forces to pull and push agricultural equipment, and loads were high.[12] Cylinders carrying tasks was appropriate for < 1% of workers population and maximum acceptable carrying weights for them was 12 kg.

Hence, ergonomic intervention must be taken to resolve this problem quickly. Ergonomic intervention was based on using the cylinders mechanical handling instead of their individual manual handling. Thus, manual handling of O_2 cylinders was totally excluded by designing and building a box and mechanizing these tasks. One of the limitations of this intervention was high consumption of oxygen that made it impossible to place fewer numbers of cylinders in the box. Before the intervention, the cylinders were placed horizontally on each other and the probability of their falling and colliding was high. Furthermore, cylinders were connected to the oxygen device separately and workers were forced to replace empty cylinders with full cylinders in short intervals. Therefore, probability of human error was high. High opening and closing of cylinders connections increased corrosion and the probability of oxygen leakage. Moreover, opening and closing of cylinders connections with greasy hands increased the risk of an explosion. Therefore, manual handling of cylinders was excluded and all loading, unloading and handling of cylinders tasks were performed by crane. Finally, safety factor and workers safety against the risk of an explosion was increased.

Conclusion

The results showed that in most cases, the MMH tasks were inappropriate for the workers and the high prevalence of MSDs in the working population can be associated with it. Thus, by designing and building a box and mechanizing handling tasks, risk of suffering from MSDs caused by manual handling of O_2 cylinders was removed.

Conflict of Interests

Authors have no conflict of interests.

Acknowledgements

Hereby, the authors thank the Zagroos steel

Company for technical support of this study.

References

1. Li KW, Yu RF, Han XL. Physiological and psychophysical responses in handling maximum acceptable weights under different footwear--floor friction conditions. Appl Ergon 2007; 38(3): 259-65.
2. Way Li K, Yu RF, Gao Y, Maikala RV, Tsai HH. Physiological and perceptual responses in male Chinese workers performing combined manual materials handling tasks. International Journal of Industrial Ergonomics 2009; 39(2): 422-7.
3. Sadeghi Naeeni H. Ergonomic principles in the design of transport systems for handheld products. Tehran, Iran: Fanavaran Publication; 2009. [In Persian].
4. Abdoliermeki M. Body mechanics and principles of work station design. Tehran, Iran: Omid Majd Publication; 2000. [In Persian].
5. Division of Workers' Compensation. Manual Material Handling an Ergonomic Approach. Texas, TX: The Texas Department of Insurance, Division of Workers' Compensation; 2004.
6. Ciriello VM, Dempsey PG, Maikala RV, O'Brien NV. Revisited: Comparison of two techniques to establish maximum acceptable forces of dynamic pushing for male industrial workers. International Journal of Industrial Ergonomics 2007; 37(11-12): 877-82.
7. Industrial Accident Prevention Association. Manual Materials Handling. Mississauga, Ontario: IAPA; 2008.
8. Dempsey PG, Maynard W. Manual Materials Handling: Using the Liberty Mutual Tables to Evaluate These Tasks. Professional Safety 2005; 50(5): 20-5.
9. NIOSH. Ergonomic Guidelines for Manual Material Handling the California Department of Industrial Relations [Online]. [cited 2007]; Available from: URL: http://www.dir.ca.gov/dosh/dosh_publications/mmh.pdf
10. Ciriello VM. The effects of box size, vertical distance, and height on lowering tasks. International Journal of Industrial Ergonomics 2001; 28(2): 61-7.
11. National Institute for Occupational Safety and Health. Work practices guide for manual load lifting. Cincinnati, OH: NIOSH; 1981.
12. Tiwari PS, Gite LP, Majumder J, Pharade SC, Singh VV. Push/pull strength of agricultural workers in central India. International Journal of Industrial Ergonomics 2010; 40(1): 1-7.
13. Snook SH. Psychophysical Tables: Lifting, Lowering, Pushing, Pulling, and Carrying. In: Stanton NA, Hedge A, Brookhuis K, Salas E, Hendrick HW, Editors. Handbook of Human Factors and Ergonomics Methods. New York, NY: CRC Press; 2004. p. 128-50.
14. Ciriello VM, Snook SH. Survey of manual handling tasks. International Journal of Industrial Ergonomics 1999; 23: 149-56.
15. Ciriello VM. The effects of box size, frequency and extended horizontal reach on maximum acceptable weights of lifting. International Journal of Industrial Ergonomics 2003; 32(2): 115-20.
16. Ciriello VM. The effects of box size, vertical distance, and height on lowering tasks for female industrial workers. International Journal of Industrial Ergonomics 2005; 35(9): 857-63.
17. Ciriello VM. The effects of container size, frequency and extended horizontal reach on maximum acceptable weights of lifting for female industrial workers. Appl Ergon 2007; 38(1): 1-5.
18. Ciriello VM, Snook SH. A study of size, distance, height, and frequency effects on manual handling tasks. The Journal of the Human Factors and Ergonomics Society 1983; 25(5): 473-83.
19. Gallagher S, Kotowski S, Davis KG, Mark C, Compton CS, Huston RL, et al. External L5-S1 Joint Moments When Lifting Wire Mesh Screen Used to Prevent Rock Falls in Underground Mines. Int J Ind Ergon 2009; 39(5): 828-34.
20. Kuorinka I, Jonsson B, Kilbom A, Vinterberg H, Biering-Sorensen F, Andersson G, et al. Standardised Nordic questionnaires for the analysis of musculoskeletal symptoms. Appl Ergon 1987; 18(3): 233-7.
21. Armstrong TJ, Marshall MM, Martin BJ, Foulke JA, Grieshaber DC, Malone G. Exposure To forceful exertions and vibration in a foundry. International Journal of Industrial Ergonomics 2002; 30(3): 163-79.
22. Faghih M, Motamedzadeh M, Mohammadi H, Habibi Mohraz M, Bayat H, Arassi M, et al. Assessment of Manual Material Handling by Snook tables in Hamadan casting manufactories. Iran Occup Health 2013; 10(1): 60-9. [In Persian].

JAEHR Journal of Advances in Environmental Health Research

Determining suitable model for zoning drinking water distribution network based on corrosion potential in Sanandaj City, Iran

Parvin Dehghani[1], Behzad Shahmoradi[1], Ata Amini[2], Mohammad Sedigh Sabeti[3]

1 Kurdistan Environmental Health Research Center, Kurdistan University of Medical Sciences Sanandaj, Iran
2 Agricultural and Natural Resources Research Center of Kurdistan, Sanandaj, Iran
3 Department of Civil Engineering, School of Technology, Islamic Azad University, Sanandaj Branch, Sanandaj, Iran

Original Article

Abstract

Corrosion in general is a complex interaction between water and metal surfaces and materials in which the water is stored or transported. Water quality monitoring in terms of corrosion and scaling is crucial, and a key element of preventive maintenance, given the economic and health hurts caused by corrosion and scaling in water utilities. The aim of this study is to determine the best model for zoning and interpolation corrosive potential of water distribution networks. For this purpose, 61 points of Sanandaj, Iran, distribution network were sampled and using Langelier indices, we investigated corrosivity potential of drinking water. Then, we used geostatistical methods such as ordinary kriging (OK), global polynomial interpolation, local polynomial interpolation, radius-based function, and inverse distance weighted for interpolation, zoning and quality mapping. Variogram analysis of variables was performed to select appropriate models. The results of the calculation of the Langelier index represented scaling potential of drinking water. Suitable model for fitness on exponential variogram was selected based on less (residual sums of squares) and high (R^2) value. Moreover, the best method for interpolation was selected using the mean error and root mean square error. Comparison of the results indicated that OK was the most suitable method for drinking water quality zoning.

KEYWORDS: Water Quality, Inverse Distance weighted, Kriging, Radius-Based Function, Zoning, Interpolation, Corrosivity, Sanandaj

Date of submission: *27 Oct 2013*, ***Date of acceptance:*** *13 Jan 2014*

Citation: Dehghani P, Shahmoradi B, Amini A, Sabeti MS. **Determining suitable model for zoning drinking water distribution network based on corrosion potential in Sanandaj City, Iran.** J Adv Environ Health Res 2014; 2(2): 72-80.

Introduction

Drinking water must be void of any mixtures that may be harmful to human health. Most of the developing countries suffer from hygienic problems resulting from lack of drinking water and absence good quality and microbiological contamination.[1] It is estimated that approximately 5 million children die annually due to inappropriate drinking water quality.[2]

One of the qualitative parameters in water distribution network is corrosion. Corrosion is one of the most complicated and costly problems facing drinking water utilities.[3] Corrosion can affect public health, public acceptance of water supply and the cost of providing safe drinking water. Corrosion in drinking water distribution system causes lots of hygienic and economic problems, for instance, internal corrosion causes pipe fractures, overflowing, pipe obstruction, quality change and odor, color and taste production. Rapid urban development brings

Corresponding Author:
Behzad Shahmoradi
Email: bshahmorady@gmail.com

about more demand and vaster development of water network system. More complexity of the water network, the more data processing. For data processing and management, systems with easier access and faster functioning are needed.[4] Determining optimized zoning method and quality model of drinking water can be a fundamental step in quality data management of water in the district. Geographical information systems (GIS) have effective usage in managing geo-spatial information and qualitative and quantitative information.[5] In such a situation, the interpolation of data points is the most suitable option that can handle the spatial characteristics.[6] Spatial interpolation models include geographical location of sample data points.[7] Some spatial interpolation models for creating qualitative model of drinking water include distance-reverse weighting inverse distance weighted (IDW), spline, Kriging and polynomial interpolation, among which ordinary Kriging (OK) and IDW are widely used.[8] Earls and Dixon compared interpolation models for IDW spline and data rainfall spatial Kriging using ArcGIS software (version 9.3, Esri, Redlands, CA, USA). She found that Kriging models (Kriging-exponential) produce better results than IDW and spline models.[9] Naoum and Tsanis rated spatial interpolation according to the decision-making systems based on GIS. They found that OK (Kriging-exponential) produce reliable estimates.[10] Evaluating geostatistical methods like Kriging, radius-based function (RBF), local estimating, and global estimating, Shaabani found that Kriging models are better tools to analyze salinity and nitrate of underground water due to their lower root mean square error (RMSE) and higher R2.[11] Taghizadeh Mehrjardi et al. studied spatial evaluation of qualitative parameters of underground water like TDS, TH, EC, SAR, SQ_4, Cl^- according to IDW, Kriging and co-Kriging models; their results show that Kriging model is better based on RMES criterion.[12] Kriging modeling nitrate pollution of underground water resulting from agricultural activities, Piccini et al. showed that it is a suitable method for identifying vulnerable areas from nitrate perspective.[13] The same findings were reported by other researchers.[14-17] Ghaneian et al. investigated corrosion and precipitation potential in Dual water distribution system in Kharanagh District of Yazd Province and determined that water had precipitative quality.[18] Dehghani et al. used Langelier saturation index (LSI) for corrosion zoning of water distribution system in Shiraz, Iran. Regular monitoring and analyzing water samples, they found that scaling potential in water samples was high.[19] The aim of the present study is to zone the corrosion potential of drinking water distribution network of Sanandaj, Iran, using LSI and the most appropriate interpolation and variogram models in GIS.

Materials and Methods

Sanandaj, the capital of Kurdistan province, covering an area of 3688.8 ha is located in the western part of Iran and the southern part of the province. Its geographical coordination is latitude N 14 35´ and longitude E 46 (Figure 1). Its height differs from 1450 to 1538 m above sea level. It is also located in the mountainous region of Zagros and has cold and semi-arid weather. Its average temperature is 15.20, 25.20, 10.40, and 1.60 °C in spring, summer, autumn, and winter respectively. The maximum temperature in July is 44 and the minimum temperature in February is −13.5 °C.

In this study, we collected water samples randomly from 61 points of the drinking water distribution network of Sanandaj. Latitude and longitude of the samples location was recorded via GPS. Each water sample was tested for corrosion perspective according to the standard methods for water and wastewater examination.[20] LSI was used to determine the corrosion potential of drinking water. It is based on pH of the water sample.[21]

LSI was determined using Equation. 1.

$$LSI=pH-pH_s \quad (1)$$

Where, pH is the pH of water sample and pHs is pH at $CaCO_3$ saturation determined using

Equation. 2.

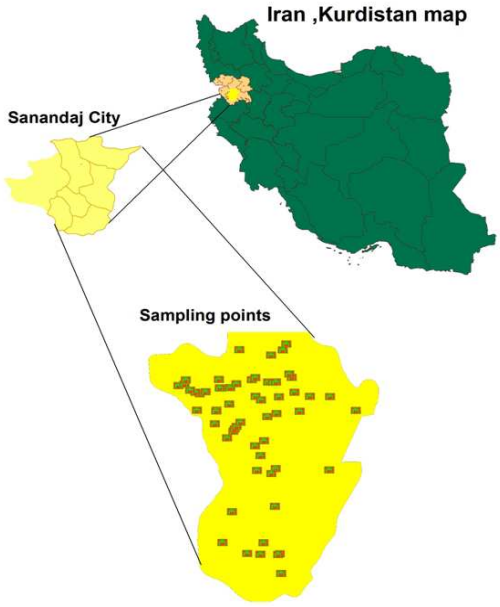

Figure 1. Location and sampling points of study area

$$pHs = (9.3+A+B)-(C+D) \quad (2)$$

Where, A = (Log10 [TDS]-1)/10 = 0.15;

B = −13.12 × Log10 (°C + 273) + 34.55 = 2.09 at 25° C and 1.09 at 82° C;

C = Log10 (Ca^{2+} as $CaCO_3$)−0.4 = 1.78, (Ca^{2+} as $CaCO_3$ is also called calcium hardness and is calculated as = 2.5(Ca^{2+});

D = Log10 (alkalinity as $CaCO_3$) = 1.53

For LSI > 0, water is supersaturated and tends to precipitate a scale layer of $CaCO_3$, whereas, for LSI = 0, water is saturated (in equilibrium) with $CaCO_3$. A scale layer of $CaCO_3$ is neither precipitated nor dissolved. For LSI < 0, water is under saturated and tends to dissolve solid $CaCO_3$.

If the actual pH of the water is below the calculated saturation pH, the LSI is negative, and the water has a very limited scaling potential. If the actual pH exceeds PH_S, the LSI is positive and being supersaturated with $CaCO_3$, the water has a tendency to form scale. At increasing positive index values, the scaling potential increases. In practice, water with an LSI between −0.5 and +0.5 will not display enhanced mineral dissolving or scale forming properties. Water with an LSI below −0.5 tends to exhibit noticeably increased dissolving abilities while water with an LSI above +0.5 tends to exhibit noticeably increased scale forming properties.

Data were analyzed according to descriptive statistics. Average, variance, standard deviation, maximum and minimum, skewness and kurtosis were calculated using SPSS for Windows (version 16.0, SPSS Inc., Chicago, IL, USA). Among various deterministic interpolation techniques OK, global polynomial interpolation (GPI), LPI, RBF and IDW were used for determining the best interpolation method. For this reason, Arc GIS 9.3 and GS+ (version 5.1, Gamma Design Software, Plainwell, MI, USA) were used. Full explanation of geostatistical methods could be found in the literature.[11,12,17,22-24] In general, geostatistical analyzing is based on this theory that measuring with smaller distances is more likely to be similar that with more distances (this means that the local coefficient exists). This theory can be verified using semivariogram examination that is an appropriate tool for measuring the coefficient among samples. Semivariogram is calculated using Eq. 3.[25,26]

$$\gamma(h)=\frac{1}{2N(h)}\sum_{i=1}^{N(h)}[Z(x_i)-Z(x_i+h)]^2 \quad (3)$$

Where, N (h) is the number of observation pairs separated by distance h, Z (x_i) is the value of the variable Z at the x_i location and (x_i + h) is the value of the variable Z at x_i + h location. Therefore, a graph is created for each variable that variance between points showed that during the modeling process of a semivariogram, the suggestions for cross-validation model are considered as a function of distance. In cross-validation method, an observational point is eliminated in each stage, and it is estimated based on other observational points. There would be a point estimated for each observational point. This method was used for verification. Variogram is composed of Nugget effect (C_0), sill (C + C_0) and range effect (A_0). The semivariogram value for h = 0 is called Nugget effect that is generally a result of the error in

sample-taking or data analyzing. By the increase of h, the semivariogram modifies increases till it reaches a specific value. Then, it becomes constant. This distance is called the Range effect, and the value of the constant semivariogram modify is called the sill that is the spatial variance of the being studied variable. The experimental semivariogram γ (h) is fitted to a theoretical model such as linear to sill, gaussian, spherical, linear and exponential. Cross-validation was conducted in order to verify the accuracy and precision of the process. The model with the highest R^2 and the lowest residual sums of squares (RSS) was selected. Nugget/sill in geostatistics can be considered as a criterion for spatial dependence. OK, GPI, local polynomial interpolation (LPI), RBF, and IDW were used for interpolation and predicting variance error of the non-sampling place.

Finally, we evaluated the model function in cross-validation using below criterion. For determining the best interpolation method, three criteria of RMSE, mean error (ME) and %RMSE were used that are computed using Eq. 4-6.[17]

$$RMSE = \sqrt{\frac{\left[\sum_{i=1}^{n}\left(Z(x_i) - Z^*(x_i)\right)^2\right]}{n}} \quad (4)$$

$$ME = \sum_{i=1}^{n} \frac{Zx_i - Z^*x_i}{n} \quad (5)$$

$$\%RMSE = (RMSE/\bar{X})100 \quad (6)$$

Where, n = number of observations or samples; $Z^*(x_i)$ = observed values; $Z(x_i)$ = predicted or estimated values, $\bar{X}$ = mean of measured parameter; and ME is the ME indication bias. Positive values of ME show values more than real and negative values show estimates less than real. The more ME is smaller, the less the interpolation is skewed. RMSE values in the optimized state (the state in which the estimated and measured values are equal) is zero. The more RMSE is smaller, the more the estimating of interpolation method is accurate.[27] RMSE is sensitive to wide values. Therefore, RMSE% can be used. This criterion being small is a reason for more accurate estimates, i.e., less difference between the real and estimated values. The accepted %RMSE value is 40 and values more than 70 show imprecision in the estimated points and high difference between the real and estimated values.[28]

Results and Discussion

A result relating to data's being normal after normalizing the data, we examined it using statistical Kolmogorov-Smirnov test in SPSS 16 software. Table 1 presents a statistical summary of the corrosion situation of the drinking water distribution network of Sanandaj. The data were distributed normally according to the Kolmogorov-Smirnov test, skewness, and histogram (Figure 2). Data normalization is a criterion only for Kriging methods.

Analysis of LSI variogram

GS+ software was used to create a semi-variogram for each variant and choosing the best theoretical corrosion model. Variogram is a useful plot by which many information could be extracted including data spatial structures, radius correlations of variants, static examination of data, and variant isotropic. Less RSS and more R^2 were used for fitting the best model on the variogram and stronger spatial structure. Nugget/sill (C_0/C_0+C) ratio in the geostatistics can be regarded as a criterion to classify the spatial dependence of quality parameters of water. If this ratio is < 25%, the

Table 1. Results of statistical analysis on Langelier saturation index

N	Minimum	Maximum	Mean	Std.	Skewness	Kurtosis
62	–0.51	1.21	0.1876	0.26415	0.541	2.820

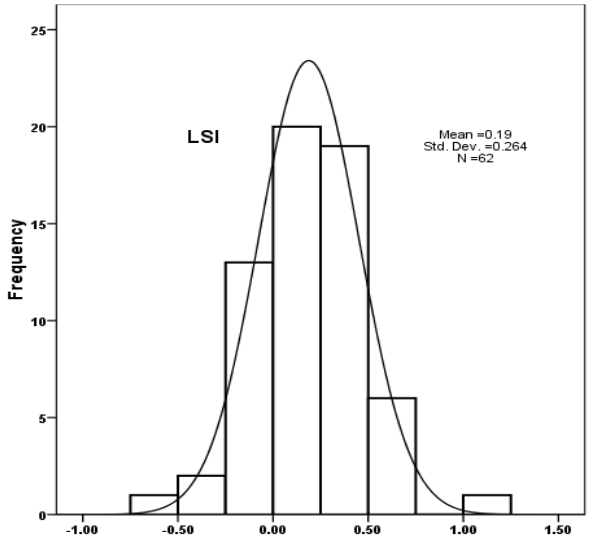

Figure 2. Data histogram of Langelier saturation index

variant owns strong spatial correlations. If the ratio is between 25% and 75% the spatial correlations is medium. And if the ratio is more than 75% the spatial correlations are weak.[25] Figure 3 shows the variogram of the measured Langelier indices. Moreover, table 2 tabulates the results of the best models of exponential, linear, spherical and Gaussian linear to sill variants for the measured indices. Nugget /Sill ratio is between 0.4 and 0.7 indicating medium spatial coefficient. Based on the criteria of higher R^2 and less RSS, exponential variogram is the best-fitted model. It has the strongest spatial correlations and Gaussian has the weakest.[10,11,15] This model was also used to describe the spatial changes.

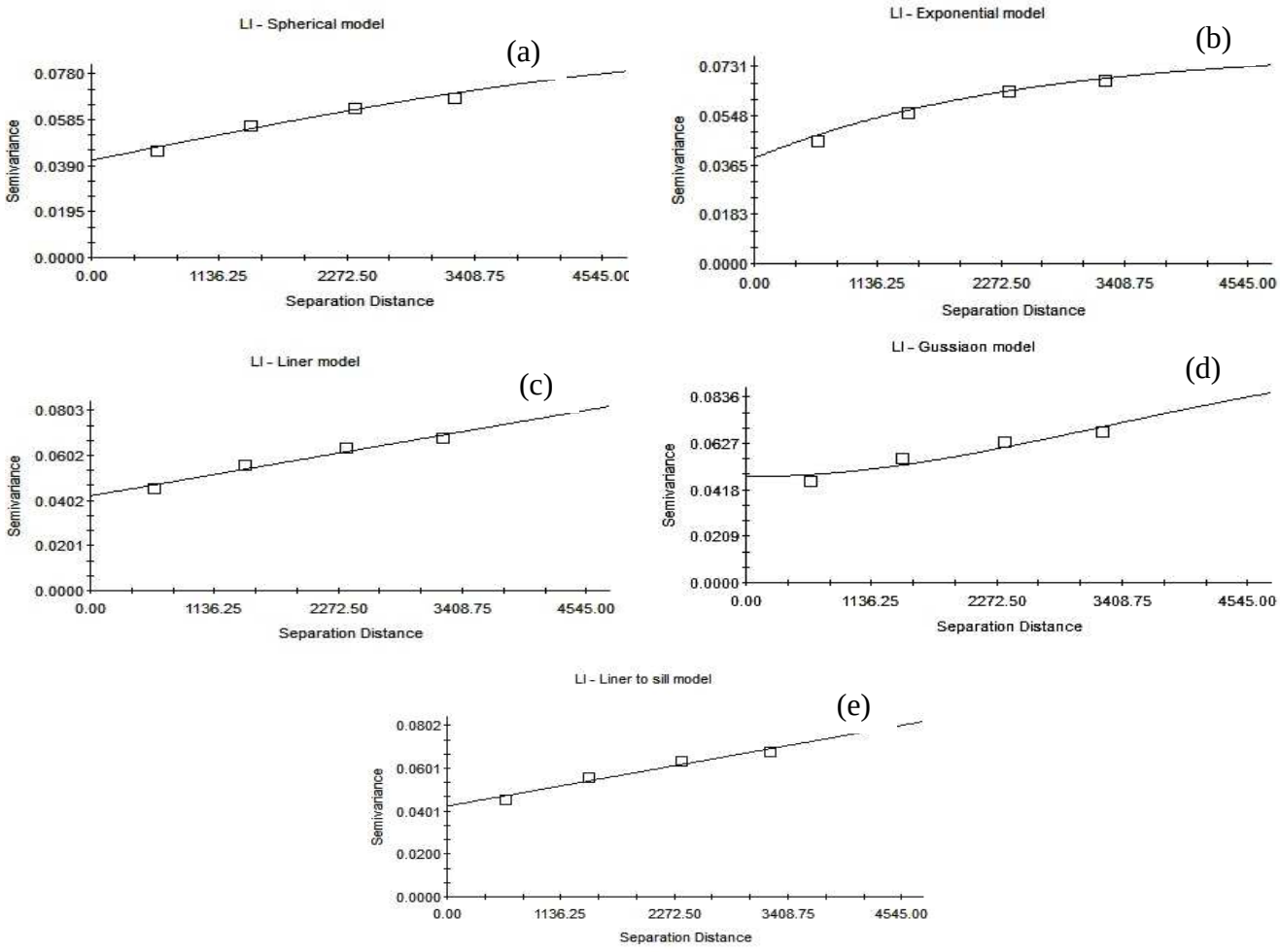

Figure 3. Fitted variogram models of Langelier saturation index (a) spherical, (b) exponential, (c) linear, (d) Gaussian, (e) linear to sill

Table 2. Best-fitted variogram models of Langelier saturation index

Model	Nugget	Sill	Range	Effective	Proportion	R^2	RSS
	C_0	$C_0 + C$	Parameter A_0	Range A_1	$C_0/(C_0 + C)$		
Spherical	0.04130	0.08370	6642	6642	0.507	0.974	8.47E-06
Spherical	0.03900	0.07910	2397	7191	0.507	0.998	7.72E-06
Linear	0.04221	0.06934	3234.4388	3234.4388	0.3910	0.961	1.301E-03
Linear to sill	0.04240	0.11800	9099	13130	0.641	0.961	1.13E-04
Gaussion	0.04770	0.10540	4608	7981.2901	0.547	0.890	3.18E-04

C_0: Nugget effect; $C + C_0$: Sill; A_0: Range effect; R^2: Regression coefficient; RSS: Residual sums of squares

Comparison of geostatistical methods

For determining the best interpolation method between the methods of geostatistical OK, GPI, LPI, RBF, IDW criteria of RMSE, ME, and %RMSE were used. As table 3 indicates, the value of ME and %RMSE in OK is less than others. The value of < 15 for %RMSE shows very good accuracy of semi-variogram in estimations.[26] The OK model is the best for zoning. Zoning results of this paper is consistent to those of Naoum and Tsanis,[10] Earls and Dixon,[9] and Goovaerts.[29] Langlier saturation index zoning is shown by OK, GPI, LPI, RBF, and IDW maps (Figure 4). Langlier index has more sediment potential in North West, South East and central parts. Sediment is not balanced. It is strong in some parts and weak in other parts. Compared with North West and South East parts, central parts have weak sediment potential. Few parts of North East, South West and West have weak corrosion potential.

Conclusion

Deterioration of materials resulting from corrosion can necessitate a colossal annual expenditure of scarce resources for repairs replacement and maintenance of distribution system. Given results obtained of drinking water in the Sanandaj distribution network has the scale formation potential. OK estimates with an exponential variogram based on RMSE and ME criteria is the most suitable technique for mapping quality spatial changes of LSI and assess the probability of exceeding the critical threshold. The advantage of kriging compared with other methods is that kriging produces better estimates than the other methods because the method takes explicit account of the effects

Table 3. Selection of the most suitable model for evaluation on variogram

ME	RMSE%	RMSE	Interpolation method
−0.001379	14.4	0.2791	Kriging_Ordinary_Exponentil
−0.003198	14.40	0.2737	Kriging_Ordinary_Spherical
−0.003374	14.30	0.2731	Kriging_Ordinary_Circular
−0.005531	14.20	0.2709	Kriging_Ordinary_Gaussian
−0.002824	14.40	0.2749	Kriging_Ordinary_pentaspherical
−0.003012	14.40	0.2743	Kriging_Ordinary_Tetraspherical
−0.002181	14.51	0.2757	Kriging_Ordinary_Rational Quadratice
−0.005879	14.20	0.2705	Kriging_Ordinary_Hole Effect
−0.00555	14.24	0.2707	Kriging_Ordinary_K-Bessel
−0.005499	14.25	0.2709	Kriging_Ordinary_J-Bessel
−0.005572	14.25	0.2708	Kriging_Ordinary_Stable
−0.0004534	14.74	0.2802	GPI
−0.0008811	15.20	0.2888	LPI
0.01493	15.54	0.2953	IDW
0.005173	14.60	0.2775	RBF

ME: Mean error; GBI: Global polynomial interpolation; LPI: Local polynomial interpolation; RBF: Radius-based function; IDW: Inverse distance weighted; RMSE: Root mean square error

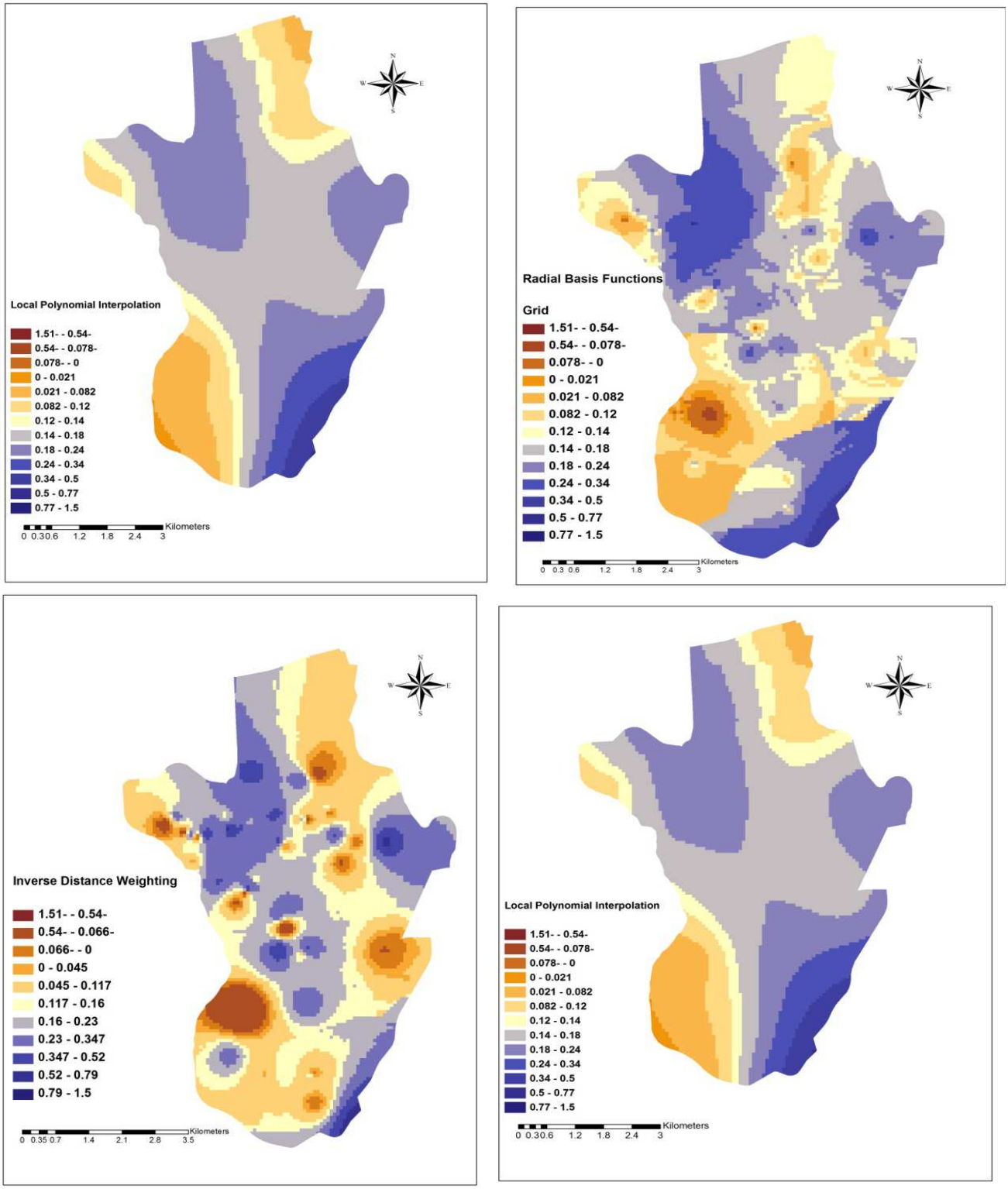

Figure 4. Spatial variations maps of Langelier saturation index by interpolation methods of OK, GPI, LPI, RBF, and IDW
Ok: Ordinary kriging; GPI: Global polynomial interpolation; LPI: Local polynomial interpolation; RBF: Radius-based function; IDW: Inverse distance weighted

of random noise and identifies the optimal interpolation weights and searches radius and provides an indication of the reliability of the estimates. Kriging analysis leads to an increased understanding of the data sets obtained for the fouling potential. The accuracy of the kriging map not only depends on the variogram and the maximum number of samples or neighboring points in kriging, but also depends on the number of classes and class boundaries. LSI calculations and plotted zoning maps revealed that the chemical quality of drinking water distribution network in Sanandaj City is imbalanced; hence, causing scale formation in water distribution network systems, and other facilities are unavoidable. Moreover, health and economic outcomes, consumers dissatisfaction due to quality changes, loss of water pressure in the distribution network are another potential drawbacks of this issue. Finally, it is suggested that the concerned authorities take crucial and required measures to make the water more stabilized from the corrosion point of view before delivering it to the customers. Moreover, analyzing other physicochemical parameters is essential in giving better figure of the water quality in the studied area.

Conflict of Interests

Authors have no conflict of interests.

Acknowledgements

The authors would like to thank Deputy of Research, Kurdistan University of Medical Sciences, Sanandaj, Iran for financial supporting this research work. The results presented in this paper is a part of M. Tech Dissertation of the first author.

References

1. van Leeuwen FX. Safe drinking water: the toxicologist's approach. Food Chem Toxicol 2000; 38(1 Suppl): S51-S58.
2. Wadud A, Chouduri AU. Microbial safety assessment of municipal water and incidence of multi-drug resistant Proteus isolates in Rajshahi, Bangladesh. Current Research in Microbiology and Biotechnology 2013; 1(4): 189-95.
3. Sander A, Berghult B, Ahlberg E, Broo AE, Johansson EL, Hedberg T. Iron corrosion in drinking water distribution systems-Surface complexation aspects. Corrosion Science 1997; 39(1): 77-93.
4. Dawoud MA, Darwish MM, El-Kady MM. GIS-Based Groundwater Management Model for Western Nile Delta. Water Resour Manage 2005; 19(5): 585-604.
5. Tabesh M, Saber H. A Prioritization Model for Rehabilitation of Water Distribution Networks Using GIS. Water Resour Manage 2012; 26(1): 225-41.
6. Cressie N, Wikle CK. Statistics for Spatio-Temporal Data. New Jersey, NJ: John Wiley & Sons; 2011.
7. Maselli F, Chiesi M. Evaluation of statistical methods to estimate forest volume in a mediterranean region. Geoscience and Remote Sensing 2006; 44(8): 2239-50.
8. Zimmerman D, Pavlik C, Ruggles A, Armstrong M. An Experimental Comparison of Ordinary and Universal Kriging and Inverse Distance Weighting. Mathematical Geology 1999; 31(4): 375-90.
9. Earls J, Dixon B. Spatial interpolation of rainfall data using ArcGIS: A comparative study. Proceedings of the 27th Annual ESRI International User Conference; 2007 Jun 18-22; San Diego, CA.
10. Naoum S, Tsanis K. Ranking spatial interpolation techniques using a GIS-based DSS. Global Nest: the Int J 2004; 6(1): 1-20.
11. Shaabani M. Evaluation Geostatistical methods for mapping of groundwater quality and their zoning Case Study: Neyriz Plain, Fars Province. Journal of Natural Geography Lar 2011; 4(13): 93-6. [In Persian].
12. Taghizadeh Mehrjardi R, Mahmoodi Sh, Heidari A, Sarmadian F. Application of geostastical methods for mapping groundwater quality in Azarbayjan Province, Iran. Am Eurasian J Agric Environ Sci 2008; 3: 726-35.
13. Piccini C, Marchetti A, Farina R, Francaviglia R. Application of Indicator kriging to Evaluate the Probability of Exceeding Nitrate Contamination Thresholds. International Journal of Environmental Research 2012; 6(4): 853.
14. Hooshmand A, Delghandi M, Izadi A, Aali A. Application of kriging and cokriging in spatial estimation of groundwater quality parameters. African Journal of Agricultural Research 2011; 6(14): 3402-8.
15. Maqami Y, Ghazavi R, Abbasali V, Sharafi S. Evaluation of spatial interpolation methods for water quality zoning using GIS Case study, Abadeh Township. Geography and Environmental Planning 2011; 22(2): 171-82.
16. Al-Mashagbah A, Al-Adamat R, Salameh E. The use of Kriging Techniques with in GIS Environment to Investigate Groundwater Quality in the Amman-Zarqa

Basin/Jordan. Research Journal of Environmental and Earth Sciences 2012; 4(2): 177-85.
17. Li J, Heap AD. A review of comparative studies of spatial interpolation methods in environmental sciences: Performance and impact factors. Ecological Informatics 2011; 6(3-4): 228-41.
18. Ghaneian MT, Ehrampoush MH, Ghanizadeh GH, Amrollahi M. Survey of corrosion and precipitation potential in dual water distribution system in kharanagh district of yazd province. Toloo-E-Behdasht 2008; 7(3-4): 65-72.
19. Dehghani M, Tex F, Zamanian Z. Assessment of the potential of scale formation and corrosivity of tap water resources and the network distribution system in Shiraz, South Iran. Pak J Biol Sci 2010; 13(2): 88-92.
20. Clesceri LS, Eaton AD, Greenberg AE. Standard Methods for the Examination of Water and Wastewater. Washington, D.C: American Public Health Association; 1998.
21. Kumar P, Sanand VS, Santhosh Kumar N, Sreerama Murthy B. Assessment of water quality of thatipudi reservoir of vizianagaram district of andhra pradesh. Innovare Journal of Science 2013; 1(2): 20-4.
22. Samanta S, Pal D, Lohar D, Pal B. Interpolation of climate variables and temperature modeling. Theor Appl Climatol 2012; 107(1-2): 35-45.
23. Rawat KS, Mishra AK, Sehgal VK. Identification of Geospatial Variability of Flouride Contamination in Ground Water of Mathura District, Uttar Pradesh, India. Journal of Applied and Natural Science 2012; 4(1): 117-22.
24. Babak O, Deutsch C. Statistical approach to inverse distance interpolation. Stoch Environ Res Risk Assess 2009; 23(5): 543-53.
25. Shi J, Wang H, Xu J, Wu J, Liu X, Zhu H, et al. Spatial distribution of heavy metals in soils: a case study of Changxing, China. Environ Geol 2007; 52(1): 1-10.
26. Hengl T, Heuvelink GBM, Stein A. A generic framework for spatial prediction of soil variables based on regression-kriging. Geoderma 2004; 120(1-2): 75-93.
27. Mishra U, Lala R, Liuc D, Van Meirvenned M. Predicting the Spatial Variation of the Soil Organic Carbon Pool at a Regional Scale. Soil Science Society of America Journal 01/2010; 74(3) 2010; 74(3): 906-14.
28. Flipo N, Jeannee N, Poulin M, Even S, Ledoux E. Assessment of nitrate pollution in the Grand Morin aquifers (France): combined use of geostatistics and physically based modeling. Environ Pollut 2007; 146(1): 241-56.
29. Goovaerts P. Geostatistical approaches for incorporating elevation into the spatial interpolation of rainfall. Journal of Hydrology 2000; 228(1-2): 113-29.

JAEHR Journal of Advances in Environmental Health Research

Chemical composition of indoor ash residues

Rameshwari Verma[1], Khageshwar Singh-Patel[1], Santosh Kumar-Verma[1]

1 School of Studies in Chemistry, Pt. Ravishankar Shukla University, Raipur, Chhattisgarh, India

Original Article

Abstract

The ash content formed after burning of materials in indoor may be harmful to environment on dumping due to high ionic and metallic concentration. Therefore, the chemical composition of various indoor ash residues derived from burning of the biomass (BM), coal (C), cow dung (CD), incense (IS) and mosquito coil (MC) materials is described in this study. Three samples each of BM, coal, CD, IS and MC materials were burnt. The ash residues were collected and sieved out the particles of mesh size ≤ 0.1 mm size. The Cl^-, NO_3^-, SO_4^{2-}, Na^+, K^+, Mg^{2+}, Ca^{2+} content (n = 15) was ranged from 0.12-8.27, 0.01-0.64, 0.74-12.53, 0.06-4.47, 0.29-15.45, 0.30-2.51 and 0.68-19.05% with mean value of 1.81 ± 1.18, 0.10 ± 0.08, 3.31 ± 1.66, 1.05 ± 0.70, 4.92 ± 2.04, 1.27 ± 0.36 and 7.68 ± 2.94%, respectively. The composition of metals, that is, Fe, Cr, Mn, Ni, Cu, Zn and Pb (n = 15) was ranged from 1100-24,600, 12-211, 109-1102, 5-142, 21-145, 25-244 and 5-42 mg/kg with mean value of 95 ± 31, 474 ± 152, 43 ± 23, 75 ± 23, 107 ± 32 and 16 ± 6 mg/kg, respectively. The enrichment and fluxes of ions and metals of indoor ash residues are described.

KEYWORDS: Ash Residue, Biomass, Coal, Cow Dung, Incense, Ions, Metals, Mosquito Coil

Date of submission: 27 Oct 2013, ***Date of acceptance:*** *13 Jan 2014*

Citation: Verma R, Singh-Patel K, Kumar-Verma S. **Chemical composition of indoor ash residues.** J Adv Environ Health Res 2014; 2(2): 81-90.

Introduction

Indoor particulate matter (PM) air pollution is being several folds more dangerous than the outdoor particulate air pollution in developing countries like India due to widespread use of solid fuels [i.e., wood, charcoal, coal, cow dung (CD), crop residues, etc.] for purposes, that is, cooking, heating, etc., The combustion of these materials generates aerosol particles as well as high content of ash in the coarse (PM_{10}), fine ($PM_{2.5}$) and ultrafine ($PM_{0.1}$) mode having a very complex chemical composition with high potential environmental and health risks.[1] In the developing countries, that is, China, India and Sub-Saharan Africa, about 80% households still use solid fuels such as wood, coal, CD and crop residues as an energy source.[2] The incense (IS) and mosquito coil (MC) materials are used to fragrance and to repel mosquitoes in indoor environments, respectively. The particulate emitted during burning causes several health problems.[3,4]

Wood ash is formed after combustion of wood that can be related to coal ash, which is a fossilized wood.[5] The study reported that all the major compounds present in wood ash were present in coal ash.[6] The elements, that is, silica, Al, Ca, Fe, K, Mg, Na, P, Si, Ti, As, Ba, Cd, Co, Cr, Cu, Hg, Mn, Mo, Ni, Pb, Tl, V, Zn, etc. are main constituents of the ash.[7,8] The wood and coal ash components cause several environmental and health effects, that is, deposit formation, aerosol emissions, corrosion, disposal of ashes, increase in pH, ion composition on the surface of the vegetation and on the upper soil horizon, organ disease, cancer, respiratory illness, neurological

Corresponding Author:
Rameshwari Verma
Email: rbaghel9@gmail.com

damage, developmental problems, and even kill plants and animals, and etc.[9-11]

The composition of metals in some ash residues, that is, biomass (BM) and coal has already been reported.[12-22] However, as far as the authors are aware of, this is the first time that the ions and metal composition in BM and coal (C), CD, IS and mosquito coil (MC) ash residues derived from indoor burning is being studied in Raipur, Chhattisgarh, India. The obtained results may be used to predict the future health hazards.

Materials and Methods

Fifteen materials (i.e., three samples of each BM, coal, CD, IS and MC materials) were burnt over a clean granite sheet in an indoor environment, (a room of 0.5 × 0.5 m^2). The cold ash residue was collected in a polyethylene bag by using a plastic spoon. The ash samples were sieved to particles with mesh size ≤ 0.1 mm. They were dried for overnight at 60°C in an oven. A 5.0 g of ash samples were used for ions extraction with 50 ml of deionized water for overnight in a 250 ml plastic conical flask. The ash was extracted with aqua regia in closed plastic vessels in the microwave accelerated reaction system 5 microwave digestion system.[23] The extracted samples were used for the analysis of metals.

The Ion Chromatograph (DX120, Dionex, USA) equipped with anion separation column (AS9-HC, 250 × 4 mm), cation separation column (CS12A, 25 × 04 mm) and conductivity detector was used for analysis of the ions. The eluents, 9 mm Na_2CO_3 (1.4 ml/min) and 20 mm methanesulfonic (0.8 ml/min) were used for leaching of the anion and cation, respectively. Standards (AR, E. Merck) were used for preparation of the calibration curves to evaluate the soluble ion content in the samples. Blank and replicate analyses were performed for 10% of all samples according to standard operating procedures. Method detection limits (MDL) of ionic species (in µg/ml) were Cl^- (0.044), NO_3^- (0.077), SO_4^{2-} (0.046), Na^+ (0.091), K^+ (0.123), Mg^{2+} (0.007), Ca^{2+} (0.143). Laboratory blanks were used to assess contamination. The blank compositions of ionic species were less than corresponding MDLs. Compositions of non-detects were taken as zero. In this study, ND indicates that the value is below the level of detection limitation.

The Varian liberty AX sequential inductively coupled plasma-atomic emission spectroscopy and varian AA280FS atomic absorption spectrophotometer equipped VGA-77 (plasma flow: 15 l/min, an auxiliary flow: 1.5 l/min, power: 1 kw, PMT voltage: 650 V) were used for analysis of the metals in the indoor ash residues. The detection limit of the instrument was 2 µg/l with percentage recovery of 102.5 at 80 µg/l. The 5% HCl/0.5% HNO_3 solution served as both the blank solution and the rinse solution.

The weighted amount of materials, that is, BM, coal (C), CD, IS and MC were burnt over a clean granite sheet. After complete burning, the cold ash residues were collected and weighted out. The ash content of the materials was calculated. The composition of the ions and metals was determined by using appropriate techniques. The flux of the species was measured using the following equation:

Flux of chemical species in materials = (Composition in ash × Ash% in a given material)/100

Results and Discussion

Composition of ions and metals in indoor ash residues

The compositions of ions and metals in the ash residues are presented in tables 1 and 2. The Cl^-, NO_3^-, SO_4^{2-}, Na^+, K^+, Mg^{2+} and Ca^{2+} composition in the ash residues (n = 15) was ranged from 0.12-8.27, 0.01-0.64, 0.74-12.53, 0.06-4.47, 0.29-15.45, 0.30-2.51 and 0.68-19.05% with the mean values of 1.81 ± 1.18, 0.10 ± 0.08, 3.31 ± 1.66, 1.05 ± 0.70, 4.92 ± 2.04, 1.27 ±0.36 and 7.68 ± 2.94%, respectively. The ions, that is, Cl^-, Mg^{2+} and Ca^{2+} showed the highest composition in the BM ash residue, as they are inherently present in the BM. Whereas, the highest

Table 1. Composition of ions in indoor ash residues (%)

Samples	Cl^-	NO_3^-	SO_4^{2-}	Na^+	K^+	Mg^{2+}	Ca^{2+}
BM_1	1.70	0.03	2.44	2.34	6.09	2.09	13.96
BM_2	8.27	0.03	4.49	1.13	4.12	2.43	10.75
BM_3	6.14	0.04	5.95	1.43	7.63	1.12	12.32
C_1	0.26	0.07	0.74	0.06	0.32	0.30	0.68
C_2	0.31	0.08	0.89	0.07	0.38	0.36	0.82
C_3	0.29	0.09	0.78	0.06	0.29	0.34	0.78
CD_1	1.08	0.01	1.90	0.15	3.54	0.99	3.38
CD_2	1.40	0.01	2.47	0.20	4.60	1.29	4.39
CD_3	1.54	0.02	2.72	0.21	5.06	1.42	4.83
IS_1	0.25	0.10	1.05	0.12	2.90	1.90	19.05
IS_2	0.12	0.03	1.56	0.11	1.00	0.84	3.30
IS_3	0.54	0.04	12.53	0.51	15.45	0.79	10.84
MC_1	2.20	0.64	8.08	1.25	5.90	1.23	15.65
MC_2	2.04	0.17	2.18	4.47	7.76	2.51	7.25
MC_3	1.07	0.14	1.90	3.57	8.75	1.51	7.21

The experiment was performed 3 times and its results are presented in detail: 1; Experiment 1, 2; Experiment 2, 3; Experiment 3; BM: Biomass; C: Coal; CD: Cow dung; IS: Incense; MC: Mosquito coil

Table 2. Composition of metals in indoor ash residues (mg/kg)

Samples	Fe	Cr	Mn	Ni	Cu	Zn	Pb
BM_1	8600	177	365	18	144	244	11
BM_2	1100	12	145	85	24	98	5
BM_3	2600	42	522	33	145	144	19
C_1	2900	164	202	101	76	25	29
C_2	3500	191	240	118	91	29	35
C_3	3300	211	278	142	109	35	42
CD_1	15700	57	848	17	21	80	6
CD_2	20400	74	981	23	27	104	8
CD_3	22500	81	1102	25	30	108	9
IS_1	14100	50	109	5	50	48	8
IS_2	24600	51	562	26	29	72	10
IS_3	6300	91	288	15	64	156	16
MC_1	14600	37	445	23	59	118	33
MC_2	21200	96	476	11	133	170	10
MC_3	16800	85	552	9	119	177	5

The experiment was performed 3 times and its results are presented in detail: 1; Experiment 1, 2; Experiment 2, 3; Experiment 3; BM: Biomass; C: Coal; CD: Cow dung; IS: Incense; MC: Mosquito coil

composition for other three ions, that is, NO_3^-, Na^+ and K^+ was marked in the MC ash residue, may be due to addition of their salts as ingredients (Figure 1).

The mean composition of anions (i.e., Cl^-, NO_3^- and SO_4^{2-}) in the BM, C, CD, IS and MC was observed to be 1.20%, 3.73%, 5.43% and 6.48%, respectively. The lowest composition of the anions was seen in the coal ash residue, may be due to their removal from the coal by the weathering. Compared with cations, the composition of anions in the CD ash residue was reduced to half. High composition of anions was observed in three ash residues, that is, BM, IS and MC. The highest composition of Cl^- and SO_4^{2-} was marked in the BM ash residue. Whereas, the composition of Cl^- was remarkably suppressed in the IS ash residue. The highest composition of NO_3^- was marked in the MC ash residue, may be due to mixing of nitrate salt as ingredients in the MC during the preparation. The increased anionic composition in ash

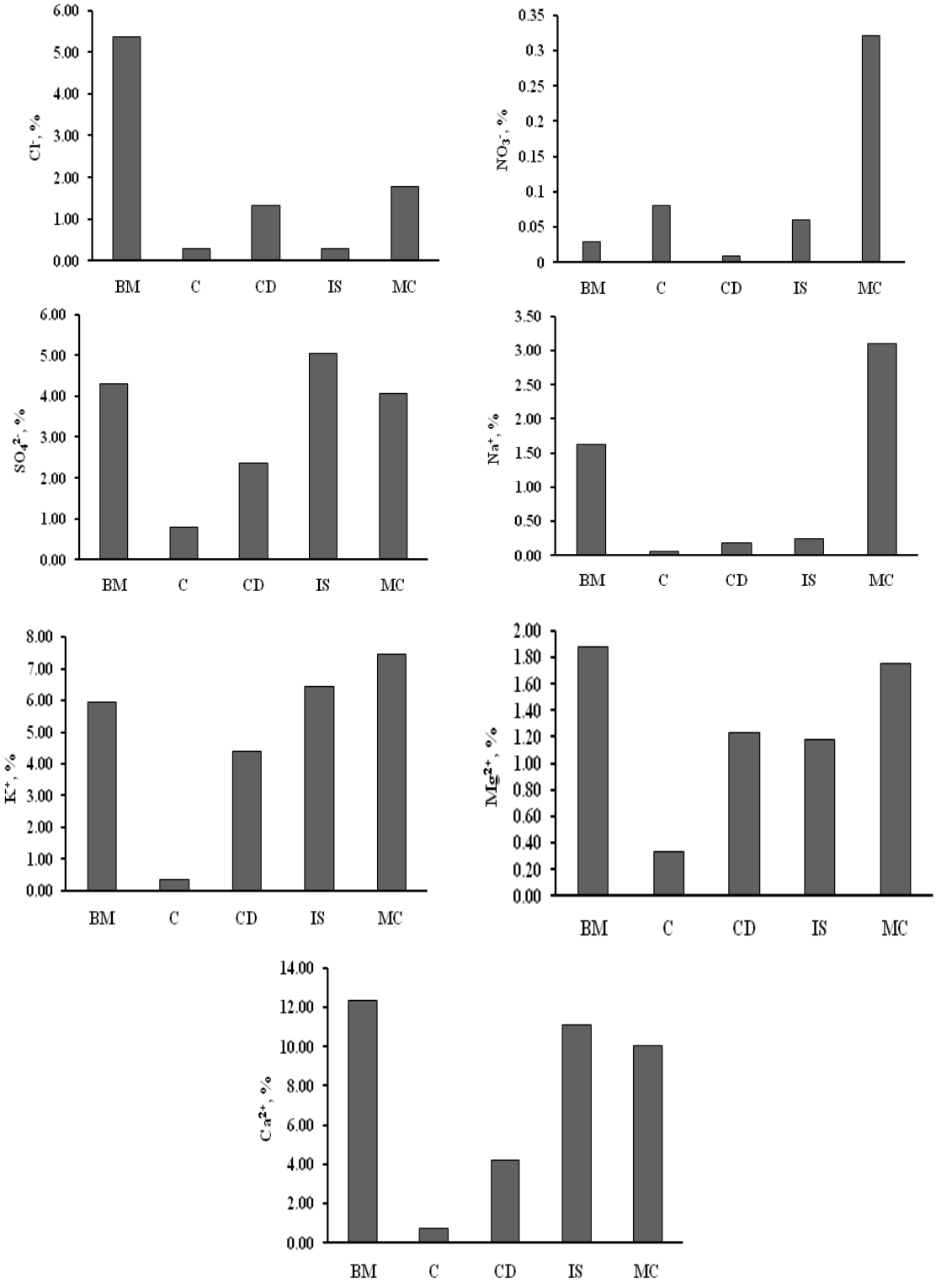

Figure 1. Mean composition of ions: Cl^-, NO_3^-, SO_4^{2-}, Na^+, K^+, Mg^{2+} and Ca^{2+} in ash residues, that is, biomass, coal, cow dung, incense and mosquito coil
BM: Biomass; C: Coal; CD: Cow dung; IS: Incense; MC: Mosquito coil

residues affects the soil fertility on their disposal in surface. Relatively higher composition of cations (i.e., Na^+, K^+, Mg^{2+} and Ca^{2+}) was observed in all ash residues, and their mean ranged from 1.48% to 22.36%. Their lowest composition was marked in the coal ash residue, may be due to their removal from the coal by the weathering. The composition of the cations in the CD ash residue was reduced at least 50% to the BM content, may be due to their sorption in the animal body from the raw food. The highest composition of the cations was observed in the BM and MC ash residues may be due to their accumulation from the soil or addition as ingredients.

The composition order of ions for the studied ash residues was as follows:

BM: $Ca^{2+} > K^+ > Cl^- > SO_4^{2-} > (Na^+, Mg^{2+}) > NO_3^-$; C (coal): $(SO_4^{2-}, Ca^{2+}) > (Cl^-, K^+, Mg^{2+}) > (NO_3^-, Na^+)$; CD: $K^+ > Ca^{2+} > SO_4^{2-} > Cl^- > Mg^{2+} > Na^+ > NO_3^-$; IS: $Ca^{2+} > K^+ > SO_4^{2-} > Mg^{2+} > Cl^- > Na^+ > NO_3^-$; and MC: $Ca^{2+} > K^+ > SO_4^{2-} > Na^+ > (Mg^{2+}, Cl^-) > NO_3^-$. Ca^{2+}, K^+ were the predominant ions in all ash residues, because plant is the base material for all of them. NO_3^- was marked as the ion with the lowest concentration in all ash residues. In general, potassium element is found as a tracer of BM burning.[24,25] However in this study, we have observed Ca^{2+} ion in a higher level. Campbell,[26] and Ohno and Susan Erich,[27] were also found calcium as the most abundant element had a mean of almost 20% of the ash. When compared to calcium, other nutrients in BM ash were about 4% potassium, and < 2% phosphorus, magnesium, aluminum and sodium. They found the mean value of elements in decreasing order as calcium, potassium, magnesium, sodium in wood ash. These mean values were from 12 different wood ashes, that is, six from Maine and six from other states. The limited composition of ions in ash residues make them useful for soil and human health.

Similarly, the composition (n = 15) of metal, that is, Fe, Cr, Mn, Ni, Cu, Zn and Pb was ranged from 1100 to 24600, 12-211, 109-1102, 5-142, 21-145, 25-244 and 5-42 mg/kg with mean value of 11880 ± 4177, 95 ± 31, 474 ± 152, 43 ± 23, 75 ± 23, 107 ± 32 and 16 ± 6 mg/kg, respectively. Among metals in indoor ash residues, iron showed strongly dominated in the all the ash residues. Whereas, Cu and Zn exhibited the highest composition in the BM ash residue, because they are micronutrients presented in plants. The increased composition of Cu and Zn has also been shown in wood and/or bark of young Norway spruce.[28] Other metals, that is, Cr, Ni and Pb showed the highest composition in the coal ash residue. These three metals are found to be harmful to plants as well as human beings. Nickel carcinogenicity has been reported in both animals and man. Increased values of Ni can cause alteration of the activity of some certain enzymes and also it can suppress immunity. Cr can be source of illnesses, that is, prolonged allergic dermatitis and potentially carcinogenicity. In general, Cr accumulates in the lung, kidney, liver, spleen. Ahigh level of Cr, therefore, causes serious some adverse effects in these organs, especially in lungs.[29,30] The increased level of Pb affects the nervous system, hemoglobin formation by interfering enzymatic activities and even every organ system. Thus, presence of such toxic metals in coal ash residue can cause harmful effect, when they mixed with air or disposed in the soil. The higher composition of Fe and Mn in the CD ash residue may be due to their lower sorption in the animal body from the raw food (Figure 2).

Enrichment of ions and metals

The BM and coal are natural solid fuel. The CD is a biodegraded fuel. Whereas, the IS MC are the synthetic fuming material. Upon burning, majority of volatile elements are emitted out, and the non-volatile elements remained in the ash residues. The enrichment of ions and metals was evaluated in the various ash residues with respect to the BM ash residue; the result shows the different level of metals due to different burning conditions (Table 3). The nitrate was strongly enriched (> 10-folds) in the MC ash residue with respect to the BM ash may be due to mixing of their salts as ingredients in the MC

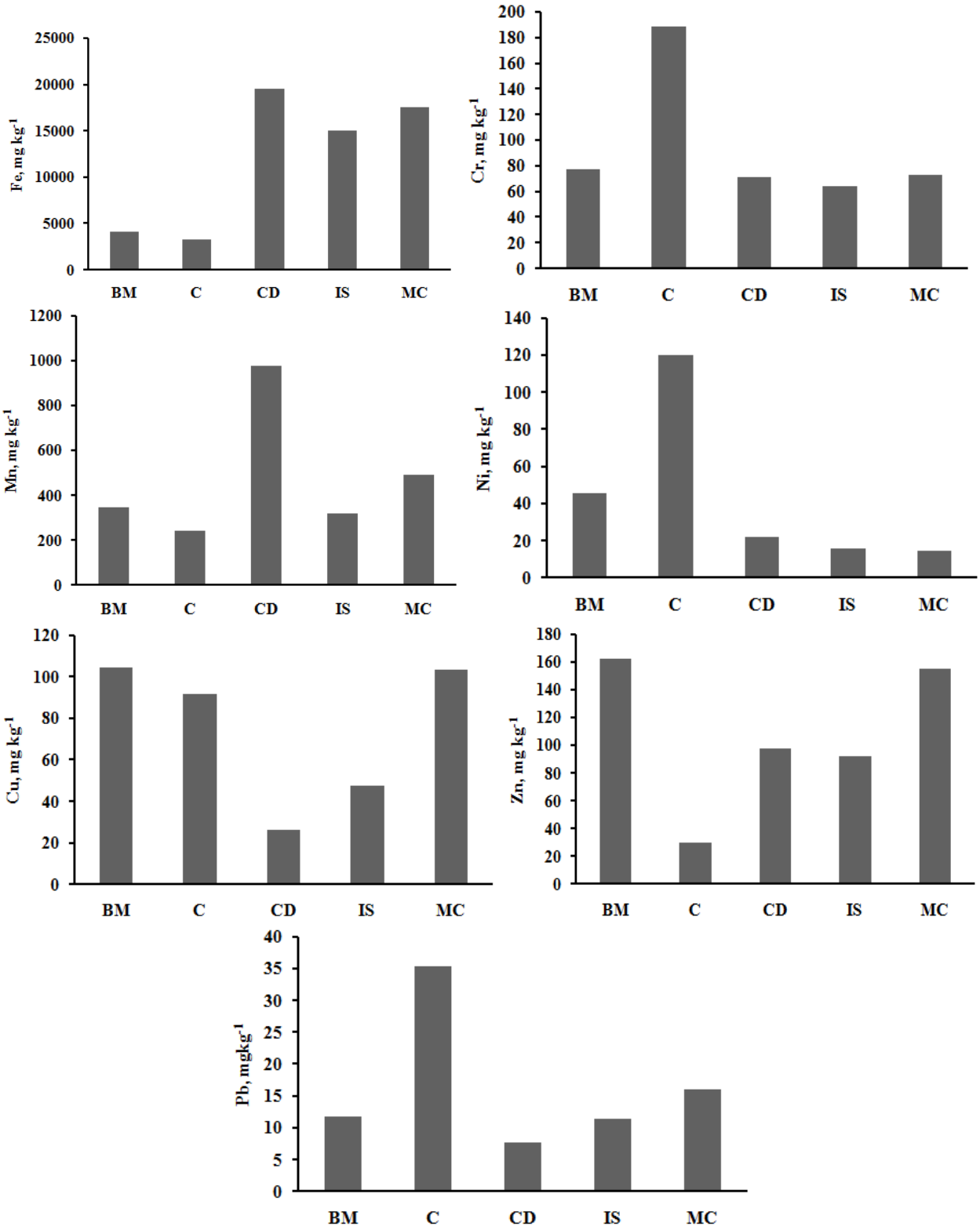

Figure 2. Mean composition of metals: Fe, Cr, Mn, Ni, Cu, Zn and Pb in ash residues, that is, biomass, coal, cow dung, incense and mosquito coil
BM: Biomass; C: Coal; CD: Cow dung; IS: Incense; MC: Mosquito coil

Table 3. Enrichment of ions and metals in the indoor ash residues with respect to the BM ash content

Ions	C	CD	IS	MC
F^-	1.10	0.60	0.70	13.70
Cl^-	0.10	0.30	0.10	0.30
NO_3^-	2.70	0.40	1.90	10.60
SO_4^{2-}	0.20	0.60	1.20	0.90
Na^+	0.00	0.10	0.20	1.90
K^+	0.10	0.70	1.10	1.30
Mg^{2+}	0.20	0.70	0.60	0.90
Ca^{2+}	0.10	0.30	0.90	0.80
Fe	0.80	4.80	3.70	4.30
Cr	2.50	0.90	0.80	0.90
Mn	0.70	2.80	0.90	1.40
Ni	2.70	0.50	0.30	0.30
Cu	0.90	0.30	0.50	1.00
Zn	0.20	0.60	0.60	1.00
Pb	2.90	0.60	0.90	1.30

BM: Biomass; C: Coal; CD: Cow dung; IS: Incense; MC: Mosquito coil

during the manufacturing time. Similarly, the higher level of Fe was found in CD, IS and MC. Whereas, the metal, that is, Cr, Ni, and Pb in coal and Cu and Zn in MC were marked in higher level. Similarly, existed Mn in CD and MC was higher than the other ash residues. The metals show no definite order in all ash residues.

Fluxes of ions and metals

The fluxes of the chemical species depend on two factors: their composition in the ash and ash percentage of the materials. The fluxes of ions and metals was evaluated in the materials that is, BM, C (coal), CD, IS and MC (Tables 4 and 5). Among five burnt materials, the CD produced the highest content of ash, 46.9%. Therefore, the highest fluxes of ions, that is, Cl^-, SO_4^{2-}, K^+, Mg^{2+}, Ca^{2+} and metals were observed with the CD. However, the highest fluxes of NO_3^- and Na^+ were marked with the MC ash residue.

Comparison of metals with other reported studies

As the best of our knowledge, the composition of metals in CD, IS and MC was not reported yet. The metal composition in wood and coal ash residues reported in different studies is summarized in table 6. The composition of metals, that is, Fe, Cr, Mn, Ni, Cu, Zn and Pb in the ash residues of the present work is found to be comparable with the previous reported wood and coal ash residues. Among all metals, in the present work, compared to other studies, higher composition of Fe and Mn in all ash residues was found.[12-14] In this study, the toxic metals, that is, Ni, Cr and Pb in coal ash residues were marked in higher level that is consistent with reported works.[16,18] Higher composition of toxic metals, in coal ash residue, make it more harmful for environment than the other tested ash residues. The Cu and Zn were found in higher level in BM.

Table 4. Fluxes of ions in indoor ash residues (g/kg)

Samples	Cl^-	NO_3^-	SO_4^{2-}	Na^+	K^+	Mg^{2+}	Ca^{2+}
BM_1	1.36	0.02	1.95	1.87	4.87	1.67	11.17
BM_2	4.14	0.02	2.25	0.57	2.06	1.22	5.38
BM_3	4.30	0.03	4.17	1.00	5.34	0.78	8.62
C_1	0.26	0.07	0.74	0.06	0.32	0.30	0.68
C_2	0.25	0.06	0.71	0.06	0.30	0.29	0.66
C_3	0.26	0.08	0.70	0.05	0.26	0.31	0.70
CD_1	5.62	0.05	9.88	0.78	18.41	5.15	17.58
CD_2	6.02	0.04	10.62	0.86	19.78	5.55	18.88
CD_3	7.08	0.09	12.51	0.97	23.28	6.53	22.22
IS_1	0.25	0.10	1.05	0.12	2.90	1.90	19.05
IS_2	0.06	0.02	0.78	0.06	0.50	0.42	1.65
IS_3	0.43	0.03	10.02	0.41	12.36	0.63	8.67
MC_1	1.98	0.58	7.27	1.13	5.31	1.11	14.09
MC_2	1.22	0.10	1.31	2.68	4.66	1.51	4.35
MC_3	0.86	0.11	1.52	2.86	7.00	1.21	5.77

The experiment was performed 3 times and its results are presented in detail: 1; Experiment 1, 2; Experiment 2, 3; Experiment 3; BM: Biomass; C: Coal; CD: Cow dung; IS: Incense; MC: Mosquito coil

Table 5. Fluxes of metals in indoor ash residues (mg/kg)

Samples	Fe	Cr	Mn	Ni	Cu	Zn	Pb*
BM_1	688	14	29	1	12	20	880
BM_2	55	1	7	4	1	5	250
BM_3	182	3	37	2	10	10	1330
C_1	290	16	20	10	8	3	2900
C_2	280	15	19	9	7	2	2800
C_3	297	19	25	13	10	3	3780
CD_1	8164	30	441	9	11	42	3120
CD_2	8772	32	422	10	12	45	3440
CD_3	10350	37	507	12	14	50	4140
IS_1	1410	5	11	1	5	5	800
IS_2	1230	3	28	1	1	4	500
IS_3	504	7	23	1	5	12	1280
MC_1	1314	3	40	2	5	11	2970
MC_2	1272	6	29	1	8	10	600
MC_3	1344	7	44	1	10	14	400

The experiment was performed 3 times and its results are presented in detail: 1; Experiment 1, 2; Experiment 2, 3; Experiment 3; * µg/kg, BM: Biomass; C: Coal; CD: Cow dung; IS: Incense; MC: Mosquito coil

Table 6. Comparison of metals in ash residues in various studies

S. No.	Ash type	Composition (mg/kg)							Reference
		Fe	Cr	Mn	Ni	Cu	Zn	Pb	
1	Wood	5000-20000	10-250	1000-30000	6-200	15-300	15-2200	15-650	12
2	Wood	2500	22	8200	18	108	675	32	13
3	Wood	3600	80	9000	38	184	935	45	14
4	Wood	-	-	-	-	84.8	3860	-	30
5	Coal	-	204.0-218.2	-	-	135.6-252.0	87.5-155.3	427.9-551.3	16
6	Coal	-	64	-	41	38	120	44	18
7	BM	1100-8600	12-177	145-522	18-85	24-145	98-244	5-19	
8	Coal	2900-3500	164-211	202-278	101-142	91-109	25-35	29-42	
9	CD	15700-22500	57-81	848-1102	17-25	21-30	80-108	6-9	Present work
10	IS	6300-24600	50-91	109-562	5-15	29-64	48-156	8-16	
11	MC	14600-21200	37-96	445-552	9-23	59-133	118-177	5-33	

BM: Biomass; C: Coal; CD: Cow dung; IS: Incense; MC: Mosquito coil

Conclusion

The highest composition of anions (i.e., Cl^-, NO_3^- and SO_4^{2-}) was observed in three ash residues, that is, BM, IS and MC, showing that their disposal can acidify the soil and affect its fertility, which is also harmful for human life. The MC ash residue was relatively enriched with a high content of NO_3^-, Na^+ and K^+ ions due to mixing of their salt (i.e., sodium benzoate and potassium nitrate) as an ingredient during making. The highest composition of cations (i.e., Na^+, K^+, Mg^{2+} and Ca^{2+}) was marked in BM and MC ash residues may be due to their accumulation from the soil and addition as ingredients, respectively.

Similarly, the high composition of toxic metal, that is, Ni, Cr and Pb was found in coal ash residue than others, showing higher toxicity of coal ash residue. The coal ash residue may harmful for living beings. Different orders of metal composition were marked in the ash residues. The highest fluxes were marked with CD, showing that it is also a major contributor of toxic metals and create harmful effect in plants and human beings.

Conflict of Interests

Authors have no conflict of interests.

Acknowledgements

I am thankful to Head of Department, School of Studies in Chemistry for providing lab facility.

References

1. Biedermann F, Obernberger I. Ash-related problems during biomass combustion and possibilities for a sustainable ash utilisation. Proceedings of the International Conference 'World Renewable Energy Congress' (WREC); 2005 May 22-27; Oxford, UK.
2. Smith KR. Indoor air pollution in developing countries: recommendations for research. Indoor Air 2002; 12(3): 198-207.
3. Ji X, Le BO, Ramalho O, Mandin C, D'Anna B, Martinon L, et al. Characterization of particles emitted by incense burning in an experimental house. Indoor Air 2010; 20(2): 147-58.
4. Liu W, Zhang J, Hashim JH, Jalaludin J, Hashim Z, Goldstein BD. Mosquito coil emissions and health implications. Environ Health Perspect 2003; 111(12): 1454-60.
5. American Coal Ash Association. Fly Ash Facts for Highway Engineers. Washington, DC: Federal Highway Administration; 2005.
6. Tarun RN, Rudolph NK, Rafat S. Use of Wood Ash in Cement-based Materials, A CBU report, CBU-2003-19 (REP-513). Proceedings of the 7th CANMET/ACI International Conference on Recent Advances in Concrete Technology; 2004 May 26-29; Las Vegas, NV.
7. Mandre M. Influence of wood ash on soil chemical composition and biochemical parameters of young Scots pine. Proceedings of the Estonian Academy of Sciences, Biology, Ecolog 2006; 55(2): 91-107.
8. Ugurlu A. Leaching characteristics of fly ash. Env Geol 2004; 46(6-7): 890-5.
9. Kellner O, Weibull H. Effects of wood ash on bryophytes and lichens in a Swedish pine forest. Scandinavian Journal of Forest Research 1998; (Supplement 2): 76-85.
10. U.S. Environmental Protection Agency, Office of Solid Waste and Emergency Response, Office of Resource Conservation and Recovery. Human and Ecological Risk Assessment of Coal Combustion Wastes. Washington, DC: Environmental Protection Agency; 2007.
11. Johnson TD. EPA considers proposals to regulate coal ash: Hundreds of coal ash dumps, waste ponds may threaten health. The Nation's Health 2010; 40(9): 1-14.
12. Augusto L, Bakker MR, Meredieu C. Wood ash applications to temperate forest ecosystems-potential benefits and drawbacks. Plant Soil 2008; 306(1-2): 181-98.
13. Sarenbo S. Wood ash dilemma-reduced quality due to poor combustion performance. Biomass and Bioenergy 2009; 33(9): 1212-20.
14. Holmberg SL, Lind BB, Claesson T. Chemical composition and leaching characteristics of granules made of wood ash and dolomite. Environmental Geology 2000; 40(1-2): 1-10.
15. Mahmoudkhani M, Richards T, Theliander H. Sustainable Use of Biofuel by Recycling Ash to Forests: Treatment of Biofuel Ash. Environ Sci Technol 2007; 41(11): 4118-23.
16. Gong X, Wu T, Qiao Y, Xu M. In Situ Leaching of Trace Elements in a Coal Ash Dump and Time Dependence Laboratory Evaluation. Energy & Fuels 2009; 24(1): 84-90.
17. Brake SS, Jensen RR, Mattox JM. Effects of coal fly ash amended soils on trace element uptake in plants. Env Geol 2004; 45(5): 680-9.
18. Smolka-Danielowska D. Heavy Metals in Fly Ash from a Coal-Fired Power Station in Poland. Polish J of Environ Stud 2006; 15(6): 943-6.
19. Abdullahi M. Characteristics of Wood. Ash/OPC Concrete. Leonardo Electr Journal Practices Technology (LEJPT) 2006; 5(8): 9-16.
20. Zhao Y, Zhang J, Tian C, Li H, Shao X, Zheng C. Mineralogy and Chemical Composition of High-Calcium Fly Ashes and Density Fractions from a Coal-Fired Power Plant in China. Energy Fuels 2010; 24(2): 834-43.
21. Rayzman VL, Shcherban SA, Dworkin RS. Technology for Chemical?Metallurgical Coal Ash Utilization. Energy Fuels 1997; 11(4): 761-73.
22. Capablo J, Jensen PA, Pedersen KH, Hjuler K, Nikolaisen L, Backman R, et al. Ash Properties of Alternative Biomass. Energy Fuels 2009; 23(4): 1965-76.
23. Murko S, Milacic R, Veber M, Scancar J. Determination of Cd, Pb and As in sediments of the Sava River by electrothermal atomic absorption spectrometry. Journal of the Serbian Chemical Society 2010; 75(1): 113-28.
24. Deshmukh DK, Tsai YI, Deb MK, Mkoma SL. Characterization of Dicarboxylates and Inorganic Ions in Urban PM10 Aerosols in the Eastern Central India. Aerosol and Air Quality Research 2012; 12(4): 592-607.
25. Deshmukh DK, Tsai YI, Deb MK, Zarmpas P. Characteristics and sources of water-soluble ionic species associated with PM10 particles in the ambient air of central India. Bull Environ Contam Toxicol 2012; 89(5): 1091-7.
26. Campbell AG. Recycling and disposing of wood ash. Tappi Journal 1990; 73: 141-6.
27. Ohno T, Susan Erich M. Effect of wood ash application on soil pH and soil test nutrient levels. Agriculture,

Ecosystems & Environment 1990; 32(3-4): 223-39.
28. Osteras AH, Greger M. Accumulation of, and interactions between, calcium and heavy metals in wood and bark of Picea abies. Journal of Plant Nutrition and Soil Science 2003; 166(2): 246-53.
29. Vardaki C, Kelepertsis A. Environmental impact of heavy metals (Fe, Ni, Cr, Co) in soils waters and plants of triada in euboea from ultrabasic rocks and nickeliferous mineralisation. Environmental Geochemistry and Health 1999; 21(3): 211-26.
30. Osteras AH, Sunnerdahl I, Greger M. The Impact of Wood Ash and Green Liquor Dregs Application on Ca, Cu, Zn and Cd Contents in Bark and Wood of Norway Spruce. Water, Air, and Soil Pollution 2005; 166(1-4): 17-29.

JAEHR Journal of Advances in Environmental Health Research

Removal of natural organic matter from aqueous solutions by electrocoagulation

Masoomeh Askari[1], Mahmood Alimohammadi[2], Mohammad Hadi Dehghani[2], Mohammad Mahdi Emamjomeh[3], Shahrokh Nazmara[2]

1 Department of Environmental Engineering, Graduate School of the Environment and Energy, Islamic Azad University, Science and Research Branch, Tehran, Iran
2 Department of Environmental Health Engineering, School of Public Health, Tehran University of Medical Sciences, Tehran, Iran
3 Department of Environmental Health, School of Health, Qazvin University of Medical Sciences, Qazvin, Iran

Original Article

Abstract

Natural organic matter (NOM) affects some qualitative parameters of water such as color. In addition, it can deteriorate the performance of water treatment process including coagulation, adsorption, and membranes. NOM also reacts with chlorine in the chlorination process and may form disinfection by-products. The present study was carried out in laboratory-scale in a batch system using a cylinder shape reactor with effective volume of 2 l. The initial NOM concentrations during the study period were 10, 25, and 50 mg/l. After specific time intervals, samples were taken from the reactor and filtered. Finally, the NOM removal according to total organic carbon (TOC) content of the samples that were analyzed with a TOC analyzer. The results showed that the highest NOM removal efficiency for three initial concentrations 10, 25, and 50 mg/l were 91, 94, and 82%, respectively. These removal efficiencies were obtained at pH 7, contact time of 20 min, and electrical current of 0.1 A. The electrical energy consumption was 0.08, 0.06, and 0.03 kWh/m^3, respectively. In this study, the application of electrocoagulation (EC) treatment method using combined Al and Fe electrode was examined to remove NOM from aqueous solution. Based on the obtained results, the EC can be used as an effective method for removing NOM from aqueous solution.

KEYWORDS: Electrocoagulation, Natural Organic Matter, Bipolar and Monopolar, Aluminum, Iron

Date of submission: *15 Oct 2013*, ***Date of acceptance:*** *18 Jan 2014*

Citation: Askari M, Alimohammadi M, Dehghani MH, Emamjomeh MM, Nazmara Sh. **Removal of natural organic matter from aqueous solutions by electrocoagulation.** J Adv Environ Health Res 2014; 2(2): 91-100.

Introduction

In recent decades, due to the sever pollution of water resources such as rivers, seas, and reservoirs by wastewater from domestic, industrial, and agricultural sources, the concentration of water contaminants has increased dramatically. Among water pollutants, organic pollutants are important due to their high quantities and ranges in water resources, an elevated concentration, specific properties, and incomplete removal by conventional water treatment plants.[1]

Natural organic matter (NOM) is a complex mixture of different organic compounds originating from both natural and anthropogenic sources and is present in all water bodies. Naturally available organic compounds provide the possibility of formation of new organic compounds in water treatment plant or distribution system due to their high reactivity.[2]

The presence of NOM not only affects some water quality parameters such as color,[3] but also interferes with the performance of treatment

Corresponding Author:
Mahmood Alimohammadi
Email: m_alimohammadi@tums.ac.ir

processes such as coagulation,[4] adsorption,[2] and membranes.[2,5] It also has negative effects on the distribution system.[6] In addition, if chlorine is used in the disinfection process, NOM reacts with chlorine and may form disinfection by-products.[7,8]

There are many methods such as chemical coagulation and sedimentation, oxidation, adsorption, ion exchange, and filtration using various membranes to remove NOM from aqueous environments.[9]

Electrocoagulation (EC) process is an environmentally-friendly method and in terms of operational cost, it can compete with other treatment methods. This method has some advantages: no need for chemicals addition;[10] requires simple equipment and less space for installation; simple operation;[11] faster and more effective separation of the pollutants than chemical coagulation; no need for pH adjustment; low retention time (high velocity for pollutants removal). Furthermore, it produces sludge with low water content in comparison with chemical coagulation,[12] and the produced sludge tends to settle easily. In addition, this process has lower effluent total dissolved solids compared with chemical treatment methods, and can remove the smallest colloidal particles.[13,14]

EC is based on the in situ formation of metallic hydroxides coagulants for removing of pollutants from aqueous medium. This can be achieved by establishing an electrical current between the electrodes. Subsequently, the sacrificial anode corrodes due to the applied current while the simultaneous evolution of hydrogen at the cathode allows for pollutant removal by flotation.[15]

Thus, in the present study, based on EC advantages, the application of an EC treatment technique using combined iron and aluminum electrodes was studied at laboratory scale to remove NOM compounds from the aqueous solutions.

Materials and Methods

In this experimental study, which was based on the treatment system setup, the performance of the EC for the removal of NOM from aqueous solution was investigated at laboratory scale in a batch system. The humic acid used in this study was purchased from across company, Germany, and used as a representative of NOM figure 1. The humic acid had a powdered appearance, and its composition was as humic acid salt 55%.

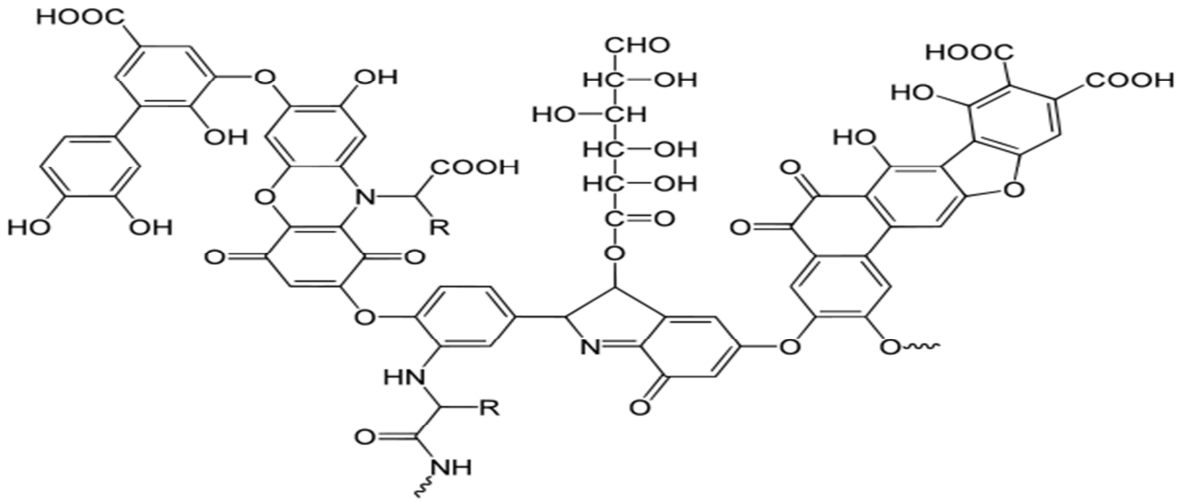

Figure 1. The proposed model for humic acid structure

1 N NaOH or 1 N HCl was used to adjust pH of the samples. The total organic carbon (TOC) of samples was measured before and after of each experimental run using a TOC analyzers of TOC-VCSH (Shimadzu, Japan). pH of The samples, and applied voltage and current were measure using a pH meter (Metrohm) and an ampere-meter (Sunwa), respectively.

In addition, electrical conductivity and turbidity of the samples were measured using a conductivity-meter and a turbidity-meter (HACH) before and after the EC treatment, respectively. A cylindrical shape reactor with effective volume of 2 lit was used to conduct the experiments. Four metal plates (2 anodes and 2 cathodes), which made of aluminum and iron were used as the electrodes. The dimensions of each electrode and the distance between the electrodes within the reactor were 110 × 110 mm and 0.5 cm, respectively.

The synthetic samples with the initial NOM concentrations of 10, 25, and 50 mg/l were prepared by dissolving the desired amount of humic acid in deionized water. In each run, the reactor was fed up with 1.250 L of these prepared samples. Initial pH of the samples was adjusted to 3, 7, and 10. The samples then were put into the reactor (equipped with aluminum and iron electrodes). The electrodes were connected as bipolar and monopolar to a direct current power supply using a wire (Figure 2a and b).

A magnetic stirrer was used to mix the solution within the reactor during the treatment. When the predetermined time for the treatment (5, 10, 15, and 20) was up, the samples were taken about 25 cc from the reactor. After settling time, the samples were filtered through a 0.45 pore size filter and analyzed. It is worth noting that all the tests were performed in duplicate, and the average value is reported in this study. After each experiment run, the electrodes were washed for 30 min with HCl 5%V and then washed with deionized water. The EC electrical energy consumption was calculated using equation 1 as follows:

$$E = U.I.t/V$$

Where E is the consumed electrical energy (kWh), U is the applied potential (V), I is the operating current in ampere (A) and t is the treatment or reaction time (h.), and V is the volume of the solution (L).

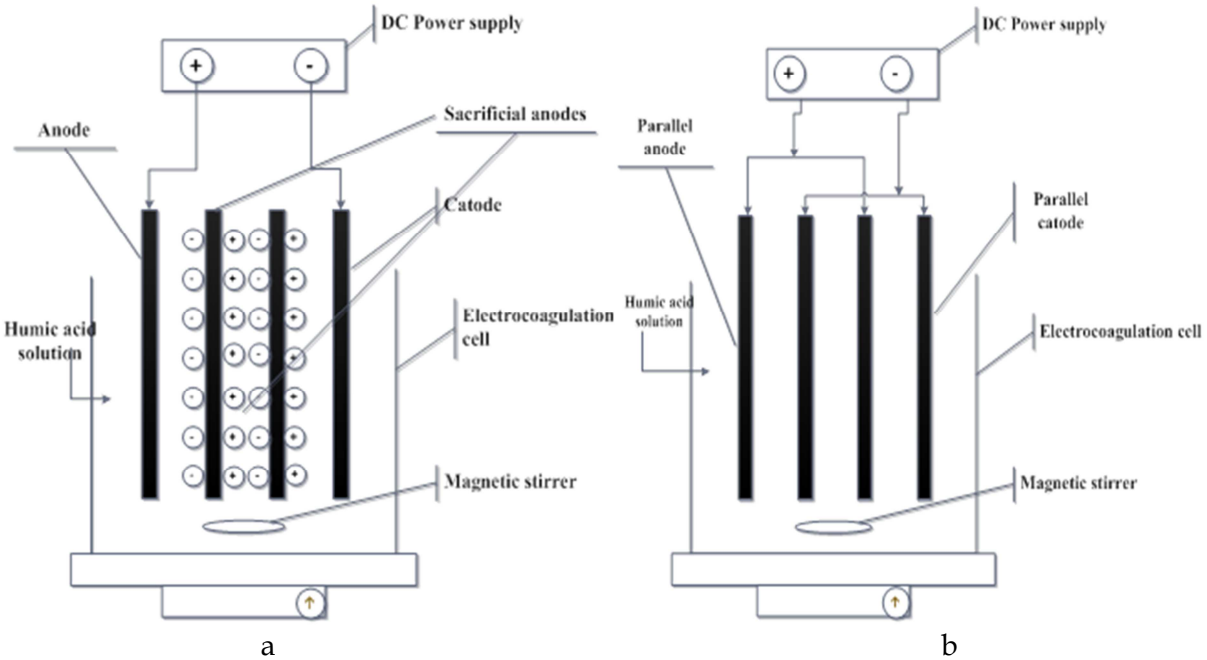

a b

Figure 2. The electrodes arrangement inside the reactor: bipolar (a) and monopolar (b)

Results and Discussion

Effect of reaction time on NOM removal

The conditions for all the experiments were the same. The experiments were carried out by multiplying the variables of each parameter to the variables of the other parameters. However, due to the large volume of data and impossibility to present a complete list of them, first, we obtained the optimum current, and then the relationship between the pH changes, and NOM removal was investigated at the optimum current. The effects of the other variables on NOM removal were investigated at optimum current and pH. Figure 3 shows the effects of electrical current and reaction time on the performance of EC for the removal of NOM at neutral pH and the highest NOM concentration.

As shown in figure 3, NOM removal efficiencies increased with increase in the reaction time. For example, at the applied current of 0.1, 0.3, and 0.5 ampere and reaction time of 20 min, NOM removal efficiencies were 82, 98, and 100%, respectively.

Reaction or treatment time is an important parameter in investigating any removal process, because it could decrease economic costs as well as will increase the applicability of the process.[15] Koparal et al. investigated the removal of humic acid by an EC process and reported that with increasing the reaction time and the energy consumption, the generation of suspended matter and removal efficiency increased until a certain time; afterwards the removal efficiency and suspended particle growth decreased.[16] Tezcan et al. evaluated the performance of the EC to treat the wastewater from a vegetable oil factory. The author stated that chemical oxygen demand removal efficiency was 98.9% for a reaction time of 90 min.[13] In the present study, NOM removal efficiency increased with increase in reaction time. The reason for this increase is the low production of aluminum and iron ions at the anode and hydroxide ions and hydrogen gas at the cathode during initial minutes of the reaction. Therefore, the formation of iron and aluminum hydroxides ions decreases because of a low contact between the metal ions formed at the anode and the hydroxides ions formed at the cathode. Consequently, the production of flocs and removal efficiency is low. With the increase in contact time, the concentration of iron and aluminum ions formed in the solution as well as the amount of hydroxides ions increases; thus,

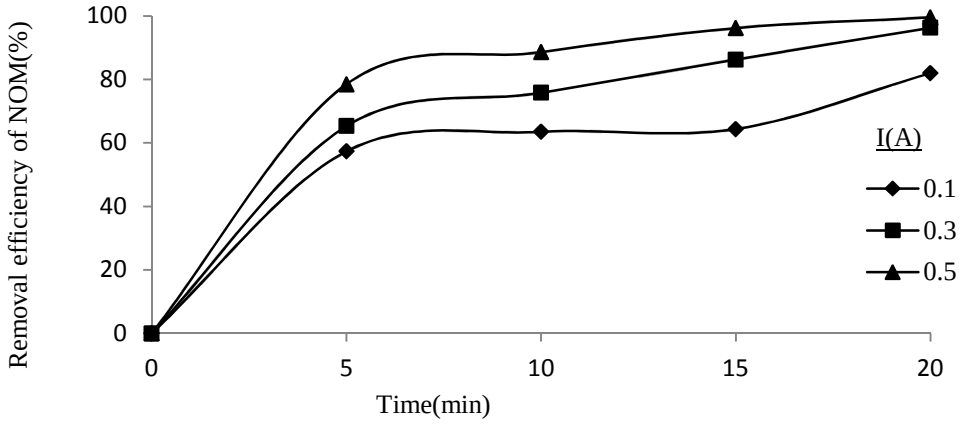

Figure 3. The relationships between natural organic matter (NOM) removal efficiencies with the current changes and reaction time
(conditions: neutral pH, initial NOM concentration of 50 mg/l)

the possibility of floc formation and removal efficiency increases.[17] Iron and aluminum hydroxide ions formed by cathodic and anodic reactions remove undesirable contaminants in the solution either by surface complexation and electrostatic attraction mechanisms or during the precipitation of heavy iron and aluminum hydroxides. Finally, organic matter physically removes by sweeping flocculation mechanism.[18]

Effect of pH on NOM removal

By considering significant effect of initial pH on NOM removal for an EC treatment and because at the reaction time of 20 min and the highest NOM concentration the removal efficiency of NOM was more than 50%, the applied current of 0.1 was selected as the optimum current for next experiments, the effects of pH changes and initial concentration were evaluated at this current.

For initial NOM concentration of 10 mg/l and reaction time of 20 min, NOM removal efficiencies were 88, 91, and 19 % for pH 3, 7, and 10, respectively (Figure 4a).

Figure 4b shows the associations between NOM removal and pH variations at optimum current and initial NOM concentration of 25 mg/l. It is apparent can be seen that NOM removal efficiencies for the EC process at pH 3, 7, and 10 were 87, 94, and 14 %, respectively.

NOM removal efficiencies for the initial NOM concentration of 50 mg/l at pH values of 3, 7, and 10 were 89, 82, and 10 %, respectively (Figure 4c).

The effect of initial pH can be attributed to the solubility of metal hydroxides formed in the solution.[19] In our study, which iron and aluminum electrodes were used together as the electrodes, pH 7 was obtained as the optimum pH because of the presence of insoluble $Al(OH)_{3(s)}$ and $Fe(OH)_{3(s)}$ and their high ability in removing NOM from the solution. In a study conducted by Ghernaout et al., the removal of humic acid was investigated by using an EC process. The authors stated that at pH 7, Al $(OH)_{3(s)}$ species was predominant in the solution and due to its insoluble nature, humic acid removal efficiency increased at this pH. In addition, at pH 7, when using iron electrodes, insoluble Fe $(OH)_{2(s)}$ and Fe $(OH)_{3(s)}$ were both present in the solution.[20]

Therefore, the presence of these species particularly Fe $(OH)_{3(s)}$ accelerates humic acid removal.[20] Chou et al. performed a study to remove TOC from the aqueous solutions by an EC treatment process. They reported that at the pH of 3 when aluminum plates were used as the electrodes, TOC removal efficiency was very low because of the presence of the insoluble species of $Al(OH)^{2+}$, $Al(OH)_3aq$, and AlO^{+} in the solution. In addition, it was stated that $Al(OH)^{4-}$ ion was the predominant species at the pH of 10; and, therefore, due to its high solubility and having negative charge were not able to remove NOM loads.[21] The other conducted studies have also indicated that in the EC treatment when using iron electrodes, at the pH of 9, $Fe(OH)^{4-}$ were dominantly present in the solutions compared with other iron hydroxides; thus, the removal efficiencies of the pollutants decreased in this pH value.[14,22-25]

Ho et al.[26] used iron electrodes to remove humic acid from the aqueous solutions. They reported that the optimum pH range for those electrodes was 2-6. The authors attributed this phenomenon to elevated concentrations of insoluble trivalent iron hydroxides species in the solution and their high capability to remove organic compounds using adsorption process. In another study, Heidmann et al.[27] investigated the performance of the EC system with Fe- and Al-electrodes for removal of Ni, Cu and Cr from a galvanic wastewater, and the highest removal efficiency was achieved at the pH values higher than 5.

Effect on initial NOM concentration on NOM removal efficiency

NOM removal efficiencies at initial NOM concentrations of 10, 25, and 50 mg/l for optimum condition are depicted in figure 5.

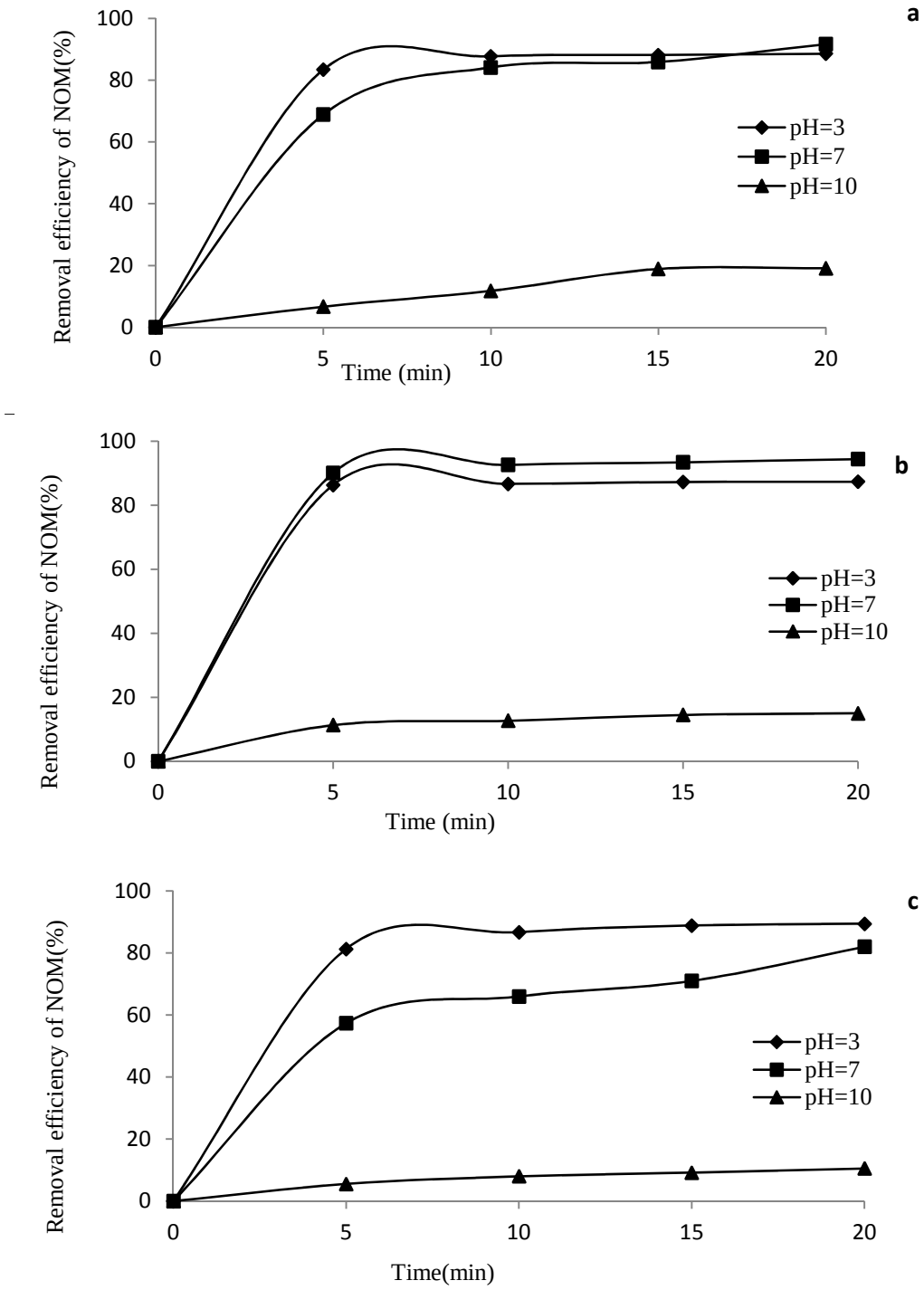

Figure 4. a: The effect of initial pH on natural organic matter (NOM) removal efficiency as a function of reaction time (condition: the applied current = 0.1 A, NOM concentration = 10 mg/l); b: The effect of initial pH on NOM removal efficiency as a function of reaction time (condition: the applied current = 0.1 A, NOM concentration = 25 mg/l); c: The effect of initial pH on NOM removal efficiency as a function of reaction time (condition: the applied current= 0.1 A, NOM concentration= 50 mg/l)

As shown in the figure at initial pH of 7 and reaction time of 20 min, for initial NOM concentrations of 10 mg/l (EC 279 µs/cm) and 25 mg/l (EC 417 µs/cm), NOM removal efficiency were about 88% and 92%, respectively. The corresponding value for NOM concentration of 50 mg/l (EC 808 µs/cm) was 82%.

The results of the present study indicated that NOM removal efficiency decreased with increase in the initial NOM concentration. Indeed, more coagulant agents are needed when initial NOM concentration increases. Since the limited iron and aluminum ions are produced at a constant current and reaction time, the removal efficiency decreases as initial concentration increases.[28] In this study, as NOM concentration increased, NOM removal efficiency decreased. The results of this study are consistent with the results obtained from the study of Gomes et al.[29] in which an EC process using a combination of iron and aluminum electrodes was evaluated to remove arsenic pollutant.

Effect of initial NOM concentration on energy consumption

As shown in figure 6, the maximum electrical energy consumption at optimum condition was observed for initial NOM concentration of 10 mg/l with the value of 0.08 kWh/m^3 of the solution. The consumed voltage for this concentration was 3 V. The minimum electrical energy consumption was detected for initial concentration of 50 mg/l with the value of 0.037 kWh/m^3 of the solution.

Electrical conductivity depends on the initial concentration of organic compounds.[23,30]

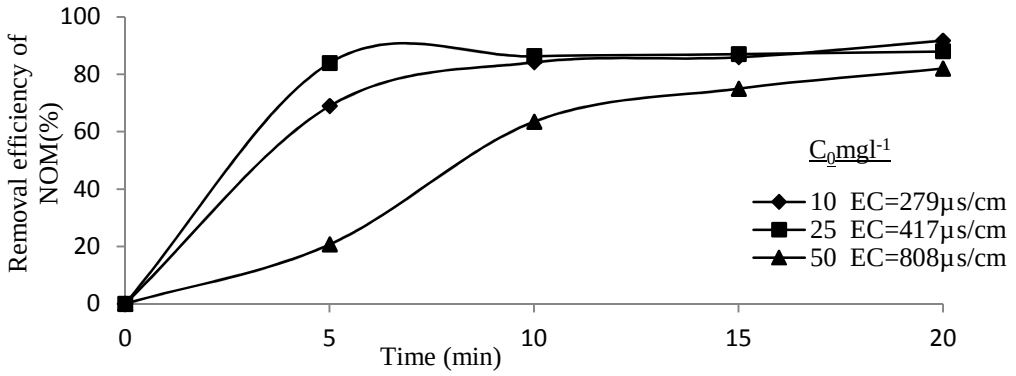

Figure 5. The effect of initial natural organic matter (NOM) concentration on NOM removal efficiencies as a function of reaction time and electrical conductivity (EC) (pH = 7, current = 0.1 A)

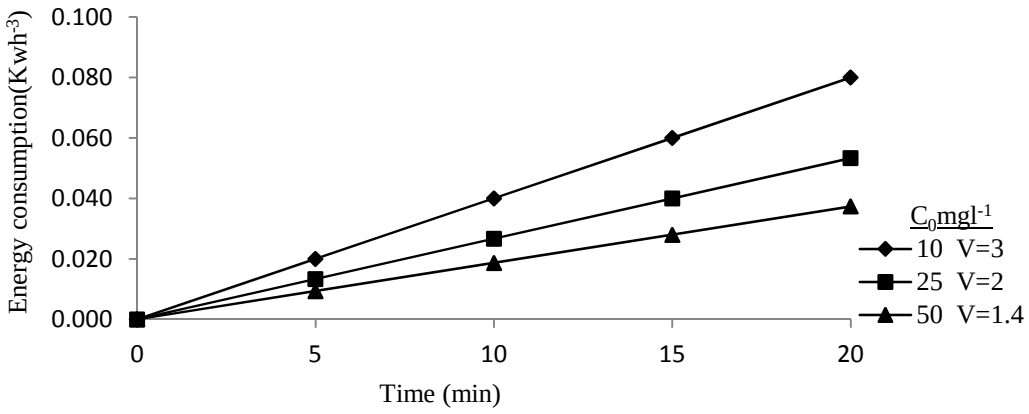

Figure 6. The effects of initial concentrations on the electrical energy consumption at optimum condition (pH = 7 and current = 0.1 A)

In the present study, by increasing initial NOM concentration, the energy consumption decreased. In this work, electrical conductivity increase in initial NOM concentration. As a result, during an EC treatment system and at a constant current, by increasing the concentration and consequently electrical conductivity of the solution the amount of potential and energy consumption decreases.

Comparison of NOM removal efficiency for bipolar and monopolar electrodes arrangement at the optimum condition

As shown in figure 7, NOM removal efficiencies at three concentrations of 10, 25, and 50 mg/l for bipolar and monopolar connections were followed by the same patterns.

Based on the performed studies, bipolar electrode connection compared to monopolar connection of the electrodes has higher removal efficiencies inorganic pollutants removal. In this study, due to the use of lower concentrations of such compounds, no significant difference was observed for both bipolar and monopolar arrangements of the electrodes. Asselin et al.[31] performed a study to remove organic pollutants by an EC process. It was noted that the higher electrical energy consumption of bipolar connection than monoplar connection was due to the potential difference between the electrodes.

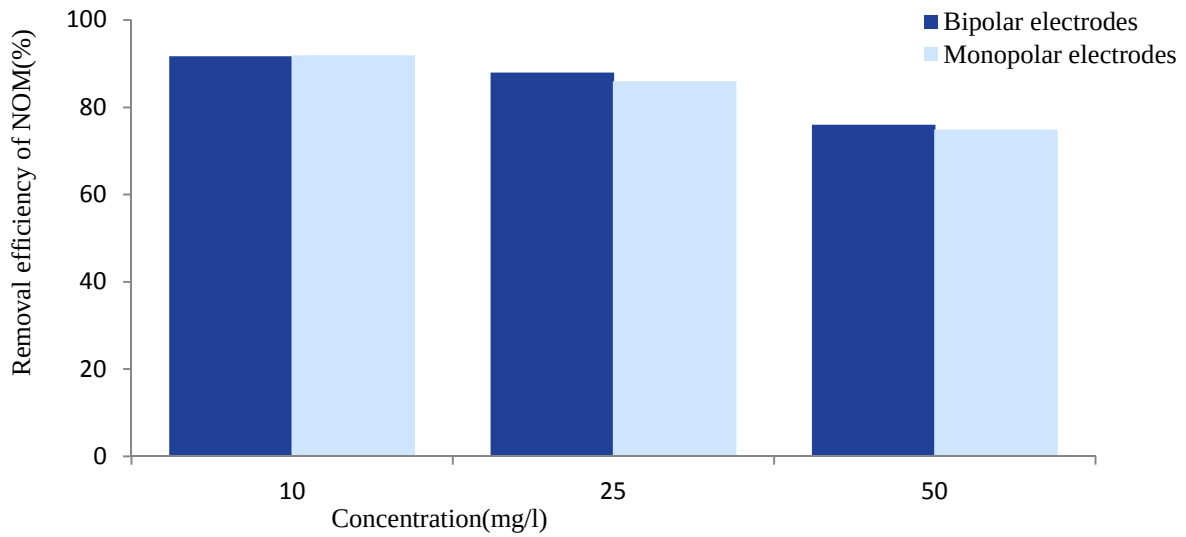

Figure 7. Natural organic matter (NOM) removal efficiencies for both bipolar and monopolar electrodes connection at optimum condition (pH = 7, current = 0.1 A, and reaction time = 20 min)

Table 1. Changes in turbidity, conductivity and pH optimum conditions for bipolar and monopolar electrodes

Electrode type	Experiments Electrode connection or arrangement (Aluminum/Iron)					
	Bipolar 1	Bipolar 2	Bipolar 3	Monopolar 1	Monopolar 2	Monopolar 3
Current intensity (A)	0.1	0.1	0.1	0.1	0.1	0.1
NOM concentration (mg/l)	10.0	25.0	50.0	10.0	25.0	50.0
Treatment time (min)	20.0	20.0	20.0	20.0	20.0	20.0
Initial pH	7.0	7.0	7.0	7.0	7.0	7.0
Final pH	7.7	7.5	7.7	7.4	7.6	8.0
Initial conductivity (µs/cm)	279	417.0	808.0	279.0	417.0	808
Final conductivity (µs/cm)	179.1	380.0	743.0	184.0	375.0	734
Initial turbidity (NTU)	5.6	10.6	20.8	5.6	10.6	20.8
Final turbidity (NTU)	0.5	1.0	3.5	0.1	0.1	2.5

NOM: Natural organic matter; NTU: Nephelometric turbidity units

In addition, they noted that electrical resistivity generated between the electrodes in bipolar EC system is higher than that for monopolar one. This increases the electrical potential and subsequently organic pollutants removal rate. Our results are consistent with the results of Asselin et al.[31]

Variations of pH, turbidity, and electrical conductivity during the process

The variations in the turbidity, electrical conductivity, and pH at optimum condition are presented in table 1.

It is obvious from table 1 that pH values for bipolar and monopolar connections of the electrodes remain in the neutral range. However, the turbidity and electrical conductivity decrease for both electrode connections.

In many studies, researchers always agree on this principle that pH parameter has a moderate variation during an EC system. It is also mentioned that pH variations depend on the electrode material and initial pH. This is an important subject because according to the final pH, after the treatment process the effluent can be discharged into water bodies such as rivers, lakes, and seas without any pH adjustment.[15] The standard of pH for discharging effluent into water bodies is in the range of 6-9.[32] In this study, the final pH after treatment process was in the standard range and it did not have any problem for discharging into the environment.

Conclusion

The results of this study showed that the EC process by using of iron and aluminum as the electrodes can remove high concentrations of NOM. Therefore, the EC process with Al-and Fe-electrodes can be used as an effective and promising method for treatment of water containing contaminants such as NOM. Additionally, its high removal efficiency allowing the discharge of the effluent into the environment.

Conflict of Interests

Authors have no conflict of interests.

Acknowledgements

The authors would like to thank the Faculty of Health of Tehran University of Medical Sciences for Technical support.

References

1. Zazouli MA, Nasseri S, Mesdaghinia A. Study of Natural Organic Matter Characteristics and Fractions in Surface Water Resources of Tehran. Iran J Health Environ 2008; 1(1): 1-7.
2. Crittenden JC, Trussell RR, Rhodes R, Hand DW, Howe KJ, Tchobanoglous G. MWH's Water Treatment: Principles and Design. New Jersey, NJ: Wiley; 2012.
3. Goslan EH, Fearing DA, Banks J, Wilson D, Hills P, Campbell AT, et al. Seasonal variations in the disinfection by-product precursor profile of a reservoir water. J Water SRT-Aqua 2002; 51: 475-82.
4. Huang H, Lee N, Young T, Gary A, Lozier JC, Jacangelo JG. Natural organic matter fouling of low-pressure, hollow-fiber membranes: Effects of NOM source and hydrodynamic conditions. Water Res 2007; 41(17): 3823-32.
5. Fan L, Harris JL, Roddick FA, Booker NA. Influence of the characteristics of natural organic matter on the fouling of microfiltration membranes. Water Res 2001; 35(18): 4455-63.
6. Huang W, Peng P, Yu Z, Fu J. Effects of organic matter heterogeneity on sorption and desorption of organic contaminants by soils and sediments. Applied Geochemistry 2003; 18(7): 955-72.
7. Saeedi R, Naddafi K, Nabizadeh R, Mesdaghinia A, Nasseri S, Alimohammadi M, et al. Simultaneous Removal of Nitrate and Natural Organic Matter from Drinking Water Using a Hybrid Heterotrophic/Autotrophic/Biological Activated Carbon Bioreactor. Environ Eng Sci 2012; 29(2): 93-100.
8. Babi KG, Koumenides KM, Nikolaou AD, Makri CA, Tzoumerkas FK, Lekkas TD. Pilot study of the removal of THMs, HAAs and DOC from drinking water by GAC adsorption. Desalination 2007; 210(1-3): 215-24.
9. Feering DA. Process options for the water treatment of humic rich waters [PhD Thesis]. Bedford, UK: School of Water Science, Cranfield University; 2004.
10. Daneshvar N, Sorkhabi HA, Kasiri MB. Decolorization of dye solution containing Acid Red 14 by electrocoagulation with a comparative investigation of different electrode connections. J Hazard Mater 2004; 112(1-2): 55-62.
11. Kim TH, Park C, Shin EB, Kim S. Decolorization of disperse and reactive dyes by continuous electrocoagulation process. Desalination 2002; 150(2): 165-75.

12. Bayramoglu M, Eyvaz M, Kobya M. Treatment of the textile wastewater by electrocoagulation: Economical evaluation. Chemical Engineering Journal 2007; 128(2-3): 155-61.
13. Tezcan UU, Koparal AS, Bakir OU. Electrocoagulation of vegetable oil refinery wastewater using aluminum electrodes. J Environ Manage 2009; 90(1): 428-33.
14. Mollah MY, Schennach R, Parga JR, Cocke DL. Electrocoagulation (EC)-science and applications. J Hazard Mater 2001; 84(1): 29-41.
15. Bazrafshan E, Joneidi Jaafari A, Kord Mostafapour F, Biglari H. Humic acid Removal from Aqueous Environments by Electrocoagulation Process Duad with Adding Hydrogen Peroxide. Iran J Health Environ 2012; 5(2): 211-24.
16. Koparal AS, Yildiz YS, Keskinler B+, Demircioglu N. Effect of initial pH on the removal of humic substances from wastewater by electrocoagulation. Separation and Purification Technology 2008; 59(2): 175-82.
17. Mollah MY, Pathak SR, Patil PK, Vayuvegula M, Agrawal TS, Gomes JA, et al. Treatment of orange II azo-dye by electrocoagulation (EC) technique in a continuous flow cell using sacrificial iron electrodes. J Hazard Mater 2004; 109(1-3): 165-71.
18. Janssen LJJ, Koene L. The role of electrochemistry and electrochemical technology in environmental protection. Chemical Engineering Journal 2002; 85 (2-3): 137-46.
19. Chen G. Electrochemical technologies in wastewater treatment. Separation and Purification Technology 2004; 38(1): 11-41.
20. Ghernaout D, Ghernaout B, Saiba A, Boucherit A, Kellil A. Removal of humic acids by continuous electromagnetic treatment followed by electrocoagulation in batch using aluminium electrodes. Desalination 2009; 239(1-3): 295-308.
21. Chou WL, Wang CT, Hsu CW, Huang KY, Liu TC. Removal of total organic carbon from aqueous solution containing polyvinyl alcohol by electrocoagulation technology. Desalination 2010; 259(1-3): 103-10.
22. Hsing HJ, Chiang PC, Chang EE, Chen MY. The decolorization and mineralization of acid orange 6 azo dye in aqueous solution by advanced oxidation processes: a comparative study. J Hazard Mater 2007; 141(1): 8-16.
23. Irdemez S, Demircioglu N, Yaldiz YS, Züleyha Bingül. The effects of current density and phosphate concentration on phosphate removal from wastewater by electrocoagulation using aluminum and iron plate electrodes. Separation and Purification Technology 2006; 52(2): 218-23.
24. Izquierdo CJ, Canizares P, Rodrigo MA, Leclerc JP, Valentin G, Lapicque F. Effect of the nature of the supporting electrolyte on the treatment of soluble oils by electrocoagulation. Desalination 2010; 255(1-3): 15-20.
25. Vepsäläinena M, Pulliainen M, Sillanpää M. Effect of electrochemical cell structure on natural organic matter (NOM) removal from surface water through electrocoagulation (EC). Separation and Purification Technology 2012; 99: 20-7.
26. Ho KJ, Liu TK, Huang TS, Lu FJ. Humic acid mediates iron release from ferritin and promotes lipid peroxidation in vitro: a possible mechanism for humic acid-induced cytotoxicity. Arch Toxicol 2003; 77(2): 100-9.
27. Heidmann I, Calmano W. Removal of Ni, Cu and Cr from a galvanic wastewater in an electrocoagulation system with Fe-and Al-electrodes. Separation and Purification Technology 2010; 71(3): 308-14.
28. Yildiz YS, Koparal AS, Irdemez S, Keskinler B. Electrocoagulation of synthetically prepared waters containing high concentration of NOM using iron cast electrodes. J Hazard Mater 2007; 139(2): 373-80.
29. Gomes JA, Daida P, Kesmez M, Weir M, Moreno H, Parga JR, et al. Arsenic removal by electrocoagulation using combined Al-Fe electrode system and characterization of products. J Hazard Mater 2007; 139(2): 220-31.
30. Gharibi H, Sowlat MH, Mahvi AH, Keshavarz M, Safari MH, Lotfi S, et al. Performance evaluation of a bipolar electrolysis/electrocoagulation (EL/EC) reactor to enhance the sludge dewaterability. Chemosphere 2013; 90(4): 1487-94.
31. Asselin M, Drogui P, Brar SK, Benmoussa H, Blais JF. Organics removal in oily bilgewater by electrocoagulation process. J Hazard Mater 2008; 151(2-3): 446-55.
32. Institute of Standards and Industrial Research of Iran. Drinking water-Specifications of industrial effluents National Standard NO.2439 [Online]. [cited 1974]. Available from: URL: http://www.isiri.org/portal/files/std/2439.htm

JAEHR Journal of Advances in Environmental Health Research

Hydrothermal synthesis of surface-modified copper oxide-doped zinc oxide nanoparticles for degradation of acid black 1: Modeling and optimization by response surface methodology

Kamal Salehi[1], Hiua Daraei[1], Pari Teymouri[1], Afshin Maleki[1]

1 Kurdistan Environmental Health Research Center, Kurdistan University of Medical Sciences, Sanandaj, Iran

Original Article

Abstract

Dyes are widely used in various industries most of them are not readily biodegradable and are consisted of number of toxic, mutagenic, and carcinogenic compounds. Therefore, it is essential to remove them from effluent before their discharge to the environment. The objective of this investigation was to synthesize copper oxide (CuO) doped zinc oxide (ZnO) nanoparticles under mild hydrothermal conditions using CuO as dopant and triethylamine as surface modifier to remove acid black 1 from aqueous solutions. Synthesized nanoparticles were characterized using powder X-ray diffractometer, Fourier transform infrared spectroscopy, scanning electron microscopy, and ultra violet-visible spectroscopy. The central composite design matrix and response surface methodology (RSM) were applied for designing the experiment, evaluating the effect of variable and modeling the degradation of acid black 1 dye. The results obtained from analyses of variance indicated that our experiments were fit with quadratic model. Moreover, the optimization R^2 and R^2 adjusted correlation coefficients for model were evaluated as 0.94 and 0.89, respectively. The optimal conditions for high efficiency (100% dye removal) was found to be at catalyst dosage of 1g/l, dye concentration of 50 mg/l, and pH = 6. This investigation introduced the RSM as an appropriate method to model and optimizes the best operating condition for maximizing dye removal. In conclusion, the results showed that nanoparticals dosage plays crucial role in this regard.

KEYWORDS: Hydrothermal, Photocatalysis, Modeling, Response Surface Methodology, Dye Removal, Acid Black 1

Date of submission: *16 Oct 2013*, ***Date of acceptance:*** *4 Jan 2014*

Citation: Salehi K, Daraei H, Teymouri P, Maleki A. **Hydrothermal synthesis of surface-modified copper oxide-doped zinc oxide nanoparticles for degradation of acid black 1: Modeling and optimization by response surface methodology.** J Adv Environ Health Res 2014; 2(2): 101-9.

Introduction

Dyes are macromolecules with high color yield, widely used in various industries such as textile, food, cosmetic, plastic and leather.[1,2] The average annual production rate of synthetic dyes by industries is about 7 million tons world-wide,[3] which about 40% of them are acid dyes. Most acid dyes contain one or more azo (-N = N-) group.[4,5] Since most of these dyes are not readily biodegradable and are consisted of number of toxic, mutagenic, and carcinogenic compounds; it is essential to remove them from effluent before their discharge to the environment.[4-7]

There are several conventional treatment methods for the removal of dyes from effluent stream including flocculation/coagulation, adsorption by activated carbon, electroflocculation, etc.[8] Nevertheless, these methods are expensive and non-destructive, because they just transfer contamination from liquid to the solid phase.[9,10] Advanced oxidation processes (AOPs) for removal of organic contamination from wastewater have attracted

Corresponding Author:
Afshin Maleki
Email: maleki43@yahoo.com

considerable attention of many researchers. AOPs are also used for oxidation, removal, and mineralization of dyes and other organic materials in wastewater and effluent.[11] They generally involve various methods, including UV/H_2O_2, O_3, O_3/H_2O_2, O_3/UV, O_3/H_2O_2/UV, Fenton, photo and electro-Fenton, and photdegradation.[12-14]

The latter, photo degradation or semiconductor-mediated photo catalyst has been given of great attention over recent years due to its potential to destruct organic contaminants at ambient temperature and pressure.[15] Until now, various semiconductors have been studied by researchers as photocatalyst.[16,17] Among these semiconductors, TiO_2 is the most widely used because it is non-toxic, inexpensive and photochemically stable.[18] However, zinc oxide (ZnO) is another semiconductor considered as not only a suitable alternative for TiO_2 but also even more efficient than TiO_2 in several applications.[19] The greatest advantage of ZnO in compared with TiO_2 is that it adsorbs a larger fraction of the solar spectrum.[20] There are a variety of strategies to tailor the morphology of ZnO nanoparticles, controlling its growth direction, reducing its agglomeration, and enhancing its photo catalytic properties. Dopping with suitable materials and using of surface modifiers or capping agents are among the excellent and confirmed techniques used.[21-23]

Therefore, we synthesized copper oxide (CuO) doped ZnO nanoparticles under mill hydrothermal conditions (T = 100 °C, and P = autogenous) using CuO and triethylamine as dopant and surface modifier, respectively. Moreover, we used response surface methodology (RSM) to design experimental and to evaluate the variable effect on photodegradation of acid black 1.

Materials and Methods

Reagent grade ZnO, CuO, triethylamine and KOH were purchased from Merck, Germany. Type I Water and distilled water were produced by a TKA smart 2 ultrapure water production system (Thermo Electron LED GmbH, Germany). The acid black 1 (Alvan Sabet Co. Iran) was used as a model pollutant from textile industry. Figure 1 shows the chemical structure and some characteristics of this dye figure 1.

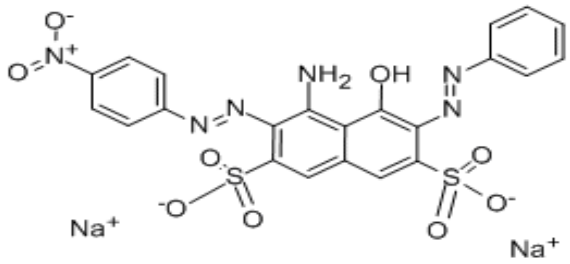

Figure 1. Chemical structure of acid black 1

Surface modified CuO-doped ZnO hybrid nanomaterials were fabricated under mild hydrothermal conditions (T = 100 °C, P = autogenous, t = 8 h). 2 mole of ZnO was taken as starting material and the dopant, CuO, at 0.5, 1, 1.5, 2 and 2.5 weight % was added into it. A certain amount of 1 mole KOH was added as mineralizer to the precursors. At the same time, a fixed concentration (1 ml) of triethylamine was added to the above-mentioned mixture and it was stirred vigorously for a few minutes. The final compound was then transferred to the Teflon liner (V_{fill} = 10 ml), which was later placed inside a general purpose autoclave. Then the assembled autoclave was kept in an oven with a temperature programmer-controller for 8h. The temperature was kept at 100 °C. After the experimental run, the autoclave was quenched to the room temperature. The product in the Teflon liner was then transferred to a clean beaker, washed with double distilled water several times, and then allowed to settle down. The surplus solution was removed using a syringe. Then, the remnant was allowed to dry naturally at room temperature. The dried particles were subjected to systematic characterization and photocatalytic studies.[21]

Fourier transform infrared spectroscopy

(FTIR) spectra of the grade reagent ZnO and the CuO-doped ZnO were obtained by employing a bruker-Tenso r27 spectrophotometer spectrum, one within wavelength range of 450-4000/cm. Powder X-ray diffraction (XRD) was performed on a Bruker D8-Advance powder XRD by monochromatized Cu KR radiation (λ = 1.5418 Å). Scanning electron microscopy (SEM) was used to analyze the morphology of the samples.

In this study, five types of synthesized xCuO: ZnO (x = 0.5, 1.0, 1.5, 2.0 and 2.5 wt. % of CuO content) were used for dye removal. A total volume of 200 mL of acid black 1 solutions was prepared using double distilled water for investigation of the photo catalyst activity of CuO:ZnO. The CuO-ZnO (0.4, 0.6, 0.8, 1.0, and 1.2 g/l) was mixed with Acid black 1 solutions (50, 100,150, 200 and 250). The initial pH of the solutions was adjusted before the experiments by 0.1 N NaOH and HCl, and controlled using pH meter (Model WTW-340I). Then, the suspensions were dispersed by vigorous stirring to make a good dispersion of nano-sized ZnO particles. Afterwards, suspension exposed to UV light (30 w) for up to 90 min. All experiments were performed at room temperature (25 °C). Dye sample of about 5-8 ml was taken out at the end of experiment using 10 ml pipettes. Each sample was centrifuged (10 min at 5000 rpm) and the absorbance was recorded using a UV-Vis spectrophotometer (Model CECIL 2021) at λ_{max} = 618 nm. The degradation efficiency (R%) was calculated using the following equation.

$$R(\%) = \frac{A_0 - A}{A_0} \times 100 \quad (1)$$

Where, A_0 and A are the dye concentration (mg/l) at time 0 and t, respectively.

In this investigation, the degradation of acid black 1 in the presence of UV radiation using CuO:ZnO was optimized by RSM using Design Expert Software (Version 7, Stat-ease, Inc., Minneapolis, MN, USA). The runs were designed in accordance with central composite and carried out batch wise. Independent variables for this investigation were catalyst dosage, pH and dye concentration, which were coded with low and high level in central composite. Table 1 shows the ranges and the level of the investigated variables.

Table 1. Experimental design of photocatalyst degradation of acid black 1 using copper oxide doped zinc oxide

Factor	Name	Low actual	High actual
X_1	Dye concentration (mg/l)	50	250
X_2	Nano dose (g/l)	0.4	1.2
X_3	Ph	4	8

The total numbers of experiments for the three independent variables were determined according to the following equation:

$$N = 2^n + 2_n + n_c = 2^3 + 2 \times 3 + 6 = 20 \quad (2)$$

Where, n and n_c are the number of independent variables and center points, respectively.[24] The center points are used to estimate the experimental error. The α value in this study was fixed at 2.

After completing the experimental design, the experiments of dye removal were carried out to obtain appropriate model. The experimental data were analyzed by quadratic models. The general form of the quadratic models is shown as follow:

$$Y = \beta_0 + \sum_{j=1}^{k} \beta_j x_j + \sum_{j=1}^{k} \beta_{jj} x_j^2 + \sum_{i}^{k} \sum_{\leq 2} \beta_{ij} x_i x_j + e_i \quad (3)$$

Where, η is response, x_i, x_j are variable, β_0 is the constant coefficient β_j is coefficient of linear, β_{jj} is coefficient of quadratic and β_{ij} is coefficient of interaction and e_i is error.[25]

Results and Discussion

Morphological characterizations

The SEM image indicates that the synthesized nanoparticles had different size and heterogeneous morphology; among them tetragonal nanoparticles were more obvious. Furthermore, there was no agglomeration on the surface of synthesized nanoparticles (Figure 2). In addition, the change in the morphology could be contributed to the applied surface modifier.[21]

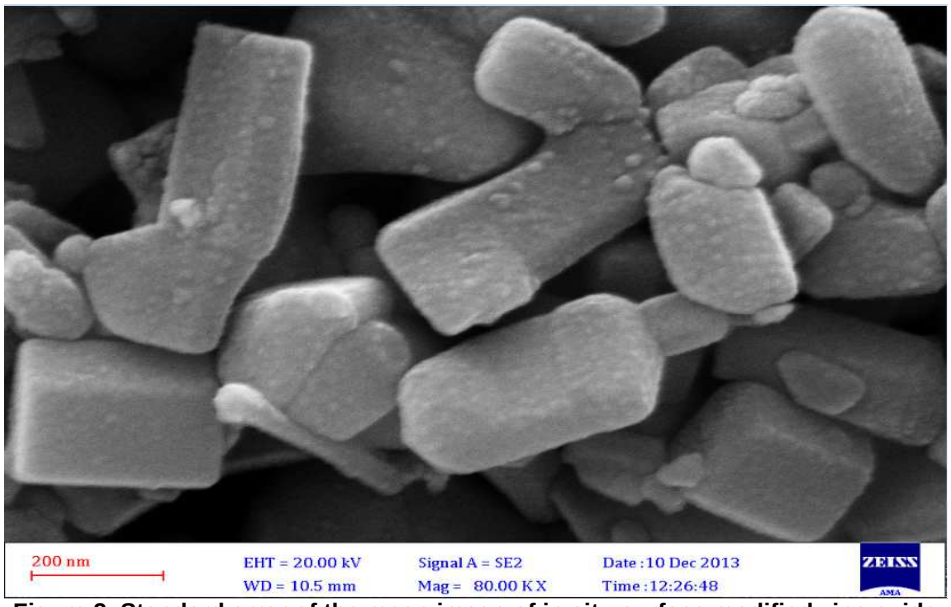

Figure 2. Standard error of the mean image of in situ surface modified zinc oxide doped copper using 1 ml triethylamine

Figure 3 shows the FT-IR spectrum of ZnO (carve A) and 1.50 % CuO-doped ZnO (carve B) nanoparticle recorded in the range of 400-4000/cm. Carve B in figure 3 shows the FT-IR spectrum of CuO-doped ZnO nanoparticle. The broadband at 2800-3000/cm is assigned to the C-H/cm group on the surface modifier. Peaks observed at 1600, 1500, 1400/cm corresponds to N-H, CH_2, CH_3 bonds stretching, respectively. Next peak around 1300/cm is due to the presence of the C-N group. The peak at 750/cm attributes to the Cu-O bond stretching and peak at 500-600/cm indicates stretching vibration of ZnO nanoparticles.

The XRD pattern of fabricated 1.50% CuO/ZnO nanoparticles is shown in figure 4 The diffraction peaks (100, 002 and 101) in figure 4 show that the fabricated nanoparticles are hexagonal structures.[26] Average crystallite size were determined using the Debye-Scherrer formula and the value was obtained 54nm for the fabricated nanoparticles. The formula is given below:

$$D_{Scherrer} = \frac{k\lambda}{\beta\cos\theta} \quad (4)$$

Where, D is the average crystallite size, λ is the radiation wavelength (1.5418Å), k is related to the crystallite shape (k = 0.089), β is the peak width at half maximum, and θ is the Bragg diffraction angle.[27] Also increased value of lattice parameter clearly indicates that the CuO ions substitute for Zn in ZnO lattice (Table 2).

Modelling and optimization of acid black 1

The experimental results of dye degradation by synthesized nanoparticles were analyzed through RSM to obtain an empirical model. Quadratic model were used to explain mathematical relationship between independent and depended variables. The mathematical expression of the relationship between acid black 1 degradation and the X_1, X_2, X_3 variables is shown in equation 3.

$$R = 78.1 - 0.072 \times X_1 + 65.36 \times X_2 + 63.75 \times X_3 + 0.2025 \times X_1 \times X_2 - 5.5 \times X_1 \times X_3 + 0.25 \times X_2 \times X_3 - 4.25 \times X_1^2 - 53.43 \times X_2^2 - 0.05 \times X_3^3 \quad (5)$$

In equation (4), R is response decolonization percent, X_1, X_2 and X_3 are corresponding to independent variables of dye concentration (mg/l), catalyst dosage (g/l) and pH, respectively. Analyses of variance results of

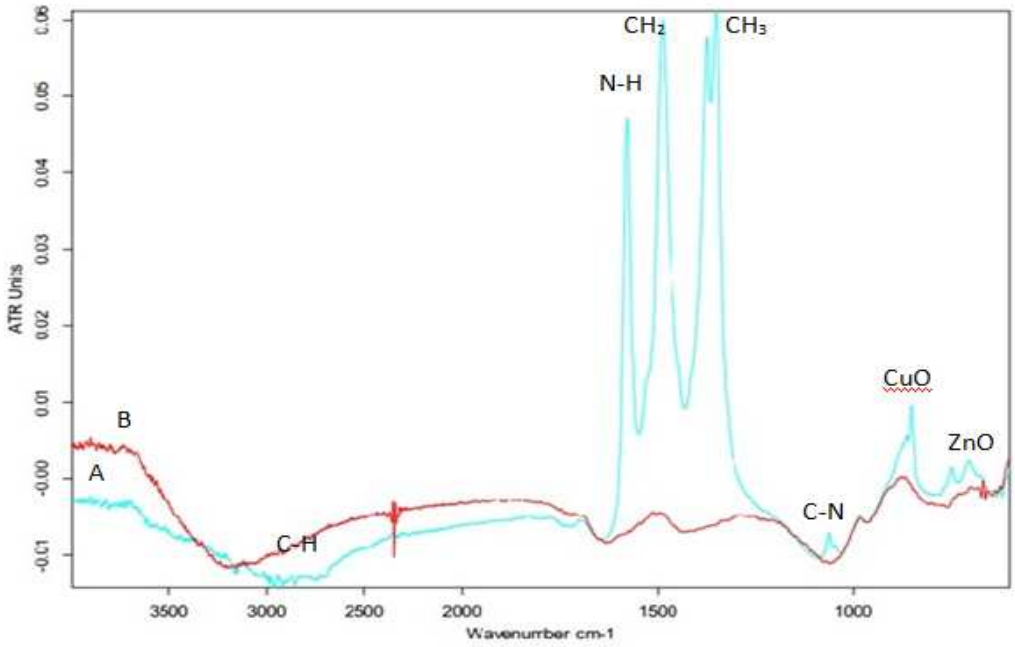

Figure 3. Fourier transform infrared spectrum of in situ surface modified zinc oxide doped copper using 1 ml triethylamine

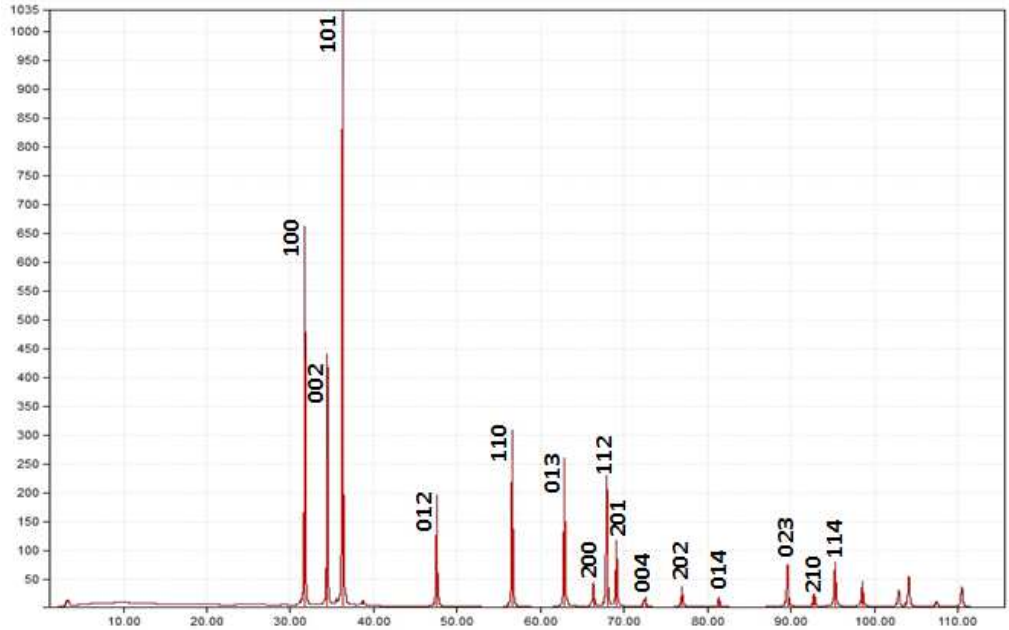

Figure 4. X-ray diffraction patter of in situ surface modified zinc oxide doped copper using 1 ml triethylamine

Table 2. Lattice parameters of surface modification copper:zinc oxide hybrid nanoparticle

Catalyst	a (A˚)	c (A˚)	a:c ratio	v (A˚)	Reference
Reagent-grade ZnO	3.249	5.207	0.6239	47.60	(8)
CuO:ZnO	3.255	5.214	0.6242	47.86	Present work

CuO: ZnO: Copper oxide: zinc oxide

these quadratic models are presented in table 3. They indicate that these quadratic models can be used to navigate the design space.

As shown in table 3, the quadratic model (F-value = 18.78) implies that the model is significant for degradation of acid black 1. With an adequate precision, the signal to noise ratio can be measured, and a ratio < 4 is generally desirable.[28] Therefore, in the quadratic models of degradation Acid black 1, the ratio of 13.79 indicates an adequate signal.

The values of Prob > F < 0.05 and > 0.1000 indicate that the model terms are significant and not significant, respectively. In this study, the Prob >F values are significant for X_1, X_2, but not significant for X_3, X^2_1, X_2X_3, X_1X_2 (Table 3). The "lack of fit F-value" of 4.51 shows that the lack of fit is not significant and the model is adequate.

The actual and predicted acid black 1 dye degradation are shown in figure 5. Actual values and perfected values were measured from response data for a particular run and the model, respectively. The results showed that the predicate values obtained are approximately close to the actual value (Figure 5). Moreover, it was found that the developed models were effectual in taking correlation between nanoparticles type variables and degradation of dye.

Table 3. ANOVA result of the quadratic model of photocatalyst degradation of acid black 1 using copper oxide doped zinc oxide

Source	Sum of Square	DF	Mean Square	F	P
Model	462.08	9	51.34	18.78	< 0.0001
X_1	203.0	1	203.6	74.29	< 0.0001
X_2	88.36	1	88.36	32.32	< 0.0001
X_3	5.52	1	5.52	2.02	0.1230
X_1X_2	32.81	1	32.81	12	0.1856
X_1X_3	0.60	1	0.60	0.22	0.0061
X_2X_3	0.02	1	0.020	7.31	0.6481
X_1^2	28.38	1	28.38	10.38	0.9335
X_2^2	114.88	1	114.88	42.03	0.0091
X_3^2	0.063	1	0.063	0.023	< 0.0001
Residual	27.33	10	2.73	-	0.8825
lack of fit	22.37	5	4.47	4.51	0.0619

DF: Degree of Freedom; X_1: Dye concentration, X_2: Nanoparticle dose, X_3: pH

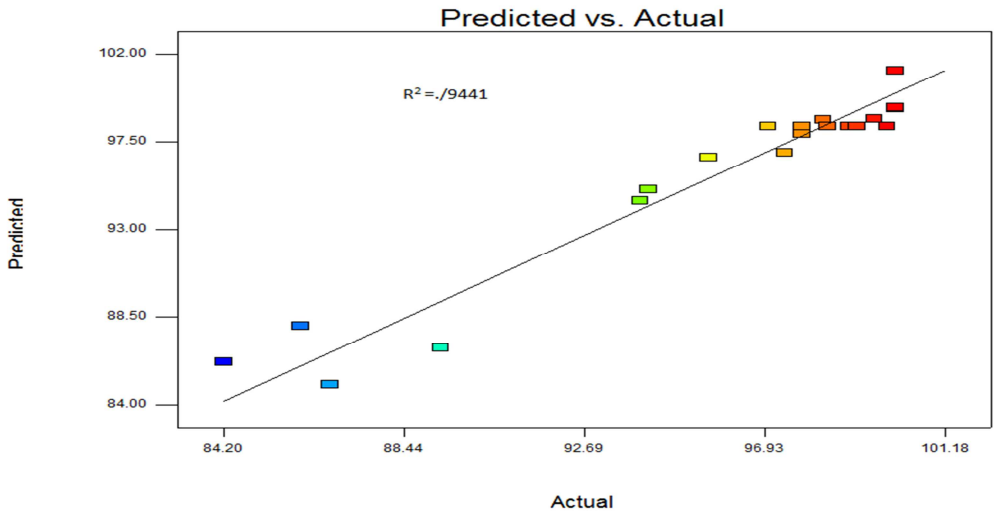

Figure 5. The actual and predicted plot of degradation of acid black 1 (R2 = 0.9441 and Radj = 0.8949)

The correlation coefficient (R^2) value is usually in range 0-1. The model is stronger and can better predict the responses when R^2 values are closer to 1.[29] The results in this study indicated that the values of R^2 and adjusted R^2 (R^2_{adj}) were found to be 0.94 and 0.89, respectively. X_3 terms in table 1 are not significant, which can be the reason for R^2_{adj} of 0.89.

The effects of variables on acid black 1 degradation are shown in figures 6 and 7 figure 6 shows the 3D response surface plot of interaction between varying concentration of dye and nanoparticles on dye degradation efficiency at pH = 6. The surface plot shows the decrease in dye degradation with increase in dye concentration. Although, degradation increased with catalyst dosage up to 1 g/l catalyst, and then decreased with its increase. The surface plot also shows that the best degradation (100%) obtained at 50 mg/l dye, pH = 6 and 1 g/l nanoparticle dosage.

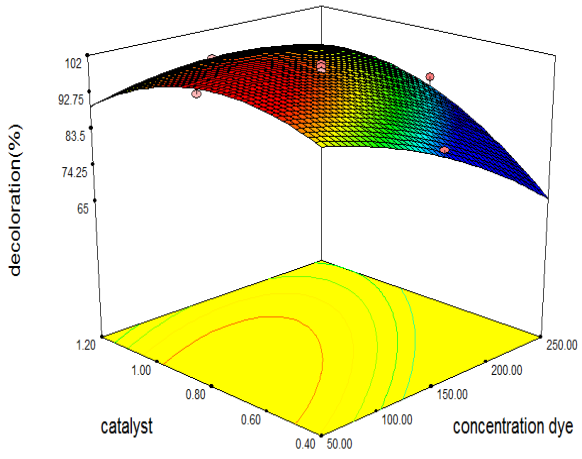

Figure 6. The effect of initial acid black 1 concentration (in mg/l) and nanoparticls (copper oxide doped zinc oxide) dose (in g/l) on decoloration of acid black 1 (pH = 6)

Bragti and Rauf reported that the decrease in degradation might be attributed to the increasing levels of catalyst causing the solution to become turbid and intercept the penetration of light.[30] A study by Marugesan et al. showed that by increasing the concentration of dye from 25 to 100 mg/l, the degradation rate for reactive black removal decreased.[31] Furthermore, Tekin and Saygi reported that by increasing the dye level from 25 to 35 mg/l, the degradation rate for acid black 1 removal decreased.[32] The degradation efficiency can prohibit light penetration, or reduce activated sits for adsorption of hydroxyl ion and generation of hydroxyl radicals. Because with increase in dye concentration, more dye substances are adsorbed on the nanoparticles' surface, and then, prevents generation of hydroxyl radicals.[33] Figure 7 illustrates the effect of changing dye concentration, nanoparticles dosage and pH on photodegradation efficiency of acid black 1. As figure 7 indicates, the dye degradation efficiency is proportion with photo catalyst dosage. Maximum degradation (η > 98%) of acid black 1 was determined at constant dye concentration of 150 mg/l, nanoparticles dosage of 1 g/l and pH = 6.

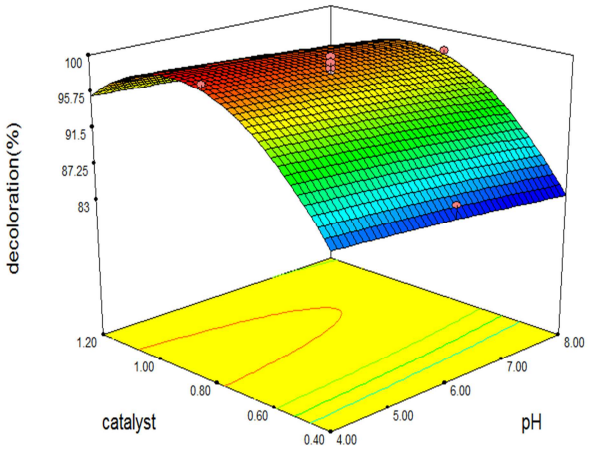

Figure 7. The effect of initial nanoparticles dose (copper oxide doped zinc oxide) and pH on degreadation of acid black 1

Conclusion

We synthesized CuO: ZnO nanoparticle under mild hydrothermal condition (P = autogenus, T = 100 °C, t = 8h). The synthesized nanoparticle

was characterized using powder XRD, FTIR, UV-VIS spectroscopy and SEM. The characterization results revealed that the CuO has been completely doped in ZnO lattice. Using triethylamine surface modifier, no agglomeration was observed. Moreover, the nanoparticles were well dispersed in the medium. FTIR results showed the appearance of new peaks after using the surface modifier. The nanoparticles were used for photodegradation of acid black 1. We carried out the systematic analysis using experimental design by RSM. This study clearly showed that RSM is a suitable method for modeling, and also optimizing the best operating conditions for maximum dye removal. In addition, we found that nanoparticle's dosage plays a crucial role in this regard.

Conflict of Interests

Authors have no conflict of interests.

Acknowledgements

The present study is a part of the master thesis of Mr. K. Salehi. The authors would like to thank the Vice-chancellor for Research and Technology, Kurdistan University of Medical Sciences for providing the grant of this research study.

References

1. Srivastava R, Rupainwar D. A comparative evaluation for adsorption of dye on Neem bark and Mango bark powder. Indian J Chem Technol 2011; 18(1): 67-75.
2. Mahmoodi NM, Hayati B, Arami M, Lan C. Adsorption of textile dyes on Pine Cone from colored wastewater: Kinetic, equilibrium and thermodynamic studies. Desalination 2011; 268(1-3): 117-25.
3. Bharathi KS, Ramesh ST. Removal of dyes using agricultural waste as low-cost adsorbents: a review. Appl Water Sci 2013; 3(4): 773-90.
4. Elmorsi TM, Riyad YM, Mohamed ZH, Abd El Bary HM. Decolorization of Mordant red 73 azo dye in water using H2O2/UV and photo-Fenton treatment. J Hazard Mater 2010; 174(1-3): 352-8.
5. Zee F. Anaerobic azo dye reduction [PhD Thesis]. Wageningen, Netherlands: Wageningen University; 2002.
6. Mahajan P, Kaushal J. Degradation of Congo Red Dye in Aqueous Solution by Using Phytoremediation Potential of Chara Vulgaris. ChitkaraChemistry ReviewVolume 1 2013; 1(1): 67-75.
7. Kousha M, Daneshvar E, Dopeikar H, Taghavi D, Bhatnagar A. Box Behnken design optimization of Acid Black 1 dye biosorption by different brown macroalgae. Chemical Engineering Journal 2012; 179(0): 158-68.
8. Giwa A, Nkeonye PO, Bello KA, Kolawole EG, Oliveira Campos AM. Solar Photocatalytic Degradation of Reactive Yellow 81 and Reactive Violet 1 in Aqueous Solution Containing Semiconductor Oxides. International Journal of Applied Science and Technology 2012; 2(4): 90-105.
9. Chong MN, Jin B, Chow CWK, Saint C. Recent developments in photocatalytic water treatment technology: A review. Water Research 2010; 44(10): 2997-3027.
10. Chakrabarti S, Dutta BK. Photocatalytic degradation of model textile dyes in wastewater using ZnO as semiconductor catalyst. J Hazard Mater 2004; 112(3): 269-78.
11. Chang SH, Chuang SH, Li HC, Liang HH, Huang LC. Comparative study on the degradation of I.C. Remazol Brilliant Blue R and I.C. Acid Black 1 by Fenton oxidation and Fe 0/air process and toxicity evaluation. J Hazard Mater 2009; 166(2-3): 1279-88.
12. Neamtu M, Yediler A, Siminiceanu I, Kettrup A. Oxidation of commercial reactive azo dye aqueous solutions by the photo-Fenton and Fenton-like processes. Journal of Photochemistry and Photobiology A: Chemistry 2003; 161(1): 87-93.
13. Chung, Kim JO. Application of advanced oxidation processes to remove refractory compounds from dye wastewater. Desalination and Water Treatment 2011; 25(1-3): 233-40.
14. Palit S. Membrane Separation Processes and Advanced Oxidation Processes of Dyes in Bubble Column Reactor-A Keen and Far Reaching Overview. International Journal of ChemTech Research 2012; 4(3): 862-6.
15. Wu YL, Tok AIY, Boey FYC, Zeng XT, Zhang XH. Surface modification of ZnO nanocrystals. Applied Surface Science 2007; 253(12): 5473-9.
16. Maleki A, Shahmoradi B. Solar degradation of Direct Blue 71 using surface modified iron doped ZnO hybrid nanomaterials. Water Sci Technol 2012; 65(11): 1923-8.
17. Shahmoradi B, Negahdary M, Maleki A. Hydrothermal Synthesis of Surface-Modified, Manganese-Doped TiO2 Nanoparticles for Photodegradation of Methylene Blue. Environmental Engineering Science 2012; 29(11): 1032-7.
18. Ullah R, Dutta J. Photocatalytic degradation of organic dyes with manganese-doped ZnO nanoparticles. J Hazard Mater 2008; 156(1-3): 194-200.

19. Qiu R, Zhang D, Mo Y, Song L, Brewer E, Huang X, et al. Photocatalytic activity of polymer-modified ZnO under visible light irradiation. J Hazard Mater 2008; 156(1-3): 80-5.
20. Subash B, Krishnakumar B, Pandiyan V, Swaminathan M, Shanthi M. An efficient nanostructured Ag_2S-ZnO for degradation of Acid Black 1 dye under day light illumination. Separation and Purification Technology 2012; 96(0): 204-13.
21. Shahmoradi B, Namratha K, Byrappa K, Soga K, Ananda S, Somashekar R. Enhancement of the photocatalytic activity of modified ZnO nanoparticles with manganese additive. Research on Chemical Intermediates 2011; 37(2-5): 329-40.
22. Chen J, Yao M, Wang X. Investigation of transition metal ion doping behaviors on TiO2 nanoparticles. J Nanopart Res 2008; 10(1): 163-71.
23. Ueda K, Tabata H, Kawai T. Magnetic and electric properties of transition-metal-doped ZnO films. Appl Phys Lett 2001; 79: 988.
24. Sahu JN, Acharya J, Meikap BC. Response surface modeling and optimization of chromium(VI) removal from aqueous solution using Tamarind wood activated carbon in batch process. J Hazard Mater 2009; 172 (2-3): 818-25.
25. Zheng Y, Wu XM, Branford-White C, Quan J, Zhu LM. Dual response surface-optimized process for feruloylated diacylglycerols by selective lipase-catalyzed transesterification in solvent free system. Bioresour Technol 2009; 100(12): 2896-901.
26. Chen YW, Liu YC, Lu SX, Xu CS, Shao CL. Photoelectric properties of ZnO: In nanorods/SiO2/Si heterostructure assembled in aqueous solution. Appl Phys B 2006; 84(3): 507-10.
27. Narayana RL, Matheswaran M, Aziz AA, Saravanan P. Photocatalytic decolourization of basic green dye by pure and Fe, Co doped TiO2 under daylight illumination. Desalination 2011; 269(1-3): 249-53.
28. Ahmadi M, Vahabzadeh F, Bonakdarpour B, Mofarrah E, Mehranian M. Application of the central composite design and response surface methodology to the advanced treatment of olive oil processing wastewater using Fenton's peroxidation. J Hazard Mater 2005; 123(1-3): 187-95.
29. Kaushik R, Saran S, Isar J, Saxena RK. Statistical optimization of medium components and growth conditions by response surface methodology to enhance lipase production by Aspergillus carneus. Journal of Molecular Catalysis B: Enzymatic 2006; 40(3-4): 121-6.
30. Korbahti BK, Rauf MA. Response surface methodology (RSM) analysis of photoinduced decoloration of toludine blue. Chemical Engineering Journal 2008; 136(1): 25-30.
31. Murugesan K, Dhamija A, Nam IH, Kim YM, Chang YS. Decolourization of reactive black 5 by laccase: Optimization by response surface methodology. Dyes and Pigments 2007; 75(1): 176-84.
32. Tekin D, Saygi B. Photoelectrocatalytic decomposition of Acid Black 1 dye using TiO2 nanotubes. Journal of Environmental Chemical Engineering 2013; 1(4): 1057-61.
33. Giahi M, Badalpoor N, Habibi S, Taghavi H. Synthesis of CuO/ZnO Nanoparticles and Their Application for Photocatalytic Degradation of Lidocaine HCl by the Trial-and-error and Taguchi Methods. Bulletin- Korean Chemical Society 2013; 34(7): 2176-82.

JAEHR Journal of Advances in Environmental Health Research

Adsorption of Zn (II) from aqueous solution by using chitin extraction from crustaceous shell

Nematollah Jaafarzadeh[1], Nezamaddin Mengelizadeh[2], Afshin Takdastan[1], Mohammad Heidari-Farsani[2], Noureddin Niknam[3]

1 Department of Environmental Health Engineering, School of Health AND Environmental Technology Research Center, Ahvaz Jundishapur University of Medical Sciences, Ahvaz, Iran
2 Department of Environmental Health Engineering, School of Health, Ahvaz Jundishapur University of Medical Sciences, Ahvaz, Iran
3 Department of Health Services Management, School of Management and Medical Information AND Health Management and Economics Research Center, Isfahan University of Medical Science, Isfahan, Iran

Original Article

Abstract

Removal of toxic heavy metals from wastewater is an important environmental challenge. In this Study, Zn (II) removal from aqueous solution by chitin extraction from crustaceous shells (shrimp and crab) was investigated. The biosorption studies were determined as a function of contact time, pH, initial metal concentration, and the amount of adsorbent. Adsorption of Zn (II) increased with decreasing concentration of the adsorbents and reached maximum uptake at 0.5 g. Effect of pH was studied in the range of 3-7 and the optimum conditions for both adsorbents were found in the range of 5-7. Zn (II) adsorption for both adsorbent was evaluated by Langmuir and Freundlich Isotherms. Results indicated that the Freundlich isotherm model was the most suitable one for the adsorption process using chitin extracted of shrimp and crab shells. The pseudo-first order and pseudo second order kinetic models were used to describe the kinetic data. The adsorption capacity (q_{max}) calculated from Langmuir isotherm and the values of the correlation coefficient obtained showed that chitin extracted from shrimp shells has the largest capacity and affinity for the removal of Zn (II) compared with the chitin extraction from the crab shells.

KEYWORDS: Adsorption, Chitin crab shells, Chitin shrimp shells, Kinetics, Zn (II)

Date of submission: *12 Oct 2013*, ***Date of acceptance:*** *25 Jan 2014*

Citation: Jaafarzadeh N, Mengelizadeh N, Takdastan A, Heidari-Farsani M, Niknam N. **Adsorption of Zn (II) from aqueous solution by using chitin extraction from crustaceous shell.** J Adv Environ Health Res 2014; 2(2): 110-9.

Introduction

Industrial wastewaters generated from industrialization activities may contain different toxic heavy metals.[1] Zinc is one of the most important metals often found in effluents discharged from industries involved in acid-mine drainage, galvanizing plants and municipal wastewater treatment plants.[2] It is important for the physiological functions of living tissue and regulates many biochemical processes. However, too much zinc can cause eminent health problems, such as stomach cramps, skin irritations, vomiting and anemia.[3] Therefore, selective separation of Zn (II) from aqueous solution, especially wastewater has drawn more and more attention in recent years. There are many techniques for Zn (II) removal, such as chemical precipitation, ion exchange, membrane filtration, electrolytic methods and

Corresponding Author:
Nezamaddin Mengelizadeh
Email: Nezam_m2008@yahoo.com

reverse osmosis. However, these methods are limited for high operational cost and inefficient in the removal of some heavy metal ions.[4] In contrast, adsorption owing to its advantages such as a variety of adsorbent materials and high efficiency is recognized as an effective and economic method for removal of pollutants from wastewaters.[5] In this method, different materials such as chitinous materials (e.g. shrimp, krill, squid, and crab shell), microbial biomass (e.g. bacteria, fungi, and yeast), and activated carbon, ion exchange resins, natural and synthetic zeolites are used.[6,7] In recent years, the use of chitin extracted from crustacean shell as biosorbents and organic substrates has gained importance.[8]

Chitin is the most important natural polysaccharide after cellulose found in crustaceous shells or in cell walls of fungi.[9] This polymer has been recommended as a suitable absorbent resource material because of its excellent properties such as biodegradability, biocompatibility, adsorption property, flocculating ability, polyelectrolisity and its possibilities of regeneration in a number of applications. The chitin structure (Figure 1) has positively charged amine (NH_2) functional groups which are responsible for the polyelectrolyte behavior. Therefore, chitin could adsorb negatively charged material with its positively charged functional groups to give electric neutrality.[10] Moreover, it has been recognized that chitin has significant potential as a biosorbent for metal removal. For example, the uptake of Cd^{2+} by chitin has been reported to be 14.9 mg/g.[11] Zhou et al.[12] investigated the adsorption of lead, cadmium, and copper onto cellulose/chitin beads; these metals were adsorbed at pH ranging from 3 to 6. Hawke et al.[13] studied the uptake of iron and manganese from seawater onto chitin; results showed low manganese (II) removal (< 10%) at pH 6-8.7 and increased removal (> 90%) at pH 9.5, while iron (II) was removed at levels of 22-30% at pH 2-8.

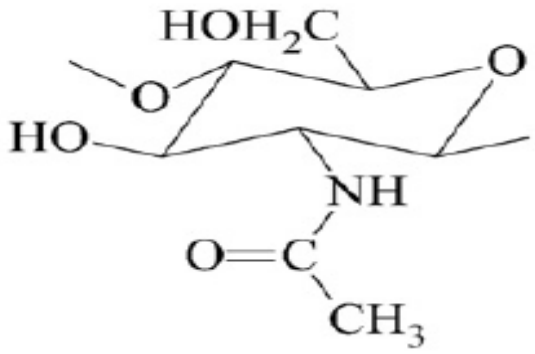

Figure 1. The basic structure of chitin[14]

In this work, we investigated the potential of chitin, extracted from shrimp and crab shells, to act as a biosorbent for Zn^{2+} removal from aqueous media. Chitin was prepared in the particle sizes range of 50-16 mesh and used in batch studies to quantify the effects of adsorbent dosage, contact time, pH and metal concentration on Zn^{2+} uptake performance.

Materials and Methods

Shrimp shells were washed several times with water and dried at 50° C overnight in a dry heat incubator. Afterwards, they were mechanically grinded in a mixer and passed through two layers of gauze. One hundred grams of shrimp shell powder were submerged in 1 L of 10% (w/w) HCl at room temperature for 24 h. After filtration with filter paper, the residue was washed with distilled water to neutral. Then the residue was submerged in 1000 ml of 10% (w/w) NaOH at room temperature for 24 h for. Then, the shrimp shell residue was washed with distilled water for removal the proteins. A volume of 250 ml of 95% ethanol was consecutively used to remove ethanol-soluble substances from the obtained crude chitin. Finally, the shrimp shell residue was subjected to the above procedure for 2 times.[14]

Chitin was extracted from the exoskeleton of crab with 1 N NaoH for 24 h at room temperature. This process was repeated 2 times with alkaline solution. The material was washed with water until the pH became neutral and demineralization was then carried out with 1 N

HCl at room temperature. The pigments were oxidized with 1% potassium permanganate and 1% oxalic acid, and then the material was washed until its pH was neutral. The material was then dried at 100° C for 2 h.[15]

In order to understand the adsorption mechanism, several characterizations were carried out on the two adsorbents. Fourier transform infrared spectrophotometer was applied to determine the presence of adsorbent functional groups (4000-400/cm). Brunauer-Emmet-Teller (BET) method was used for the samples specific surface determination. Water binding capacity (WBC) and fat binding capacities (FBC) of chitin were measured using the method of Kucukgulmez et al.[16] The degree of acetylation (DA) was calculated from the absorbance (A) ratios by using the following equation:

$$DA(\%) = \frac{A_{1655}}{A_{3450}} \times 115 \qquad (1)$$

Finally, the pH values of the chitin samples were determined according to the ASTMD 4972-01 standard method while the ash content was determined by heating at 530° C for 20 h.

A stock solution of 1000 mg/l of Zn (II) ions was prepared using analytical-reagent grade zinc chloride salt. The stock solution was diluted to appropriate concentrations accordingly. Each experiment was carried out in duplicates, and the average values were presented. All filtrate was analyzed using atomic absorption spectrometer (AAS 5FL model, Germany).

The effect of initial pH on the adsorption of Zn (II) ions was conducted using 1 g of adsorbent with 250 ml of 50 mg/l Zn (II) ions solution. The pH of the solution was adjusted in the range 3-7 using 0.1 M HCl or 0.1 M NaOH. The adsorbent was stirred in the Zn (II) ions solution at 300 rpm for 180 min. Since the optimum pH has been determined, the effect of adsorbate concentration was studied by varying the amount of adsorbent from 0.5 to 10 g under the optimum pH and agitation period of 180 min. The effect of metal concentration was investigated by mixing 250 ml of Zn (II) solution with metal concentration various under optimal conditions. Adsorption kinetic studies were carried out by shaking 250 ml of 50 mg/l Zn(II) solution with different contact time (0.5-4 h).

The amount of adsorbed Zn (II) on adsorbent (q_e, mg/g), and percent removals (%R) were calculated as follows:

$$q = \frac{(C_0 - C_e)V}{W} \qquad (2)$$

$$\%R = \frac{(C_0 - C_e)V}{C_0} \qquad (3)$$

Where q is the adsorption amount (mg/g), C_0 and C_e the initial and final concentrations (mg/l), V the volume of solution (l) and W is the mass of biosorbent used (g).

Results and Discussion

Characterization of chitin extraction from crustaceous shell

Chitin was obtained from shrimp and crab shells with a yield of 25.21% and 37.5% respectively. According to Muzzarelli, crustaceous shells consist mainly of chitin, protein and calcium carbonate with an average composition of 15-40%, 20-40% and 20-50% by weight, respectively.[17] This means that the yield of chitin was high on the laboratory scale. On the other hand, this value is similar to other studies.[18-20] The calculated DA values of crab and shrimp chitin using the formula (1) were 58% and 90%, respectively. These differences in DA could be attributed to the different isolation conditions of chitin, demineralization step or the deproteinization step under different alkaline conditions.[21] Majtan et al. obtained same results and showed the DA values of bumblebee and shrimp chitin were 87.3% and 99.0%, respectively.[22] Moreover, previous studies have shown the DA of chitin from various marine sources, including 79.5% in the king crab shell, 95.1% in the squid shell, and 84.6% in the Lobster.[23] Water and FBC of different chitin

derivatives (chitosan) were reported as 355-611% and 217-477 %, respectively, by Kucukgulmez et al.[16] The WBC and FBC of crustaceous chitin in the present study were compatible to those reported by Kucukgulmez et al.[16] The moisture content of chitin obtained from crustaceous shells was measured to be 2.8% as shown in table 1, which is in agreement with Abdulkarim et al.[24] The ash content of crab chitin was higher than that of shrimp shell, this could be attributed the presence of high acetyl group and $CaCO_3$ in the crab chitin sample. Furthermore, table 1 indicates that a very small amount of ash (0.8%) was found in the chitin shrimp. This proves that a demineralization process for the isolation of chitin from shrimp shells was enough.

Table 1. Physico-chemical characteristic of adsorbents

Characterization	Chitin shrimp shells	Chitin crab shells
Yield (%)	25.21	37.5
PZC	6.7	7.2
Moisture (%)	2.813	2.86
Ash content (%)	0.8	10.75
Water binding capacities (%)	452	402
Fat binding capacities (%)	387	306
Surface area (m^2/g)	3.95	3.2

PZC: Point of zero charge

The pH_Z values for chitin shrimp and chitin crab were 6.7 and 7.2, respectively. Based on these values, the prepared adsorbents were almost similar. However, for chitin crab the pH_Z was higher than the pH_Z of chitin shrimp. This could be due to the presence $CaCO_3$ in the crab chitin sample. The BET surface area of the crab and shrimp chitin was 3.2 and 3.95 m^2/g, respectively.

The infrared spectra of chitin from shrimp and crab are shown in figure 2. According this figure, Fourier transform infrared (FTIR) spectra of two chitins were quite similar. The spectra were characterized by three significant amide bands at 1632, 1574 and 1315/cm, which correspond to the amide I stretching of C = O, the amide II of N-H and amide III of C-N, respectively. The vibrational absorption bands at 1063 and 1073/cm are assigned to the C-O stretching. Bands at 3500 and 3200/cm corresponded to O-H and N-H stretching vibration, respectively. In addition, absorption bands at 3000-2850/cm assigned to -CH stretching vibrations; at 2517.95 and 2563.91/cm assigned to O-H vibrations. Moreover, figure 2 also shows the FTIR spectra of (a) chitin shrimp-Zn (II) and (b) chitin crab-Zn (II). With respect to the FTIR spectrum of chitin, the FTIR spectra of chitin-zinc ion show changes in the intensity of the adsorption bands at 3500-3300/cm, 1419/cm and 1632/cm attributable to -OH and $-NH_2$ groups. These changes indicate complex formation, which decreases the energies of the bonds due to the adsorbed zinc ions.

Effect of pH

The pH of an adsorption system is a crucial parameter in any adsorption system as it describes the mechanism involved in the adsorption process. Figure 3 shows the biosorption efficiency of Zn (II) at different pH values from 3 to 7. As shown in figure 3, the adsorption capacities were very low for adsorbents at pH < 4, due to an increase in the positively charged active sites (NH_3^+). Moreover, in this pH, electrostatic repulsion between the positive protons of the surface of chitin and H^+ lead to decrease of adsorption capacity. At pH > 5, a decrease in the protonation of the active sites increased the adsorption capacities for chitin shrimp and crab. According to these results the maximum adsorption of Zn (II) ions onto the two adsorbents occurred at pH 7, therefore, this pH value was selected as the optimum pH throughout this study. On the comparison between chitin shrimp and chitin crab the adsorption of zinc was much higher in chitin shrimp than that of chitin crab due to the DA high, maximum surface area and free amino groups. Karthikeyan et al.[25] reported the neutral condition for a favorable removal of Zn (II) using chitosan. According to Vijayaraghavan et al.[26] report, a strong adsorption of Zn (II) occurs

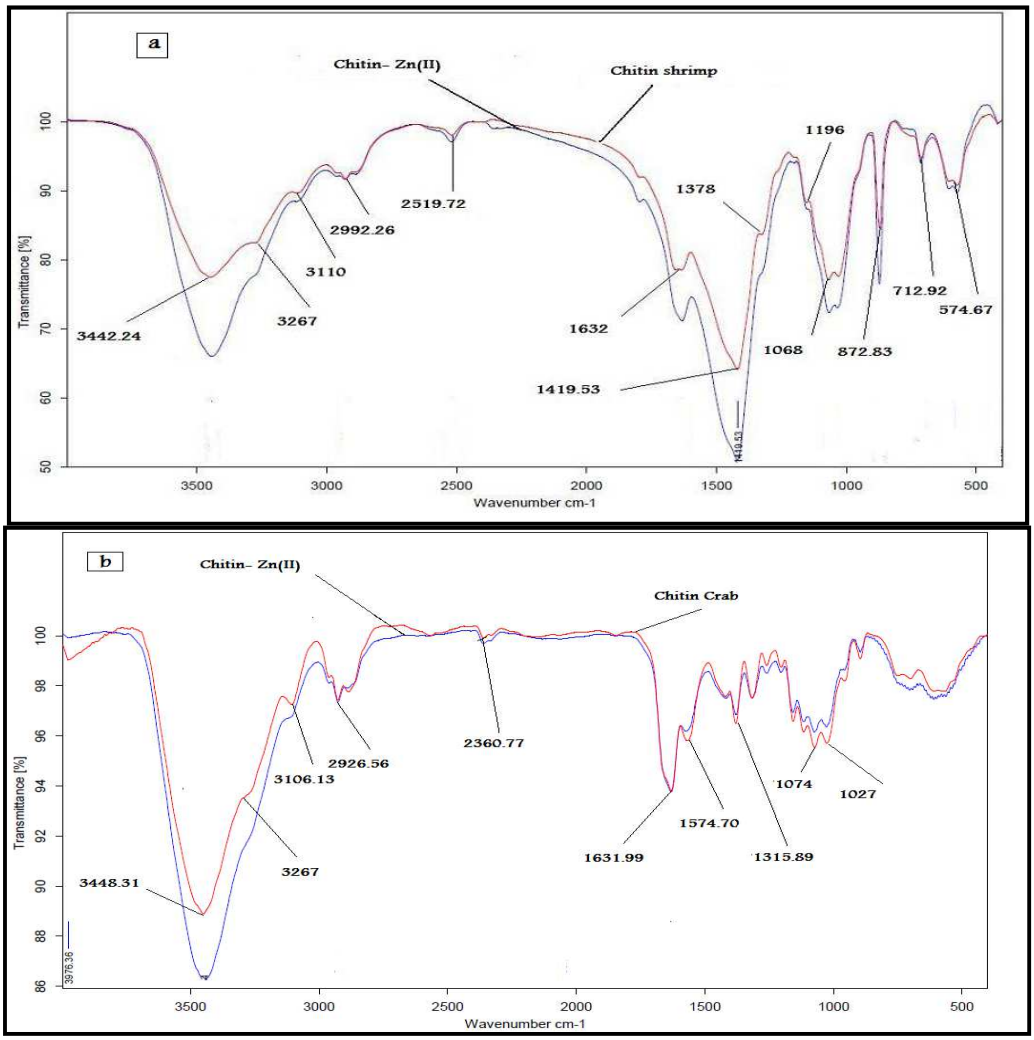

Figure 2. Infrared spectra of (a) chitin shrimp-Zn (II), and (b) chitin crab-Zn (II)

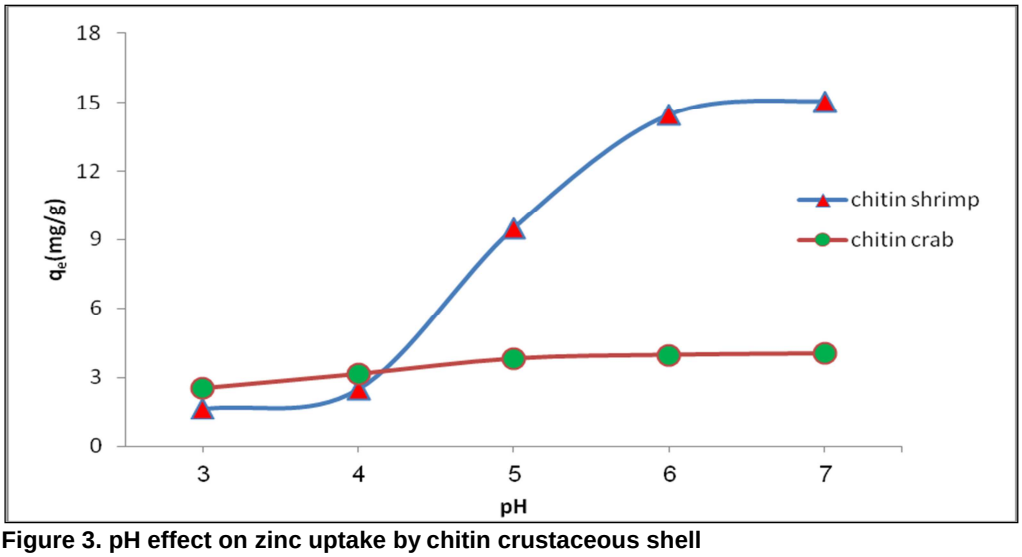

Figure 3. pH effect on zinc uptake by chitin crustaceous shell

on the crab shell particles in pH = 6. Lee et al.[27] reported that the presence of acetyl groups (DA high) in polymer increased their ability to bind with ferric ion.

Effect of initial metal concentration

Figure 4 shows the effect of initial metal concentration on the adsorption kinetics of the chitin at pH 7. An increase in the initial metal concentration leads to an increase in the adsorption capacity of the Zn (II) on chitin. This is due to the increase in the driving force of the concentration gradient, as an increase in the initial metal concentration. Figure 4 also shows that the adsorption of Zn (II) was much higher in chitin shrimp than that of chitin crab. This may be due to availability of DA and higher special surface area, or larger adsorption site compared with chitin crab. Gonçalves et al.[28] studied the adsorption of food dyes in a binary system by chitosan with different deacetylation degrees. Their results showed that the best conditions for the adsorption of food dyes onto chitosan were DD of 95%. Kurita[29] have shown that removal of mercury and copper ions increased with increasing deacetylation degrees of chitin. Wuertz et al.[30] demonstrated that the DA of polymers can affect the binding capacity for cations. Ho et al.[31] studied adsorption of metal ions on tree. In this study, it is confirmed that the adsorption efficiency is dependent on the specific surface area.

Effect of adsorbent dosage

The effect of adsorbent dosage on the adsorption of Zn (II) was shown in figure 5. It could be seen from figure 5 that the removal efficiency of Zn (II) considerably increased with the increase of adsorbent dosage. This was due to the greater availability of exchangeable sites for Zn (II) ions. However, the adsorption capacity decreased with increasing the adsorbent dosage. This was due to the higher number of unsaturated adsorption sites as the adsorbent dosage was increased. Bhattacharya et al.[32] studied the effect of adsorbent dose on the Zn (II) adsorption capacity. Their results showed that with increasing adsorbent dosage more surface area is available for adsorption due to increasing in active sites on the adsorbent.

Adsorption kinetics

Figure 6 shows the change in the adsorption capacity of Zn (II) by chitin crustaceous shell as a function of time at pH 7. The adsorption capacity increases with the increase in contact time and the adsorption equilibrium occurs after 3 h.

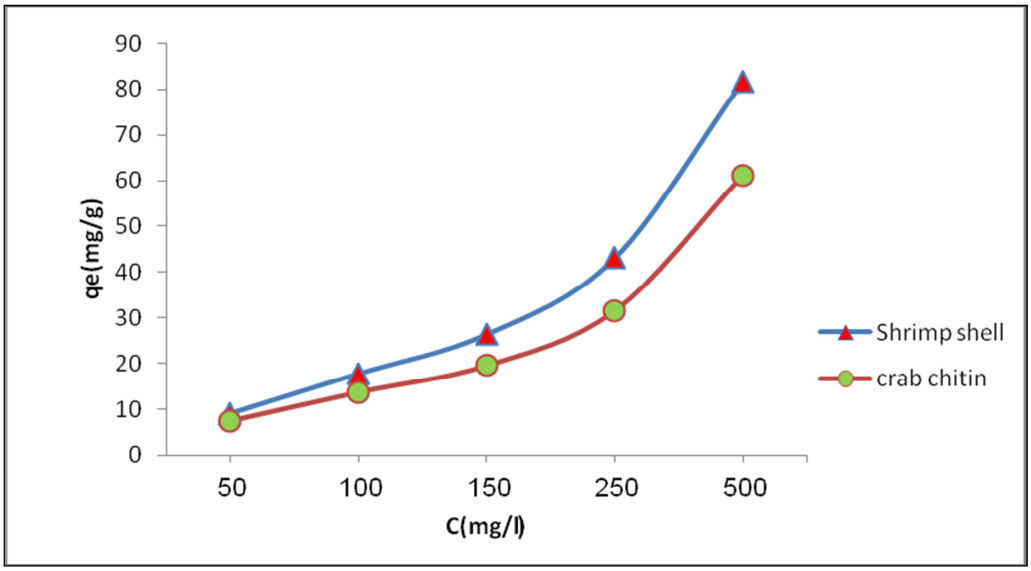

Figure 4. Effect of initial metal concentration on zinc uptake by chitin crustaceous shell

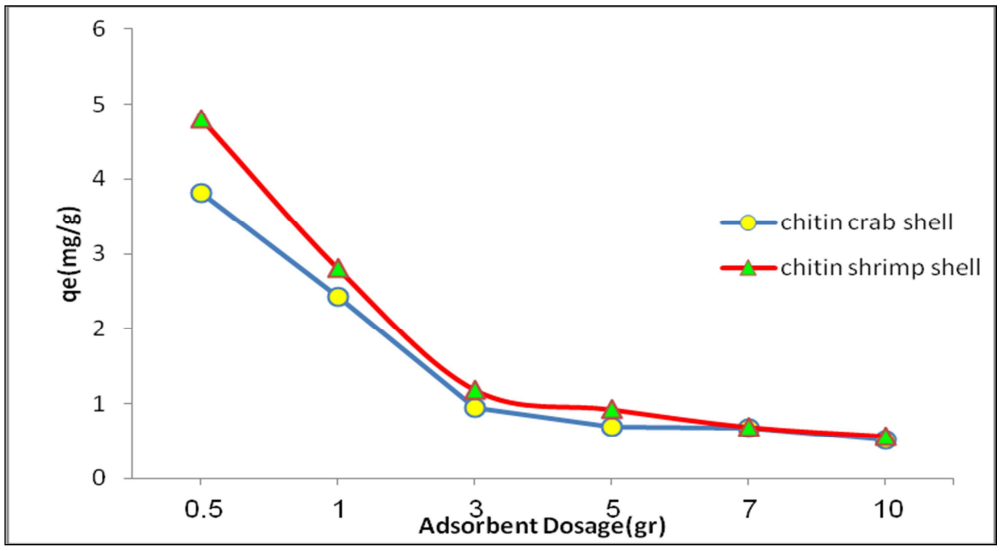

Figure 5. Effect of adsorbent dosage on the adsorption of Zn (II)

The kinetic data in table 2 is explicitly analyzed according to pseudo first-order and second-order. The R^2 and q_e values (Table 2) complied with experimental results, show that the pseudo second-order equation is the best one. Arshad et al.[33] studied the kinetics of adsorption Zn onto neem biomass. They found that pseudo-second order model provided better correlation than pseudo first-order model. Li et al.[4] computed the pseudo-second order model for their experimental data of studies on adsorption characteristics of Zn removal by magnetic chitosan modified with diethylenetriamine.

The adsorption isotherms

In order to determine the adsorption capacity the chitin crustaceous shell for Zn (II), and to identify the nature of this adsorption, the equilibrium adsorption isotherm is of basic importance. The Langmuir and Freundlich adsorption isotherm models were used to depict equilibrium sorption isotherms, and the calculated results of these models are given in table 3. As shown in table 3, the R^2 value of the Freundlich isotherm was greater than that of the Langmuir isotherm for the adsorption of Zn (II). This indicates that the adsorption of Zn (II) on chitin particles is better described by the Freundlich model than the Langmuir model. Kalyani et al.[34] reported that adsorption of zinc and copper on Gallus Domesticus shell powder followed both Freundlich and Langmuir models. Souag et al.[35] and Israel et al.[36] computed the Freundlich adsorption isotherm for their experimental data.

In order to anticipate the Zn (II) adsorption efficiency by chitin crustaceous shell and to understand whether the process is favorable or unfavorable for the Langmuir type adsorption process, the isotherm shape can be classified by the dimensionless equilibrium parameter (R), and can be calculated as following:

$$R_L = \frac{1}{1+bC_0} \qquad (4)$$

Where R_L, C_o, and b are the dimensionless equilibrium parameter or separation factor, the initial Zn (II) concentration (mg/l), and the Langmuir constant (mg/l), respectively. The value of RL (constant separation factor) indicates the shape of the isotherms to be either linear (RL = 1), favorable (0 < RL < 1), irreversible (RL = 0) or unfavorable (RL > 1). The data obtained in table 3 represent a favorable adsorption for both adsorbents.

A comparison of the maximum capacity q_{max} of chitin crustaceous shell with those of some other adsorbents reported in the literature is

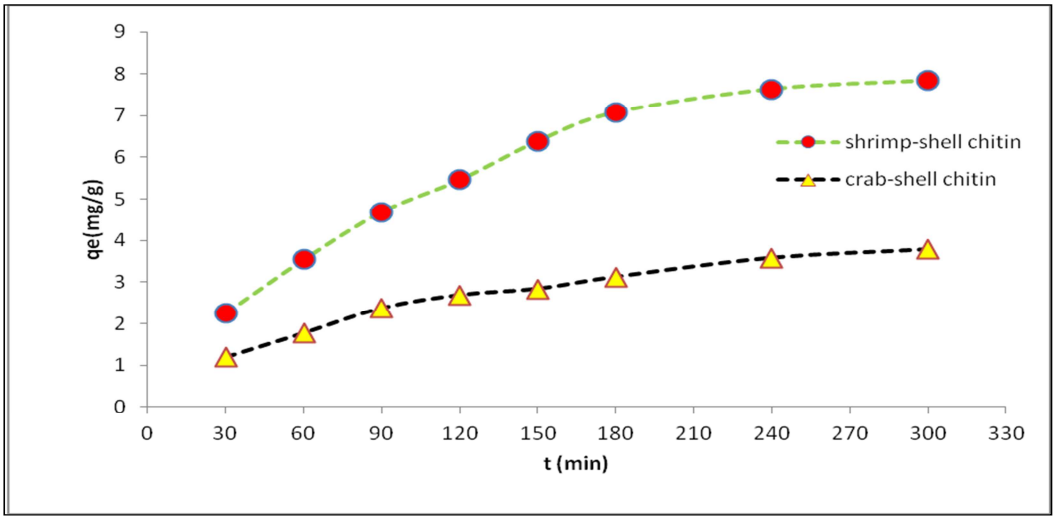

Figure 6. Influence of contact time on Zn (II) uptake by chitin crustaceous shell

Table 2. Kinetic model constants during Zn (II) biosorption at pH 7

Adsorbents	q_e (exp) mg/g	Pseudo first-order kinetics			Pseudo second-order kinetics		
		K_1 (10^{-4})	q_e	R^2	K_2(10^{-4})	q_e	R^2
Chitin shrimp shells	7.64	149	10.01	0.9577	5.4	12.562	0.9815
Chitin crab shells	3.58	156	4.8128	0.9686	23	4.677	0.9918

K_1: The pseudo-first order rate constant (1/min); q_e: The amount of metal sorption at equilibrium (mg/g); R^2: Correlation coefficient; K_2: The pseudo-second order rate constant (g/mg/min)

Table 3. Langmuir and freundlich isotherm constants and correlation coefficients

Adsorbents	RL	Freundlich model			Langmuir model		
		K_f	n	R^2	q_m	b	R^2
Chitin shrimp shells	0.447-0.89	0.9664	1.1544	0.9992	270.270	0.00247	0.9783
Chitin crab shells	0.52-0.915	0.6013	1.2119	0.9973	181.181	0.00184	0.7391

RL: Constant separation factor; R^2: Correlation coefficient; K_f: Freundlich isotherm constant; q_m: The maximum adsorption capacity (mg/g); n: The Freundlich constant; b: The Langmuir constant

given in table 4. Differences of metal uptake are due to the differences in properties of each adsorbent such as structure, functional groups and surface area.

Conclusion

The results of the present investigation show that chitin crustaceous shell has considerable potential for the removal of Zn (II) ions from aqueous solution. The adsorbed amounts of Zn (II) increased with a decrease in adsorbent dosage due to the decreasing number of unsaturated adsorption sites. The solution pH plays a significant role in influencing the capacity of an adsorbent towards Zn (II) ions. An increase in the pH of solutions leads to a significant increase in the adsorption capacities

Table 4. Comparison of maximum capacity of chitin crustaceous shell for zinc adsorption with other adsorbents

Adsorbent	Uptake (mg/g)	Reference
Bentonite	52.91	37
Red mud	12.59	37
Bacillus subtilis	137.00	37
Fungal biomass	98.00	37
Lignin	95.00	37
Scarp rubber	100.00	37
Crab carapace	172.50	37
Amberlite IRC-718	156.89	37
Chitosan	58.83	37
Lewatit TP-207	89.56	33
Biosolids	36.87	33
Powered waste sludge	168.00	33
Neem bark	137.67	33
Neem leaves	147.08	33
Chitin shrimp shells	270.27	This study
Chitin crab shells	181.18	This study

of Zn (II) on the chitin crustaceous shell. The adsorbed amounts of Zn (II) ions increased with increase in contact time and reached the equilibrium after 180 min. The equilibrium data have been analyzed using Langmuir and Freundlich isotherms. The Freundlich isotherm was demonstrated to provide the best correlation for the adsorption of Zn (II) on the chitin crustaceous shell. The pseudo-first-order and second-order kinetic models were used to describe the kinetic data. The dynamical data fit well with the second-order kinetic model. The uptake of zinc by chitin crustaceous shell in this study is comparable with other adsorbents reported in the literature. The results showed that zinc uptake by chitin crustaceous shell in this study was significantly higher than most of the selected biosorbents.

Conflict of Interests

Authors have no conflict of interests.

Acknowledgements

The authors are grateful for the financial support of this project by Environmental Technology Research center Ahvaz Jundishapur University of Medical Sciences, Iran, under grant number E-9009.

References

1. Veli S, Alyuz B. Adsorption of copper and zinc from aqueous solutions by using natural clay. J Hazard Mater 2007; 149(1): 226-33.
2. King P, Anuradha K, Lahari SB, Prasanna KY, Prasad VS. Biosorption of zinc from aqueous solution using Azadirachta indica bark: equilibrium and kinetic studies. J Hazard Mater 2008; 152(1): 324-9.
3. Fu F, Wang Q. Removal of heavy metal ions from wastewaters: a review. J Environ Manage 2011; 92(3): 407-18.
4. Li H, Bi S, Liu L, Dong W, Wang X. Separation and accumulation of Cu(II), Zn(II) and Cr(VI) from aqueous solution by magnetic chitosan modified with diethylenetriamine. Desalination 2011; 278(1-3): 397-404.
5. Aydin YA, Aksoy ND. Adsorption of chromium on chitosan: Optimization, kinetics and thermodynamics. Chemical Engineering Journal 2009; 151(1-3): 188-94.
6. Apiratikul R, Pavasant P. Batch and column studies of biosorption of heavy metals by Caulerpa lentillifera. Bioresour Technol 2008; 99(8): 2766-77.
7. Sari A, Tuzen M, Soylak M. Adsorption of Pb(II) and Cr(III) from aqueous solution on Celtek clay. J Hazard Mater 2007; 144(1-2): 41-6.
8. Pinto PX, Al-Abed SR, Reisman DJ. Biosorption of heavy metals from mining influenced water onto chitin products. Chemical Engineering Journal 2011; 166(3): 1002-9.
9. Brugnerotto J, Lizardi J, Goycoolea FM, Arguelles-Monal W, Desbrieres J, Rinaudo M. An infrared investigation in relation with chitin and chitosan characterization. Polymer 2001; 42(8): 3569-80.
10. Ahmad AL, Sumathi S, Hameed BH. Coagulation of residue oil and suspended solid in palm oil mill effluent by chitosan, alum and PAC. Chemical Engineering Journal 2006; 118(1-2): 99-105.
11. Benguella B, Benaissa H. Cadmium removal from aqueous solutions by chitin: kinetic and equilibrium studies. Water Res 2002; 36(10): 2463-74.
12. Zhou D, Zhang L, Zhou J, Guo S. Cellulose/chitin bead for adsorption of heavy metals in aqueous solution. Water research 2004; 38(11): 2643 50.
13. Hawke D J, Sotolongo S, Millero F J. Uptake of Fe(II) and Mn(II) on chitin as a model organic phase. Marine chemistry 1991; 33(3): 201-212.
14. Du Y, Zhao Y, Dai S, Yang B. Preparation of water-soluble chitosan from shrimp shell and its antibacterial activity. Innovative Food Science & Emerging Technologies 2009; 10(1): 103-7.
15. Yen MT, Yang JH, Mau JL. Physicochemical characterization of chitin and chitosan from crab shells. Carbohydrate Polymers 2009; 75(1): 15-21.
16. Kucukgulmez A, Celik M, Yanar Y, Sen D, Polat H, Kadak AE. Physicochemical characterization of chitosan extracted from Metapenaeus stebbingi shells. Food Chemistry 2011; 126(3): 1144-8.
17. Kim SK. Chitin, Chitosan, Oligosaccharides and Their Derivatives: Biological Activities and Applications. New York, NY: Taylor & Francis Group; 2010.
18. Benavente M, Moreno L, Martinez J. Sorption of heavy metals from gold mining wastewater using chitosan. Journal of the Taiwan Institute of Chemical Engineers 2011; 42(6): 976-88.
19. Sagheer FAA, Al-Sughayer MA, Muslim S, Elsabee MZ. Extraction and characterization of chitin and chitosan from marine sources in Arabian Gulf. Carbohydrate Polymers 2009; 77(2): 410-9.
20. Wang Y, Chang Y, Yu L, Zhang C, Xu X, Xue Y, et al. Crystalline structure and thermal property characterization of chitin from Antarctic krill

(Euphausia superba). Carbohydr Polym 2013; 92(1): 90-7.
21. Susana Cortizo M, Berghoff CF, Alessandrini JL. Characterization of chitin from Illex argentinus squid pen. Carbohydrate Polymers 2008; 74(1): 10-5.
22. Majtan J, Bilikova K, Markovic O, Grof J, Kogan G, Simuth J. Isolation and characterization of chitin from bumblebee (Bombus terrestris). Int J Biol Macromol 2007; 40(3): 237-41.
23. Cardenas G, Cabrera G, Taboada E, Miranda SP. Chitin characterization by SEM, FTIR, XRD, and 13C cross polarization/mass angle spinning NMR. Journal of Applied Polymer Science 2004; 93(4): 1876-85.
24. Abdulkarim A, Isa MT, Abdulsalam S, Muhammad AJ, Ameh AO. Extraction and Characterisation of Chitin and Chitosan from Mussel Shell. Civil & Environmental Research 2013; 3(2): 108-14.
25. Karthikeyan G, Anbalagan K, Andal NM. Adsorption dynamics and equilibrium studies of Zn (II) onto chitosan. J Chem Sci 2004; 116(2): 119-27.
26. Vijayaraghavan K, Winnie HYN, Balasubramanian R. Biosorption characteristics of crab shell particles for the removal of manganese(II) and zinc(II) from aqueous solutions. Desalination 2011; 266(1-3): 195-200.
27. Lee JW, Ashby RD, Day DF. Role of acetylation on metal induced precipitation of alginates. Carbohydrate Polymers 1996; 29(4): 337-45.
28. Gonçalves JO, Duarte DA, Dotto GL, Luiz AA. Use of Chitosan with Different Deacetylation Degrees for the Adsorption of Food Dyes in a Binary System. CLEAN - Soil, Air, Water 2014; 42(6): 767-74.
29. Kurita K. Controlled functionalization of the polysaccharide chitin. Progress in Polymer Science 2001; 26(9): 1921-71.
30. Wuertz S, Muller E, Spaeth R, Pfleiderer P, Flemming HC. Detection of heavy metals in bacterial biofilms and microbial flocs with the fluorescent complexing agent Newport Green. J Ind Microbiol Biotech 2000; 24(2): 116-23.
31. Ho YS, Huang CT, Huang HW. Equilibrium sorption isotherm for metal ions on tree fern. Process Biochemistry 2002; 37(12): 1421-30.
32. Bhattacharya AK, Mandal SN, Das SK. Adsorption of Zn(II) from aqueous solution by using different adsorbents. Chemical Engineering Journal 2006; 123(1-2): 43-51.
33. Arshad M, Zafar MN, Younis S, Nadeem R. The use of Neem biomass for the biosorption of zinc from aqueous solutions. J Hazard Mater 2008; 157(2-3): 534-40.
34. Kalyani G, Babu Rao G, Saradhi V, Kumar YP. Equilibrium and kinetic studies on biosorption of zinc onto Gallus Domesticus shell powder. ARPN Journal of Engineering and Applied Sciences 2006; 4(1): 39-49.
35. Souag R, Touaibia D, Benayada B, Boucenna A. Adsorption of Heavy Metals (Cd, Zn and Pb) from Water Using Keratin Powder from Algerien Sheep Hoofs. European Journal of Scientific Research 2009; 35(3): 416-25.
36. Israel U, Eduok UM. Biosorption of zinc from aqueous solution using coconut (Cocos nucifera L) coir dust. Archives of Applied Science Research 2012; 4(2): 809-19.
37. Lu S, Gibb SW, Cochrane E. Effective removal of zinc ions from aqueous solutions using crab carapace biosorbent. Journal of Hazardous Materials 2007; 149(1): 208-17.

JAEHR Journal of Advances in Environmental Health Research

Assessment of dental waste production rate and management in Sari, Iran

Mohammad Ali Zazouli[1], Rostamali Ehsan[2], Mansour Barafrashtehpour[2]

1 Department of Environmental Health Engineering, School of Health AND Health Sciences Research Center, Mazandaran University of Medical Sciences, Sari, Iran
2 Department of Environmental Health, Student Research Committee, School of Health, Mazandaran University of Medical Sciences, Sari, Iran

Original Article

Abstract

Dental offices produce a variety of dangerous wastes during normal business day. Most of these waste are non-hazardous that can be managed as household wastes; however, some component are hazardous and can pose a risk to human and the environment if discarded to Municipal Solid Wastes. These types of wastes must be managed separately. Therefore, the aim of this study was to assess the component and production rate of dental waste in Sari city, northern of Iran in 2011-2012. A descriptive cross-sectional study was conducted on 64 private dental practices from 146 available dental clinics in Sari city using a checklist and questionnaires which contain 25 questions and items. Dental wastes were weighed to determined qualitative and quantitative analysis. The data were analyzed using SPSS and MS-Excel. The results indicated that 77% of produced wastes were non-hazardous. The acceptable level management was observed only in 3.7% offices. The most desirable element management was accurate collecting (30.88%) in these offices. In general, it can be concluded that there is no proper management of wastes in dental centers of Sari. The mercury recycling is required for optimal management of dental waste. Furthermore, the dentists' education must be takes place to perform the management activities including reduction, separation and recycling inside the office.

KEYWORDS: Waste Management, Dental Waste, production

Date of submission: *23 Oct 2013*, ***Date of acceptance:*** *28 Jan 2014*

Citation: Zazouli MA, Ehsan R, Barafrashtehpour M. **Assessment of dental waste production rate and management in Sari city, Iran.** J Adv Environ Health Res 2014; 2(2): 120-5.

Introduction

Dental waste is one of the high sensitivity environmental problems due to its hazardous toxic and pathogenic factors, including pharmaceutical, chemical, radioactive, infectious and sharp wastes.[1] Dental wastes are relatively new environmental issues that have been focused more in recent years and have been conducting several studies in different countries.[2]

Generated wastes at the dental centers are contained various types. Blood and bloody tissues, sharp objects, heavy metals, paper, cardboard, glass, gloves and many other materials, which are produced in these centers can be classified as infectious, non-infectious, hazardous, household and administrative wastes, etc.[3,4] The fixer and developer drugs, which are used in advent and X-ray processes contain hazardous material.[5] The conservation and recovery act Section11008(a) includes guidelines and information toward the medical waste and production centers. This information includes the quantity and quality of waste and

Corresponding Author:
Mansour Barafrashtehpour
Email: bmansoor50@yahoo.com

its production facility and its proper management method. Dental clinics and offices produce such wastes.[6]

Some products in dentistry clinics, such as amalgam, contain mercury. Approximately, 10,000 tons per year of mercury is extracted, and it is estimated that about 3-4% is used in dentistry of Australia.[7] The most important work that can be performed in the field of efficient dental waste management is to prevent waste component to be mixed, because of their different characteristics. Therefore, management method must be regulated based on such properties.[5] Although hazardous wastes have a small fraction of dental wastes, however, they need to be managed correctly, otherwise they can transmit the disease agents, such as HIV and hepatitis B virus, and other infectious agents. They also can have negative environmental impacts, caused by heavy metals and radioactive components.[4,8]

Collection, recycling and disposal of dental wastes depend on their component. Radioactive waste must be separated from other wastes. However, infectious and sharp wastes must be collected separately in a puncture resistant container.[8] The studies in Hamadan[2] and Qazvin,[9] Iran, Palestine and India[8,10] showed the amount of produced and specific dental waste management.

Therefore, the aim of this research was to assess the component and production rate of dental wastes in Sari, Iran.

Materials and Methods

This is a descriptive cross-sectional study which it is conducted on 64 offices (which participate in this study) from 146 private dentistry offices and dentists clinics in Sari city. The data about management method of each parameter was collected by observation, interviews and questionnaires. The questionnaires were consisted the 25 questions.[5] The offices with negative total points had poor management level, point of 0-5 had average management level and more than 5 point had top management level.[5] The produced wastes were weighed using a scale (Vidas, model: vi4051). The production per capita was determined by referring to 14 randomly selected offices. Various components of wastes (non-hazardous, sharp and infectious wastes, etc.) were weighed, and the number of visiting people was recorded at a special table. Then, the amount of production per capita was calculated with whole produced waste divided to the number of visiting people. The collected data were analyzed by the descriptive statistic using the using SPSS for Windows (version 18.0, SPSS Inc., Chicago, IL, USA).

Results and Discussion

Quality and quantity of dental wastes

The amount of generated waste generated wastes per capita and percent of each part of the wastes are shown in table 1. The maximum production rate in dental clinics was related to common waste (77.06%).

Dental waste management

The results indicated that there are low, average and acceptable levels of management in the studied offices, 51.85%, 44.45% and 3.7%, respectively.

Table 1. Produced waste in dental offices of Sari with 6 ± 2 visited persons per day

	Infectious waste	Safety box wastes	Common wastes
Average of waste produced in day (g)	98.16 ± 24.38	19.66 ± 3.55	395.83 ± 96.56
Maximum (g)	122.00	25.00	520.00
Minimum (g)	60.00	15.00	270.00
Per capita (g)	16.82	3.37	67.85
Percentage (%)	19.10	3.83	77.06

Figure 1 shows that the positive activity in various stages of dental waste management is very poor except for waste separation.

According to the results obtained by the questionnaire, proper waste disposal was observed in 3.84% of clinics. Also, the proper wastes are collecting, with regarding time, place and collecting along with municipal wastes observed in 30.88% of the studied clinics.

Table 2 presents the management methods of different parts of dental wastes, obtained by questionnaires. Mostly, the recycling and separation was poor, and the dangerous wastes were released directly into the trash or sewer system.

The reduction of waste generation is the first priority in solid waste management. While the results of this study indicated that there is no program for waste reduction in 69.2% of the Dental offices of Sari (Figure 1).

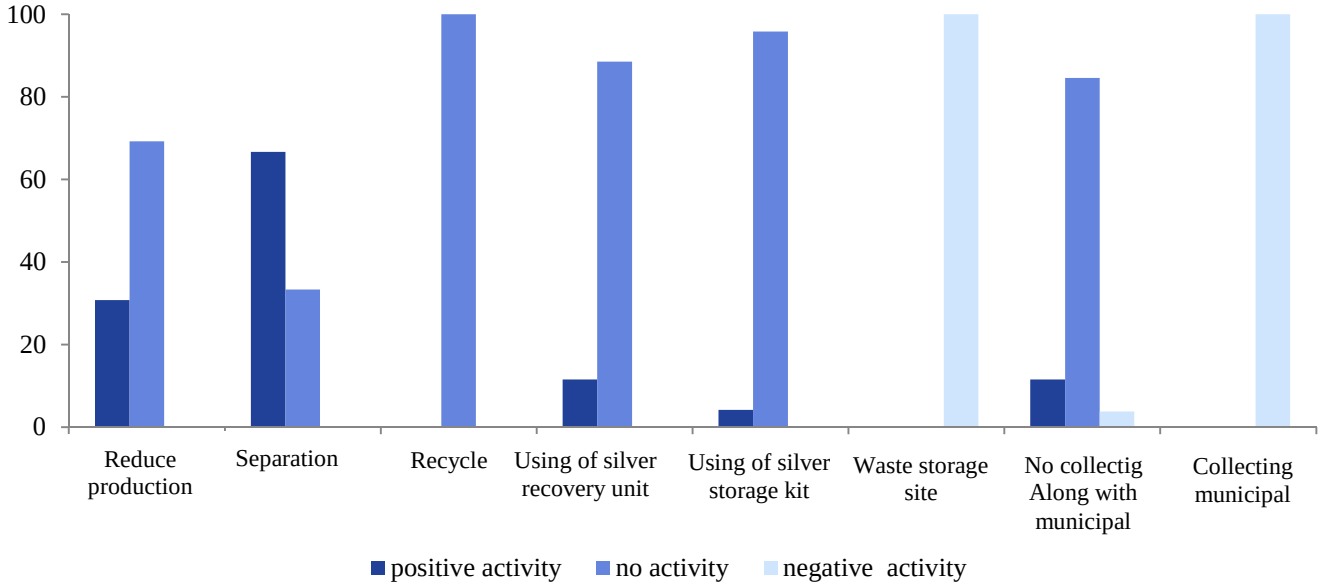

Figure 1. The percentage of the functional element of dental solid waste management in Sari

Table 2. Method for dentistry offices waste management in Sari based on questionnaires

Type of waste	Management method	Percent of clinics
Amalgam wastes	Discharge into toilet, Trash and sewer system	91.7
	Recycling	8.3
Empty amalgam capsules	Recycling of residues amalgam and then disposed to trash	30.4
	Unloading to trash	69.6
Radiographic film pocket	Unloading to trash	78.9
	Separation and recycling of lead foil and disposal of residues part into trash	21.1
Fixer	Discharge to toilet and sewer system	94.4
	Recycling	5.6
Developer	Discharge to toilet and sewer system	94.7
	Recycling	5.3
Sharp wastes	Using of Safety box, cutter	78.9
	Temporary storage in various containers and then disposed of them with the container into the trash	11.5
	Directly dispose in trash	9.6
Method of sterilization of dental instrument and equipment	Using of autoclave and combination of sterilizing agents (oven, autoclave, disinfecting and sterilizing solutions)	100

Therefore, to gain the optimum waste management, it is vital to pay attention to waste reduction. Waste reduction program is applicable by using reusable dental equipment and instrument, and products with less packaging.[5] A study by Sudhakar and Chandrashekar indicated that 39.1% of respondents did not separate their extra amalgam or mercury; but, disposed it to municipal solid wastes.[11] According to the results, dentists had no plan for waste recycling in their offices. Therefore, educational programs are essential to improving their knowledge and attitudes on waste management programs, which can lead to increase their participation in such programs. As can be seen from table 1, the highest percent of the wastes are common or semi-domestic wastes. The most important work that can be performed for optimum dental waste management is to prevent dental wastes to be mixed up, due to their different component and characteristics (infectious, toxic, semi-domestic and etc.), which requires different management methods. Kizlary et al. investigated the composition and production rate of solid waste in 4 dental labs in Xanthium of Greece. These four centers produced 75% of total solid waste of this state. The sampling was done in 2 month and the samples were divided in to three groups: (a) the infectious and potentially infectious wastes, (b) none-infectious wastes, (c) house hold wastes. The amount of these groups was 74%, 26%, 0.5%, respectively. This amount was 0.007% of municipal solid wastes in this state.[3] Rezai et al. conducted a survey on the weight and volume of the infectious waste from offices, laboratories, dressings and private radiology in Shiraz city in 2004. They observed that the maximum amount of infectious waste (62.2 Kg and 666 L) was produced in dental clinics.[12]

A part of the results from the questionnaire is shown in table 2. According to this table, 84% of the dug-out amalgam particle from patient's teeth and 4.2% of the excess residual amalgam is discharged to the wastewater. One of most common material in tooth restoration is amalgam.[9] The study of Sushma et al. indicated that 97.9% of dentists were aware of waste management policy. About 47.9% of them delivered the wastes without separation and disinfection to municipal waste collectors, 42.7% of gases and bloody swabs were placed in special color-coded plastics. 32.2% of dentists were delivered the collected residual amalgam to waste management services and 85.4% of dug-out amalgam from teeth is poured into wastes directly.[10] A study by Ogden et al. in dental clinics of northern Sweden showed that only 36% of dentists separated the mercury or the residual amalgam.[13] Treasure and Treasure were studied disposal of hazardous wastes in dental offices in New Zealand. The results of 767 filled questionnaires showed that 56.4% of dentists were covered the bloody swabs by wastes paper. Only 24.4% of infected and sharp wastes were collected in common wastes. Qualitative interviews with dentists indicated that they did not have the knowledge on the infected wastes disposal. The Government regulations on waste disposal did not motivate dentists to care for the guidelines. There were no specific waste disposal services in some areas, and some dentists did not embrace special services due to the high cost.[14] Results of this study showed that dental's units were not equipped by amalgam filter. Thus, using units equipped by amalgam filter is effective to achieve optimal management of generated wastes. For example, Germany has decreed all dentistry to use an amalgam separator and remover with at least 95% removal efficiency.[15] The study of Jamie in Montana of USA indicated that the mercury was disposed of by 79% of dental offices in Bio-hazardous materials storage containers and is burned along with other bio-medical wastes. 13% of the dug-out amalgam from teeth was poured in wastes. Only 5% of dentists recovered the empty capsules of amalgam. 70% of dentistry disposed of the empty capsules in municipal solid wastes, and 20% of capsules were putted in bio-hazardous containers.[16] In the present study, 69.6% of empty

amalgam capsules were disposed of in the trash. Using of mercury storage kit is another method to manage the generated amalgam. The results of this study showed that 95.85% of dentistry did not use storage kits. Fixer liquid along with advent solution is widely used for oral radiology. The fixer liquid is classified as a hazardous material because it contains a high concentration of silver, and should not be directly discharged into sewer or trash. Silver recycling is the best method for its management. However, only 5.6 percent of the offices in the present study used this method for the management of fixer drug. If fixer liquid is not mixed with the developer solution (hydroquinone + potassium hydroxide), it can be discharged in sewer.[15]

It is contained 50% of mercury approximately which are combined with silver, tin and other metal in lower amount.[17] Mercury should not be entered into the septic tank because it is a toxic and hazardous material and can lead to groundwater contamination.[15] Several methods may be used to control dental's mercury discharges, e.g. dental mercury control by development of Best Management Practices (BMP) is one of the choices. For example, laws of installation of amalgam separator in many states of USA are considered as a type of BMP.[18] In this study, the autoclave were applied in 48.1% of the offices to sterilize the dentistry equipment, and 51.9% used the combined methods (autoclave, oven, disinfecting and sterilizing solution). In another survey by Cannata et al. it was reported that all clinics used autoclave for sterilization. Chemical disinfectant solutions were used in 12 clinics from 14 clinics that were performed the superficial disinfection mainly. In five clinics, there was a separate section for contaminated wastes storage.[7]

Although, in recent decades, the institutions, dental associations and government agencies have been issued various guidelines and recommendations to observe the principles of infection control,[19] which can lead to improve the principles observance; but, these recommendations and guidelines was not enough. Failure to comply with the law by dentists, increasing the number of patient with AIDS and hepatitis B and C, and, consequently, the increasing transmission risk of these diseases in the dental center has led many people to be frightened and anxious about being treated by the dentist, and going to the centers.[1]

Assurance of proper sterilization operation by these devices is effective step to controlling the transmission of infectious via dentistry's equipment. In addition, knowledge on the proper application of disinfectant solutions can reduce contaminations discharged into sewer systems.

Conclusion

Generally, it concluded that there is no proper management of wastes in dental centers of Sari. It is recommended that the increasing the knowledge of dentists about reduction, separation, and recycling of wastes is essential to achieve the proper management of dental wastes. In the next step, clear codification must be done to restrict the using of certain toxic compound and their discharge to sewer and trash, and, also, continuous monitoring implementation of such codifications.

Conflict of Interests

Authors have no conflict of interests.

Acknowledgements

The research was performed with the assistance and cooperation of the research committee of the Mazandaran University of Medical Science and dentists of Sari. The authors are thankful because of their cooperation.

References

1. Arenholt-Bindslev D. Environmental aspects of dental filling materials. Eur J Oral Sci 1998; 106(2 Pt 2): 713-20.
2. Kulivand A, Nabizadeh R, Joneidy A, Yunesian M, Omrany G. Quantity and Quality Analysis and Management of Solid Waste Produced in Dentistry Laboratories and Practical Dentist Offices in Hamedan

2007. Iran J Health Environ 2009; 2(1): 36-45. [In Persian].
3. Kizlary E, Iosifidis N, Voudrias E, Panagiotakopoulos D. Composition and production rate of dental solid waste in Xanthi, Greece: variability among dentist groups. Waste Manag 2005; 25(6): 582-91.
4. Ozbek M, Sanin FD. A study of the dental solid waste produced in a school of dentistry in Turkey. Waste Manag 2004; 24(4): 339-45.
5. Barafrashteh M, Rezayi S, Alinejad A, Sadat A. Evaluation of dental wastes management in Yasouj. Proceedings of the 13th Congress of Iran Environmental Health; 2010 Nov 2-4; Kerman, Iran; 2010. p. 131-9. [In Persian].
6. Landrum VJ. Medical Waste Management and Disposal. Park Ridge, NJ: Noyes Data Corporation; 1991.
7. Cannata S, Bek M, Baker P, Fett M. Infection control and contaminated waste disposal practices in Southern Sydney Area Health Service Dental Clinics. Aust Dent J 1997; 42(3): 199-202.
8. Darwish RO, Al-Khatib IA. Evaluation of dental waste management in two cities in Palestine. East Mediterr Health J 2006; 12(Suppl 2): S217-S222.
9. Nafez A. Quantitative and qualitative survey of dentistry wastes in Qazvin city. Proceedings of the 12th Congress of Iran Environmental Health; 2009 Nov 2-4; Tehran, Iran; 2009. p. 2092-9. [In Persian].
10. Sushma MK, Bhat S, Shetty SR, Babu SG. Biomedical dental waste management and awareness of waste management policy among private dental practitioners in Mangalore city, India. Tanzania Dental Journal 2010; 16(2): 39-43.
11. Sudhakar V, Chandrashekar J. Dental health care waste disposal among private dental practices in Bangalore City, India. Int Dent J 2008; 58(1): 51-4.
12. Rezai A ea. Survey of volume and weight of Infectious wastes in offices, laboratories, dressing, private radiology in Shiraz city. Proceedings of the 9th Congress of Iran Environmental Health; 2006 Nov 7-9; Isfahan, Iran; 2006. p. 219. [In Persian].
13. Ogden GR, Bahrami M, Sivarajasingam V, Phillips G. Dental students' knowledge and compliance in cross infection control procedures at a UK dental hospital. Oral Dis 1997; 3(1): 25-30.
14. Treasure ET, Treasure P. An investigation of the disposal of hazardous wastes from New Zealand dental practices. Community Dent Oral Epidemiol 1997; 25(4): 328-31.
15. Nabizadeh R, Kulivand A, Jonidi Jafari A, Younesian M, Omrani G. Evaluation of dental solid waste in Hamedan. Journal of Dental Medicine 2009; 22(1): 66-73. [In Persian].
16. Silberberger JE. Reducing Dental Mercury Discharge in Missoula, Montana: Collaborative Opportunities [Thesis]. Missoula, MT: University of Montana; 2007.
17. Van Boom G, Richardson MK, Trip LJ. Waste Mercury in Dentistry: The Need for Management. Environmental Health Review 2003; 47(2): 33-9.
18. Saunders TR, Guillory VL, Gregoire ST, Pimsler M, Mitchell MS. The effect of bioburden on in-depth disinfection of denture base acrylic resin. J Calif Dent Assoc 1998; 26(11): 846-50.
19. Najafi Dolatabadi S, Mohebbi Nobandegani .Z, Ghafarian shirazi.H. Self-assessment of Yasuj dentists in field of regarding to principles of infection control. Dena Scientific Quarterly 2008; 3(1-2): 65-73. [In Persian].

JAEHR Journal of Advances in Environmental Health Research

Removal of nickel and total chromium using Escherichia coli biofilm supported on clinoptilolite

Roya Ebrahimi[1], Shiva Zandi[1], Fardin Gharibi[2]

1 Kurdistan Environmental Health Research Center, Kurdistan University of Medical Sciences, Sanandaj, Iran
2 Deputy of Research, Kurdistan University of Medical Sciences, Sanandaj, Iran

Original Article

Abstract

Biofilm is communities of microorganisms attached to the surface and is able to concentrate metal species within their cell structure. Therefore, the aim of this study was to produce *Escherichia coli* biofilm on zeolite (clinoptilolite) and evaluate its ability for nickel (Ni) and chromium (Cr) adsorption from aqueous solutions. A laboratory-scale batch model was used for biodsorption assay. The effect of initial metal concentrations and pH on the removal efficiency was studied. Two isotherm equations were used for analyzing the experimental data. The results showed that Ni uptake by biofilm were higher than Cr. The biosorption process was best described by the Langmuir model. Fourier transform infrared confirmed that there are some functional groups on the biomass surface that may interact with the metal ions. It is concluded that the biofilm is very promising for the removal of metal ions from aqueous solution and hence may be encourage the utilization of biofilm in environmental applications.

KEYWORDS: Nickel, Chromium, Biofilm, Biosorption, Zeolite, Escherichia coli

Date of submission: *1 Oct 2013*, ***Date of acceptance:*** *19 Jan 2014*

Citation: Ebrahimi R, Zandi Sh, Gharibi F. **Removal of nickel and total chromium using *Escherichia coli* biofilm supported on clinoptilolite.** J Adv Environ Health Res 2014; 2(2): 126-33.

Introduction

Environmental pollution by heavy metals has led to serious problems for humans and other organisms in the environment due to their nonbiodegradability and accumulation in the living organisms.[1-3] Conventional methods for removing heavy metals from industrial effluents contains various processes such as precipitation, coagulation, ion exchange, electrodialysis, electrocoagulation, reverse osmosis, evaporation and filtration.[4,5] However, most of the above mentioned processes have significant economic and technical limitations such as low efficiency, high sludge production, disposal of sludges containing large amounts of heavy metals, need for specific chemicals and expensive regeneration process.[4,6] Therefore, it is recommended to find new alternatives and biosorption can be considered as a new method.[3]

Biosorption is a process in which formation of usually chemical bonds between metal ions and functional groups on the surface of some biomaterials; such as bacteria, fungi, algae and agricultural residues; leads to separation of metals from aqueous solution. Biosorption mechanism is usually related to the chemical bonding between the adsorbent functional groups (metabolically mediation uptake) and the metal ions or ion-exchange reaction due to the high ion exchange capacity of the biosorbent (physicochemical adsorption). Economical nature and an ecofriendly behavior are the major advantages of a biosorption. Hence, is

Corresponding Author:
Roya Ebrahimi
Email: ebrahimi83@yahoo.com

being developed as an alternative to conventional methods for the removal of heavy metals. However, high affinity for metal uptake, rapid uptake and maximum adsorption capacity are some of the significant factors that should be considered in biosorbent selection. Most microorganisms such as bacteria, fungi, yeasts and algae are able to concentrate metals from aqueous solutions and to accumulate in their cell structure.[7] Among the various biosorbents, bacteria because of their small size, ubiquity, growing under controlled conditions and adaptation to a broad range of the environmental situation are used as an efficient biosorbents.[5,7] Bacteria can produce macro-molecules, known as extracellular polymeric substances (EPSs), which is important in the development of biofilms.[5,8] ESP is mainly composed of polysaccharides, nucleic acids, proteins, lipids or humic substances which contain several functional groups such as the carboxyl, amine, hydroxyl and phosphoric groups.[5,9] Among various functions of ESP in biosorption processes , the most important ones are adhesion to cell surfaces and accumulation of elements from the environment.[9,10] However, batch adsorption of pollutants and possible exiting from the reactor are two major problems of biofilm that reduce efficiency and cause operational problems.[3,6,9] Therefore, a supported media for biofilm can be useful to reduce the above problems.

Several synthetic and natural materials have been used as supporting materials for bacterial biofilms. Among the various media, materials with a porous structure and high adsorption affinity to pollutants and biofilm would be a suitable alternative. Since zeolite has ion-exchange properties, thus it can be used as a supporting media for the bacterial biofilms. Zeolite is a mineral with a crystalline structure and contains numerous microscopic pores.[11] Ion-exchange properties of zeolite are the main reason for metals uptake. However, other mechanisms such as pore structure and surface charge are also involved in metals uptake.[12] Based on the zeolites chemical structure, and the amount of exchangeable cations in their chemical structure, zeolites can show different capacities for metals uptake.[12,13] As other researchers have pointed out, raw zeolite is considered as an available and low cost material with different capacity for heavy metals' uptake.[11,13] Wingenfelder showed raw zeolite has a high capacity to absorb lead but, its ability to adsorb cadmium is less.[14] Adsorption capacity of zeolite can be increased by modification of their chemical structure or surface properties. A new method for this purpose is surface coverage of zeolite by a specific biofilm by which not only continuous treatment is applicable by biofilm, but also keeps it within the reactor.[3,6,7] For example, Quintelas et al. used Escherichia coli biofilm on granular activated carbon for the adsorption of hexavalent chromium (Cr) from industrial wastewater.[3] this study aimed to investigate the ability of a E. coli biofilm , an effective agent for metal adsorption, supported on zeolite (clinoptilolite) for the removal of nickel (Ni) and Cr from aqueous solutions.

Materials and Methods

The bacterium E. coli (PTCC 1330) was obtained from Iranian Research Organization for Science and Technology. Heavy metals stock solutions were prepared by diluting $K_2Cr_2O_7$ and $NiCl_2$ ($6H_2O$) in distilled water. Atomic absorption spectrometric standards were prepared from 1000 mg/l metal solutions. The clinoptilolite (a natural zeolite) was obtained from Afrandtooska Co. The chemical compositions of clinoptilolite are given in table 1.

Medium for growth of E. coli was prepared using 5 g/l beef extract, 10 g/l peptone, 5 g/l NaCl at pH 7.2. The prepared medium was sterilized for 20 min at 121°C, cooled to room temperature, Inoculated with bacteria and kept at 37°C for 24 h with moderate stirring in incubator. Batch adsorption experiments were conducted using 2 g of clinoptilolite with 15 ml of E. coli culture media and without E. coli (for comparison purposes) and 100 ml of the

different concentration of Ni and Cr solutions varied between 50 mg/l and 1000 mg/l in 250 mL beaker. The beakers were stirred at a constant rate of 120 rpm at 37°C for about 10 days (time required to reach an equilibrium, accordingly to previous studies).[1,3] Then, 1 ml samples were taken, centrifuged and analyzed for metal ions concentrations. The determination of metal ions concentrations was performed by atomic absorption spectrometry (PG-990, England). The Fourier transform infrared (FT-IR) spectra of biosorbents were taken in KBr pellets using a Tensor 27 spectrophotometer (Bruker Optik GmbH, Germany).

Table 1. Chemical composition of clinoptilolite

Component	Weight (%)
SiO_2	66.50
Al_2O_3	11.80
TiO_2	0.20
Fe_2O_3	1.30
CaO	3.10
MgO	0.70
K_2O	3.00
Na_2O	2.00
P_2O_5	0.01
L.O.I.	12.00

Biosorption capacity was determined from the difference between the initial and residual concentrations of the metal ion in the solution at the sampling time as follows:[15]

$$Q_t = \frac{V(C_i - C_t)}{m}$$

where Q_t is the amount of metal adsorbed per unit mass of biodsorbent at a given time (mg/g), V the volume of solution (L), C_i and C_t are the initial concentration and the residual concentration of metal ions at a given time (mg/l), and m is the dry weight of the biosorbent (g). In order to evaluate the biodsorption capacity, the experimental data were fitted to Langmuir and Freundlich isotherm models.

Results and Discussion

The solution pH is one of the most important factors that affect biological sorption process, because of its effect on the charge state of metals and also adsorbent surface. Therefore, effect of pH on studied metals uptake by zeolite and biofilm was evaluated and shown in figure 1. As is known, the cationic metals' adsorption efficiency is lower at acidic pH. It was observed that Ni and Cr uptake increased with increase in pH up to pH of 6 and then it decreased with any further increase in pH. It is clear that at pH below 6, hydrogen ions compete with positive charge ions for adsorption sites. Therefore, this condition limits the access of Ni ions to the adsorption sites and decreases Ni removal.[3] Furthermore, at alkaline pH values, the adsorption of Ni decreases because soluble hydroxylated complexes of the metal ions is formed and compete with Ni for adsorption sites.[16] According to Bhattacharyya and Gupta, biological uptake of Ni decreases at pH values higher than 8 due to precipitation of Ni ion as a hydroxide.[17] Based on other studies, the optimal pH for the biosorption of Ni was around 6 due to the effect of pH on metal speciation and metal binding sites on the biomass surface.[18-20]

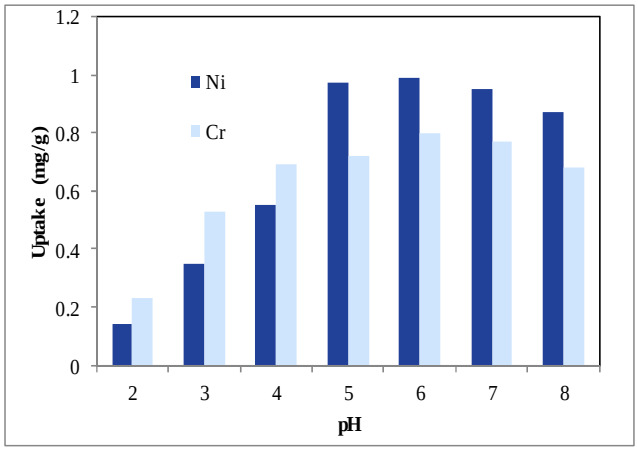

Figure 1. Effect of pH on the uptake of nickel and chromium by zeolite/biofilm (C0 = 10 mg/l)

Cr adsorption changes trend at different pH

is similar to Ni. For pH values higher than 6, the formation of hydroxyl complexes of Cr and increasing the number of hydroxyl ions in the solution and its competition with CrO_4^{2-} for adsorption sites on the surface of the adsorbent, are the most reason for decreasing of Cr uptake.[7] At pH lower than 6, Cr is in an anionic state and its biosorption decreases due to the competition with ions like nitrate ion from nitric acid that is used to adjust the pH and maintenance of low acidic condition.[20] Hence, in this study all adsorption experiments carried out in pH value of 6.

Figure 2 shows the effect of initial concentration of Cr and Ni on the removal of studied metals and their uptake. As is clear, the equilibrium adsorption capacity for the adsorption of Ni and Cr ions increased with increasing their initial concentration. In fact, in the solution with a high metal concentration, ions can be adsorbed better. While the removal efficiency showed the reverse trend. Hence, the metal removal rate decreased with increase in initial concentration. The maximum amount of Ni adsorbed per mass of adsorbent (zeolite and zeolite/biofilm) for concentrations of 10, 30, 50, 70, 90 and 110 mg/l were obtained 0.53, 1.26, 1.85, 2.45, 2.7 and 2.75 for zeolite and 1.01, 2.41, 3.96, 5.23, 6.21 and 7.46 for zeolite/biofilm, respectively. Instead, the removal percentage decreased from 53% to 25% for zeolite and from 88 to 59 for zeolite/biofilm with increasing of Ni concentration from 10 to 110 mg/l. Similarly, the maximum amount of Cr adsorbed per mass of adsorbent (zeolite and zeolite/biofilm) for concentrations of 10, 30, 50, 70, 90 and 110 mg/l were obtained 0.4, 1.14, 1.9, 2.1, 1.98 and 2 for zeolite and 0.8, 2, 2.81, 3.22, 3.2 and 3.3 for zeolite/biofilm, respectively. Instead, the removal percentage decreased from 40% to 18% for zeolite and from 70 to 26 for zeolite/biofilm with increasing of Cr concentration from 10 to 110 mg/l. These results are shown in figure 2.

In the adsorption process, the initial concentration of ions in solution has a key role as a driving force to overcome the mass transfer

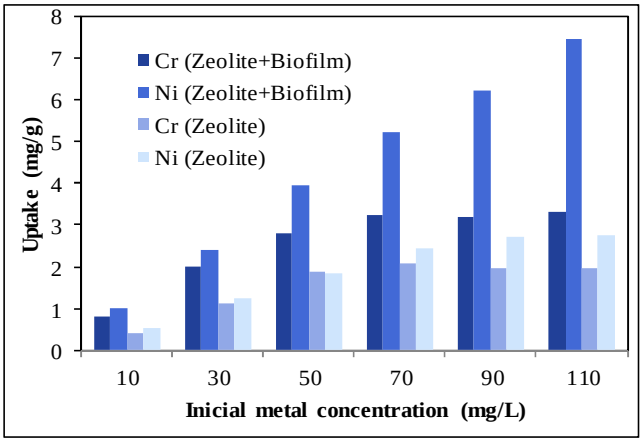

Figure 2. Effect of initial metal concentration on uptake values of nickel and chromium

resistance between the liquid phase and solid phase. Thus, it is expected that with an increase in metal ions the metal uptake will increase.[21] The results showed that Ni and Cr uptake rate were relatively high at the beginning of the process due to abundance available adsorption sites. However, the number of active sites for the adsorption gradually decreases with an increase in process time and the adsorption rate slightly decreased, leading to the formation of the adsorption equilibrium. At low metal concentrations, adsorption sites are available and could easily be occupied since the ratio between the number of metal moles in solution and available surface area is low. Therefore, absorption is independent of the initial concentration. Nevertheless, at high concentrations of metal the removal efficiency is dependent on the initial concentration because the number of available sites is less than the number of metal moles. Horsfall et al. stated when the initial concentration increases, the removal rate decreases. At higher concentration, the number of ions competing for the available binding sites on the biomass surface increases and thus reduces the number of binding sites.[22] Meanwhile, at higher concentration, the average distance between the adsorbed species will be reduced, which affects the distribution of surface charge. Thus, the ability of adsorbate to migrate to the adsorbent surface changes and, as a result,

the fixation reduces.[7] Akhtar et al. showed that at high concentrations, the absorption is insignificant due to saturation of the binding sites of biosorbent.[23] However, increase in the biomass capacity at higher concentrations can be related to differences in metal ion concentration gradient between the solution and inside of the microbial mass.[7] Finally, at very high concentrations of metal ions, solid-liquid equilibrium is limited by diffusion of metal ions into the microbial mass.[7] In other words, the metal ions should diffuse through intraparticle diffusion into the biomass surface, and this mechanism is slow.[20] Also, comparison of the results of the adsorption of studied metal ions by zeolite with and without biofilm bacteria showed better results in the adsorption process when the bacterial biofilm is used, which confirms the important role of biofilms in biological uptake. In fact, zeolite provides necessary surface for biofilm development and then biofilm provides a high concentration of biomass per unit volume hence bacteria can remain inside the reactor for an unlimited period, resulting in increased electrostatic interactions between metal ions and extracellular polymers.[7] Functional groups responsible for the bioadsorption process are mainly carboxyl, hydroxyl, carbonyl, sulfonate, amide, imidazole, phosphonate and phosphodiester groups. Most of these groups exist on E. coli biofilms, leading to their interaction with metal ions.[20] This fact has been confirmed by Pradhan et al.[24]

Comparison of biosorption performance showed differences between Ni and Cr uptake. As Ni showed better results. Chemical properties of metals (valence, electronegativity, ionic radius and atomic weight) and properties of the biomass (structure, functional groups and surface area) cause the main differences in biosorption capacity.[16] Accordingly, the electronegativity, ionic radius and atomic weight of Ni are 1.8 Pauling, 69pm and 58.7 u, respectively, and for Cr they are 1.6 pauling, 44 pm and 51.99 u, respectively.[16,20] Ni has a higher electronegativity than Cr and then better retentions on the biomass surface, which promotes the penetration into the EPSs.[20]

Despite the lower ionic radius and atomic weight of Cr, which promotes Cr ions penetration into the polymeric net, low adsorption capacity of Cr is justified by its anionic state.[20] This unexpected result may also be related to xenobiotic effect caused by the Cr ions on the bacterium biofilm. Since metal binding to the bacterial biofilm is a metabolic pathway that is sensitive to the metal toxicity.[20] Barros et al. expressed the low removal of Cr by the zeolite is related to the difference between big anionic radius of Cr and the porous diameter of the zeolite and also the strong propensity of Cr to form complexes in the aqueous solution.[25]

Adsorption isotherms are an important factor in system design and describe the interaction between the adsorbent and adsorbate. Two different models–Langmuir and Freundlich – were fitted, and sorption isotherm parameters calculated by linear regression (Figures 3 and 4) for the best fit and are shown in table 2.

When zeolite was used as the adsorbent, the best fit for Cr was obtained with the Langmuir isotherm ($R^2 = 0.95$) and for Ni the best fit was the obtained with the Freundlich isotherm ($R^2 = 0.98$). However, when zeolite/biofilm was used, the best fit for Ni and Cr was obtained with the Langmuir isotherm. Langmuir coefficients of determination (R^2) for Ni and Cr adsorption were obtained 0.98 and 0.95, respectively, which indicating a good fit of the Langmuir monolayer model for the uptake of Ni and implies a good mathematics adaptation. It may due to the homogeneous distribution of adsorption sites on the adsorbent surface. Langmuir isotherm assumes the adsorbent surface as homogeneous. However, Freundlich isotherm is important because it do not assume a homogeneous surface. According to the results, it is observed that the Freundlich model well describes the uptake of Ni

by zeolite. As shown in table 2, the value of Q_L for Ni is 3.96 mg/g, which is about 1.52 times larger than that for Cr, showing a higher biodsorption capacity of the biosorbent for Ni than that for Cr. A similar observation was reported by Quintelas et al.[3] for higher biodsorption capacity of the biosorbent for Ni.[5,20]

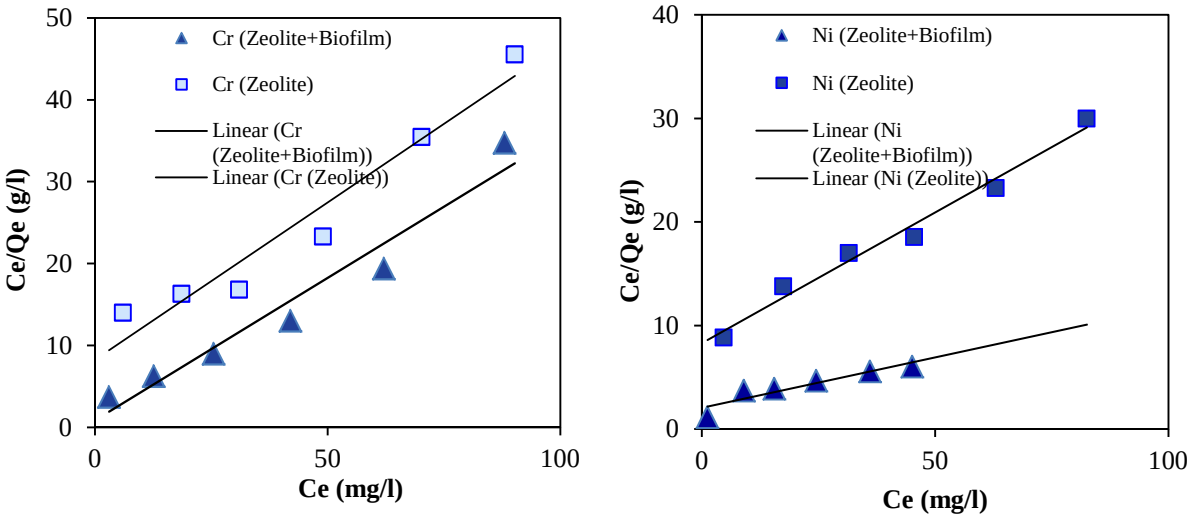

Figure 3. Biosorption isotherms of nickel and chromium based on the Langmuir model

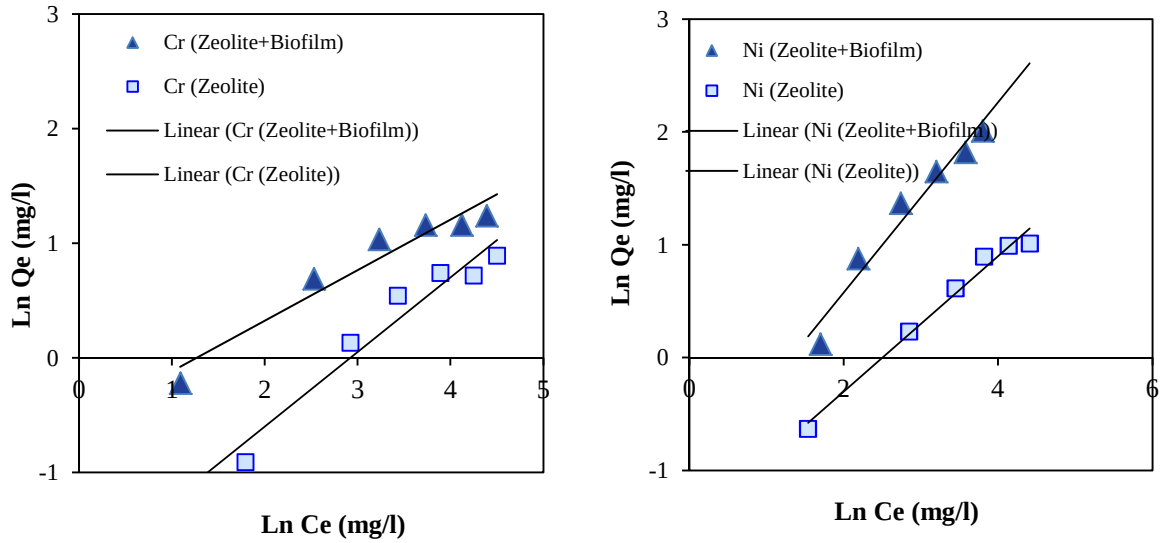

Figure 4. Biosorption isotherms of nickel and chromium based on the Freundlich model

Table 2. Parameters of Langmuir and Freundlich isotherms for biosorption of Ni and Cr

Type of adsorbent	Type of metal	Freundlich model			Langmuir model		
		K_F (mg/g)	b_F (l/g)	R^2	K_L (L/g)	Q_L (mg/g)	R^2
Zeolite	Ni	0.21	0.60	0.98	0.047	10.29	0.87
Zeolite + biofilm		0.33	0.84	0.96	0.031	3.96	0.98
Zeolite	Cr	0.15	0.65	0.94	0.400	2.87	0.95
Zeolite + biofilm		0.57	0.44	0.94	0.046	2.60	0.95

Ni: Nickel; Cr: Chromium; K_F: Freundlich constant; b_F: Degree of linearity between the solution concentration and the amount adsorbed; R_2: Linear regression coefficient; K_L: Langmuir constant related to the affinity of binding sites; Q_L: Lagmuir adsorption capacity

Figure 5 shows the FT-IR spectra of unloaded and metal loaded microbial biomass in the range of 1000-4000/cm. This spectrum was performed to determine the functional groups that might be responsible for the biosorption process. As the unloaded biomass spectrum shows, there are a number of absorption peaks, which reflecting the complex nature of the biomass. Based on the results obtained by Volesky[26] and Pavan et al.[27] hydroxyl, carbonyl, carboxyl, sulfonate, amide, imidazole, phosphonate and phosphodiester groups are main functional groups responsible for a biosorption process which some of them present on the E. coli biomass. Comparison between the spectra showed that unloaded biomass spectrum has a slight change in certain bands after uptake of metals. Therefore, these changes indicate a possible role of those functional groups in biosorption process.

Conclusion

This study was conducted to determine the ability of zeolite with and without E. coli biofilm for biosorption of Ni and Cr. It was found that the biosorption process is pH-dependent for both metals, and the maximum uptake was obtained in the pH of 6.

The equilibrium adsorption capacity for metal uptake increased with increasing initial concentration while the removal efficiency showed a reverse trend. The best isotherm fit for Ni and Cr was obtained with Langmuir model. FT-IR analyses showed that the main functional groups on the biomass were hydroxyl, carboxyl and phosphate groups that may be the main binding sites for biosorption of the Ni and Cr by E. coli. The presence of the biofilm increased the uptake efficiency of the zeolite that confirms the important role of biofilms in the adsorption process.

Conflict of Interests

Authors have no conflict of interests.

Acknowledgements

The authors would like to thank the Vice-chancellor for Research and Technology, the Kurdistan University of Medical Sciences, Iran for providing the grant of this research study.

References

1. Maleki A, Zarasvand MA. Heavy metals in selected edible vegetables and estimation of their daily intake in Sanandaj, Iran. Southeast Asian J Trop Med Public Health 2008; 39(2): 335-40.

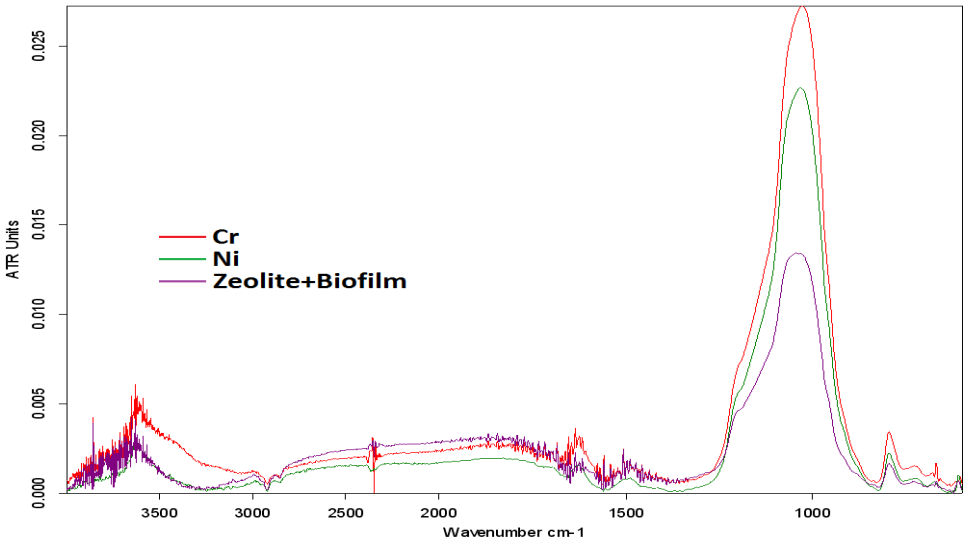

Figure 5. Fourier transform infrared spectra of zeolite/biofilm before and after metal loading

2. Maleki A, Mahvi AH, Zazouli MA, Izanloo H, Barati AH. Aqueous Cadmium Removal by Adsorption on Barley Hull and Barley Hull Ash. Asian J Chem 2011; 23(3): 1373-6.
3. Quintelas C, Rocha Z, Silva B, Fonseca B, Figueiredo H, Tavares T. Biosorptive performance of an Escherichia coli biofilm supported on zeolite NaY for the removal of Cr(VI), Cd(II), Fe(III) and Ni(II). Chemical Engineering Journal 2009; 152(1): 110-5.
4. Maleki A, Erfan MB, Mohammadi AS, Ebrahimi R. Application of commercial powdered activated carbon for adsorption of carbolic acid in aqueous solution. Pak J Biol Sci 2007; 10(14): 2348-52.
5. Quintelas C, Fernandes B, Castro J, Figueiredo H, Tavares T. Biosorption of Cr(VI) by a Bacillus coagulans biofilm supported on granular activated carbon (GAC). Chemical Engineering Journal 2008; 136: 195-203.
6. Lameiras S, Quintelas C, Tavares T. Biosorption of Cr (VI) using a bacterial biofilm supported on granular activated carbon and on zeolite. Bioresour Technol 2008; 99(4): 801-6.
7. Quintelas C, Fonseca B, Silva B, Figueiredo H, Tavares T. Treatment of chromium(VI) solutions in a pilot-scale bioreactor through a biofilm of Arthrobacter viscosus supported on GAC. Bioresour Technol 2009; 100(1): 220-6.
8. Comte S, Guibaud G, Baudu M. Biosorption properties of extracellular polymeric substances (EPS) towards Cd, Cu and Pb for different pH values. J Hazard Mater 2008; 151(1): 185-93.
9. Eboigbodin KE, Biggs CA. Characterization of the extracellular polymeric substances produced by Escherichia coli using infrared spectroscopic, proteomic, and aggregation studies. Biomacromolecules 2008; 9(2): 686-95.
10. Wang W, Wang W, Zhang X, Wang D. Adsorption of p-chlorophenol by biofilm components. Water Res 2002; 36(3): 551-60.
11. Leung S, Barrington S, Wan Y, Zhao X, El-Husseini B. Zeolite (clinoptilolite) as feed additive to reduce manure mineral content. Bioresour Technol 2007; 98(17): 3309-16.
12. Kocaoba S, Orhan Y+, Akyuz T. Kinetics and equilibrium studies of heavy metal ions removalby use of natural zeolite. Desalination 2007; 214(1-3): 1-10.
13. Castaldi P, Santona L, Enzo S, Melis P. Sorption processes and XRD analysis of a natural zeolite exchanged with Pb(2+), Cd(2+) and Zn(2+) cations. J Hazard Mater 2008; 156(1-3): 428-34.
14. Wingenfelder U, Nowack B, Furrer G, Schulin R. Adsorption of Pb and Cd by amine-modified zeolite. Water Res 2005; 39(14): 3287-97.
15. Dang VB, Doan HD, Dang-Vu T, Lohi A. Equilibrium and kinetics of biosorption of cadmium(II) and copper(II) ions by wheat straw. Bioresour Technol 2009; 100(1): 211-9.
16. Sari A TMUOSM. Biosorption of Pb(II) and Ni(II) from aqueous solution by lichen (Cladonia furcata) biomass. Biochemical Engineering Journal 2007; 37(2): 151-8.
17. Bhattacharyya KG, Gupta SS. Influence of acid activation on adsorption of Ni(II) and Cu(II) on kaolinite and montmorillonite: Kinetic and thermodynamic study. Chemical Engineering Journal 2008; 136(1): 1-13.
18. Carvalho WA, Vignado C, Fontana J. Ni(II) removal from aqueous effluents by silylated clays. J Hazard Mater 2008; 153(3): 1240-7.
19. Vijayaraghavan K, Lee MW, Yun YS. Evaluation of fermentation waste (Corynebacterium glutamicum) as a biosorbent for the treatment of nickel(II)-bearing solutions. Biochemical Engineering Journal 2008; 41(3): 228-33.
20. Quintelas C, Rocha Z+, Silva B, Fonseca B, Figueiredo H, Tavares T. Removal of Cd(II), Cr(VI), Fe(III) and Ni(II) from aqueous solutions by an E. coli biofilm supported on kaolin. Chemical Engineering Journal 2009; 149(1-3): 319-24.
21. Wan Ngah WS, Hanafiah MAKM. Adsorption of copper on rubber (Hevea brasiliensis) leaf powder: Kinetic, equilibrium and thermodynamic studies. Biochemical Engineering Journal 2008; 39(3): 521-30.
22. Horsfall M, Ogban F, Akporhonor EE. Sorption of chromium (VI) from aqueous solution by cassava (Manihot sculenta Cranz.) waste biomass. Chem Biodivers 2006; 3(2): 161-74.
23. Akhtar K, Akhtar MW, Khalid AM. Removal and recovery of uranium from aqueous solutions by Trichoderma harzianum. Water Res 2007; 41(6): 1366-78.
24. Pradhan S, Singh S, Rai LC. Characterization of various functional groups present in the capsule of Microcystis and study of their role in biosorption of Fe, Ni and Cr. Bioresour Technol 2007; 98(3): 595-601.
25. Barros MA, Machado N, Sousa-Aguiar E, Alves F, Pedroza S. Removal of Cr^{3+} from industrial and synthetic wastewater by naturally occurring clinoptilolite. In: Blanco J, Avila P, Editors. Catalizadores y adsorbentes para la protección ambiental en la Región Iberoamericana. Madrid, Spain: Cyted; 2001. p. 219-24. [In Spanish].
26. Volesky B. Biosorption and me. Water Res 2007; 41(18): 4017-29.
27. Pavan FA, Mazzocato AC, Jacques RA, Dias SLP. Ponkan peel: A potential biosorbent for removal of Pb(II) ions from aqueous solution. Biochemical Engineering Journal 2008; 40(2): 357-62.